

Medical University of South Carolina

MEDICA

MUSC Theses and Dissertations

2010

Regulation of VCAM-1 Expression by Tgf β 2 during the Formation of the Epicardium

Margaret Elizabeth Grant Burton
Medical University of South Carolina

Follow this and additional works at: <https://medica-musc.researchcommons.org/theses>

Recommended Citation

Burton, Margaret Elizabeth Grant, "Regulation of VCAM-1 Expression by Tgf β 2 during the Formation of the Epicardium" (2010). *MUSC Theses and Dissertations*. 198.
<https://medica-musc.researchcommons.org/theses/198>

This Dissertation is brought to you for free and open access by MEDICA. It has been accepted for inclusion in MUSC Theses and Dissertations by an authorized administrator of MEDICA. For more information, please contact medica@musc.edu.

**Regulation of VCAM-1 expression by TGF β 2 During the Formation of
the Epicardium**

by

Margaret Elizabeth Grant Burton

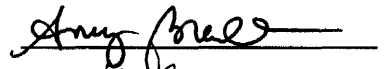
A dissertation submitted to the faculty of the Medical University of South Carolina in
partial fulfillment of the requirements for the degree of Doctor of Philosophy in the
College of Graduate Studies

Molecular and Cellular Biology and Pathobiology


2010

Approved by:


Chair, Advisory Committee







Acknowledgements

First I would like to thank my wonderful husband Grady for always being supportive of me and believing that I can achieve whatever I set my mind to and my daughter Isabelle for making me smile everyday. I would also like to thank my parents who have always encouraged me to pursue my interests and to believe in myself even when things seemed impossible.

I would also like to thank my mentor Dr. Steve Kubalak who has helped me become a scientist and encouraged me to find the next question to answer. I would like to thank my committee members Drs. Scott Argraves, Amy Bradshaw, Dhan Kuppuswamy and Andy Wessels for their continued guidance throughout my dissertation work.

The members of the Kubalak lab, past and present, have been supportive and helpful throughout this work. Loretta Hoover has been a great friend and colleague who was willing to go above and beyond. Laura Brichler has been helpful in generating some of this work.

Finally, I would like to thank my other family and friends who have been there for me throughout this process.

Table of Contents

	<u>Page</u>
ACKNOWLEDGEMENTS.....	ii
LIST OF TABLES.....	iv
LIST OF FIGURES.....	v
ABBREVIATIONS.....	viii
ABSTRACT.....	xi
CHAPTERS	
1. REVIEW OF LITERATURE.....	1
A. Congenital Heart Disease.....	1
B. Cardiac Morphogenesis.....	2
C. Formation of the Epicardium.....	8
D. Mouse Models of Aberrant Epicardium Formation.....	11
E. Cell Adhesion.....	28
F. Retinoid Signaling During Heart Development.....	33
G. Transforming Growth Factor- β signaling.....	41
H. The Retinoid X Receptor α Knockout Mouse (RXR α -/-).....	46
2. MATERIALS AND METHODS.....	55
3. RESULTS AND DISCUSSION.....	75
A. Expression patterns of VCAM-1 in RXR α -/- hearts at E9.5 and E10.5 are similar to WT.....	75
B. Transmission Electron Microscopy of WT and RXR α -/- hearts at E10.5.....	83
C. VCAM-1 is misexpressed in the epicardium in the RXR α -/- at E11.5.....	86
D. VCAM-1 expression is increased in RXR α -/- hearts at E12.5 and E13.5.....	98
E. Epicardial explants from E13.5 RXR α -/- have a higher level of VCAM-1 than WT.....	114
F. Smad binding and Retinoid responsive elements are located on the VCAM-1 promoter.....	114
G. RXR α and Smad4 will bind to the VCAM-1 promoter.....	117
H. TGF β 2 treatment increases VCAM-1 expression in epicardial explants.....	121
I. TGF β 2 treatment causes VCAM-1 expression in the epicardium and epicardial bubbling.....	126
J. TGF β 2 treatment causes activation of the VCAM-1 promoter.....	129
4. CONCLUSIONS AND FUTURE DIRECTIONS.....	136
REFERENCES.....	152

List of Tables

Page

Table 1: Knockout mice with an epicardial phenotype.....	14
--	----

List of Figures

	<u>Page</u>
Figure 1: Mammalian heart development	4
Figure 2: Illustration of epicardium formation in the E9.5 mouse.....	7
Figure 3: Epicardial phenotype of the integrin $\alpha 4$ knockout mouse.....	16
Figure 4: Epicardial phenotype of the VCAM-1 knockout mouse.....	18
Figure 5: Epicardial phenotype of the N-cadherin conditional knockout mouse.....	21
Figure 6: Epicardial Phenotype of the RXR α ^{-/-} mouse	27
Figure 7: Signaling pathways downstream of VCAM-1 or FN binding to integrin $\alpha 4\beta 1$	31
Figure 8: Retinoid Signaling and cardiovascular phenotypes resulting from knockout of pathway components.....	36
Figure 9: Immunohistochemical (IHC) analysis of RALDH2 expression in the mouse heart from E9.5-E11.5.....	38
Figure 10: TGF β mRNA expression in the mouse heart at E9.5	43
Figure 11: TGF β signaling pathway.....	45
Figure 12: Elevated TGF $\beta 2$ protein and mRNA in heart of the RXR α ^{-/-} mouse	49
Figure 13: Real time PCR analysis of VCAM-1 mRNA in the heart of the RXR α ^{-/-} mouse at E11.5	51
Figure 14: Regulatory elements contained within the mouse VCAM-1 promoter region.....	63
Figure 15: Diagram of the VCAM-1 promoter luciferase plasmid.....	68
Figure 16: VC1889 plasmid restriction digest and VCAM-1 promoter PCR	70
Figure 17: Western blot of luciferase protein following transfection with VC1889	73
Figure 18: IHC analysis of VCAM-1 expression at E9.5 in the WT and RXR α ^{-/-} mouse heart.....	78
Figure 19: IHC analysis of integrin $\alpha 4$ expression at E9.5 and E10.5 in the WT and RXR α ^{-/-} mouse heart.....	80

Figure 20: IHC analysis of VCAM-1 expression at E10.5 in the WT and RXR α ^{-/-} mouse heart.....	82
Figure 21: Immunogold-Transmission electron microscopic analysis of epicardium/myocardium junctions in E10.5 WT and RXR α ^{-/-}	85
Figure 22: IHC analysis of VCAM-1 expression in hearts of E11.5 WT and RXR α ^{-/-} mice.....	88
Figure 23: Real time PCR analysis of VCAM-1 mRNA at E11.5 in hearts of WT and RXR α ^{-/-} mice.....	91
Figure 24: Western blot analysis of VCAM-1 protein at E11.5 in WT and RXR α ^{-/-} hearts.....	93
Figure 25: IHC analysis of integrin α 4 expression at E11.5 and E12.5 in the WT and RXR α ^{-/-} hearts.....	95
Figure 26: Real time PCR analysis of N-cadherin, integrin α 4 and TGF β 2 at E11.5 in the WT and RXR α ^{-/-} heart.....	97
Figure 27: IHC analysis of VCAM-1 expression at E12.5 in the WT and RXR α ^{-/-} heart.....	100
Figure 28: IHC analysis of VCAM-1 expression at E13.5 in the WT and RXR α ^{-/-} heart.....	102
Figure 29: Real time PCR analysis of VCAM-1 mRNA at E12.5 in WT and RXR α ^{-/-} heart.....	104
Figure 30: Real time PCR analysis of VCAM-1 mRNA at E13.5 in WT and RXR α ^{-/-} heart.....	106
Figure 31: Western blot analysis VCAM-1 protein at E12.5 in the WT and RXR α ^{-/-} heart.....	108
Figure 32: Western blot analysis of VCAM-1 protein at E13.5 in the WT and RXR α ^{-/-} heart...	110
Figure 33: Real time PCR analysis of N-cadherin, integrin α 4 and TGF β 2 in WT and RXR α ^{-/-} heart.....	112
Figure 34: IHC analysis of VCAM-1 protein expression in E13.5 RXR α ^{-/-} epicardial explants versus WT.....	116
Figure 35: Chromatin immunoprecipitation analysis showing RXR α and Smad4 bind to the VCAM-1 promoter.....	119
Figure 36: IHC analysis of VCAM-1 expression following TGF β 2 treatment in 12 hour whole embryo culture.....	123
Figure 37: IHC analysis showing that VCAM-1 expression increases and the epicardium detaches following 18 hours of TGF β 2 treatment in whole embryo culture.....	125
Figure 38: TGF β 2 treatment of epicardial explant cultures results in increased VCAM-1 expression in epicardial.....	128

Figure 39: TGF β 2 treatment of cells transfected with the VC1889 luciferase expression plasmid increases VCAM-1-driven luciferase expression	132
Figure 40: Concentration-response study of cells transfected with VC1889 luciferase expression plasmid and treated with varying TGF β 2 concentrations	134
Figure 41: Diagrammatic representation of the current working hypothesis.....	149

Abbreviations

9-cisRA, 9-cis retinoic acid

aPKC, Atypical protein kinase C

ATP- Adenosine tri-phosphate

atRA- all-trans retinoic acid

BMP, Bone morphogenetic protein

BSA, Bovine serum albumin

cDNA, Complementary deoxyribonucleic acid

CHD, Congenital heart disease

ChIP, Chromatin immunoprecipitation

CKO, Conditional knockout

CMV, Cytomegalovirus

Ct, Cycle threshold

Cx43, Connexin 43

Cyp26, Cytochrome P450 26

DMEM, Dulbecco's modified eagle medium

DMSO, Dimethyl sulfoxide

E, Embryonic day

ECM, Extracellular matrix

EDTA, Ethylenediaminetetraacetic acid

EMT, Epithelial to mesenchymal transformation

EPDCs, Epicardially-derived cells

EPO, Erythropoietin

Erk, Extracellular receptor kinase

FAK, Focal adhesion kinase

FGF2, Fibroblast growth factor 2

FN, Fibronectin

FOG2, Friend of GATA 2

Foxc, Forkhead box C protein

GAPDH, Glyceraldehyde 3-phosphate dehydrogenase

H&E, Hemotoxylin and Eosin

HRP, Horseradish peroxidase

ICRS, Immediately centrifuged rat serum

m-MLV, Moloney murine leukemia virus reverse transcriptase

NADH, Nicotinamide adenine dinucleotide (reduced form)

OFT, Outflow tract

PAR, Partitioning defective protein

PBS, Phosphate buffered saline

PE, Proepicardium

PI3K, Phosphatidylinositol 3-kinase

PMSF, Phenylmethanesulfonyl fluoride

PPAR, Peroxisome proliferator-activated receptor

PVDF, Polyvinylidene fluoride

RALDH2, Retinaldehyde dehydrogenase 2

RAR, Retinoic acid receptor

RARE, Retinoic acid responsive element

RBP, Retinol binding protein

REC, Rat epicardial cells

RGD, Arginine-Glycine-Aspartate

RT, Room temperature

RT PCR, Real time polymerase chain reaction

RXR α , Retinoic X receptor alpha

SBE, Smad binding element

STRA6, retinol binding protein receptor

TBST, Tris-buffered saline containing Tween20

TEM, Transmission electron microscopy

TESS, Transcription element search system

TGF β , Transforming growth factor beta

VAD, Vitamin A deficiency

VCAM-1, Vascular cell adhesion molecule 1

WEC, Whole embryo culture

WT1, Wilms' tumor 1 transcription factor

Abstract

M. ELIZABETH G. BURTON. Regulation of VCAM-1 expression by TGF β 2 during formation of the epicardium. (Under the direction of STEVEN W. KUBALAK, Ph.D.)

The normal formation of the epicardium, the outer cell layer of the heart, is critical for subsequent development of the heart to proceed normally. Abnormalities in the epicardium lead to cardiac defects as shown in mice deficient in retinoid X receptor α (RXR α -/-), a model of congenital heart disease that exhibits many cardiac malformations including epicardial defects. The RXR α -/- epicardium is slower to form and once formed, it detaches from the myocardium. Previously an elevation of transforming growth factor β 2 (TGF β 2) has been observed in RXR α -/- hearts at midgestation and an alteration in vascular cell adhesion molecule 1 (VCAM-1) was found at E11.5. Based on these findings it was hypothesized that proper expression of VCAM-1 is essential for normal cardiac morphogenesis and is regulated by TGF β 2 and/or retinoid signaling. VCAM-1 is a transmembrane protein known to be involved in epicardial cell adhesion and has been reported to inhibit epithelial to mesenchymal transformation (EMT) of epicardial cells. In this study the expression of VCAM-1 was analyzed from E9.5-E13.5 in the wild type (WT) and RXR α -/- mice using real time quantitative PCR, immunohistochemistry and western blotting. At E11.5, VCAM-1 protein expression levels were similar to WT in the RXR α -/- mouse, but later (E12.5 and E13.5) misexpression of VCAM-1 was found in the epicardium of RXR α -/- mice. Specifically, VCAM-1 mRNA and protein were increased in the myocardium of the RXR α -/- heart compared to the WT at E12.5 and E13.5. Elevation of VCAM-1 protein was also found in E13.5 epicardial explants from RXR α -/- embryos. To investigate possible involvement of TGF β 2 in VCAM-1 regulation, E11.5 epicardial explants were treated with TGF β 2 and the treatment was found to promote upregulation of VCAM-1 in the epicardial cells. Treatment of embryos in whole embryo culture with TGF β 2 resulted in elevation of VCAM-1 and also caused

epicardial detachment after 18 hours of treatment. $RXR\alpha$ and Smad4 were shown to bind to the mouse VCAM-1 promoter using ChIP analysis and the VCAM-1 promoter can be activated by $TGF\beta 2$ treatment (shown through use of a luciferase expression plasmid containing the VCAM-1 promoter). Together the findings show that VCAM-1 is elevated in the hearts of $RXR\alpha^{-/-}$ mice and $TGF\beta 2$ can regulate VCAM-1 expression in the embryonic heart, particularly in the epicardium. Elevated $TGF\beta 2$ in the heart, such as that observed in the $RXR\alpha^{-/-}$ mouse, can cause upregulation of VCAM-1 in the myocardium and epicardium. Upregulation of VCAM-1 could decrease epicardial EMT, which is also observed in the $RXR\alpha$. From our study we show that proper expression (levels and location) of VCAM-1 is essential for normal heart development and that misexpression of VCAM-1 can negatively affect formation of the heart.

Chapter 1: Review of Literature

A. Congenital Heart Disease

Congenital heart defects (CHDs) are the most common birth defect, affecting approximately 1% of all live births. Presently, treatment of CHDs is limited to surgical and pharmaceutical intervention. Major CHDs are usually seen during the neonate period while some minor CHDs may not be found until adulthood making the prevalence of CHD likely much higher than reported. Currently there are few options to reduce the occurrence of CHD. Taking prenatal vitamins has been shown to reduce the occurrence as well as avoiding environmental exposure to risky medications, chemicals and certain illnesses (Jenkins et al., 2007). Even with these precautions, CHDs are quite prevalent so other interventions are necessary to prevent their occurrence.

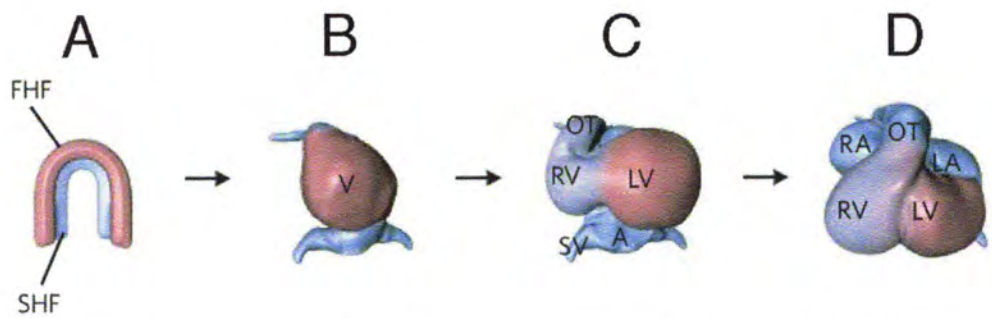
Retinoid signaling is known to play a role in the development of the heart with too much or too little signaling resulting in heart defects. The effects of retinoid signaling on the developing heart have been shown in models such as that of the vitamin A deficiency (VAD) rat (Wilson and Warkany, 1949) and human birth defects that result from exposure to the drug Accutane (isotretinoin- Roche), a retinoid receptor ligand (de la Cruz et al., 1984). The retinoic acid synthesizing enzyme retinaldehyde dehydrogenase 2 (RALDH2) is expressed in the epicardium of the heart indicating that retinoid signaling is important within the epicardium. In the mouse, loss of the retinoid X receptor alpha ($RXR\alpha$) results in embryos displaying defects in all regions of the developing heart. Specifically, the $RXR\alpha^{-/-}$ embryo displays hypoplastic endocardial cushions, thinning of the ventricular myocardium and detachment of the epicardium.

Dysfunction of the epicardium could cause common congenital abnormalities that are seen throughout the heart in the human population including coronary artery anomalies, septal and valve defects. Currently there are no reported epicardial-specific defects (loss of epicardium or bubbling of the epicardium) in the human congenital heart defect population. There are, however, rare reports of congenital absence of the pericardium (structure derived from the epicardium) (Abbas et al., 2005).

B. Cardiac Morphogenesis

The heart is derived from cardiac progenitor cells that are found in the epiblast of the developing embryo (Martinsen, 2005). These cardiac progenitor cells form the bilateral primary heart field and the secondary heart field (Buckingham et al., 2005; Cohen-Gould and Mikawa, 1996; Garcia-Martinez and Schoenwolf, 1993; Martinsen, 2005). The primary heart field is located on either side of the primitive streak forming two separate but paired regions (the cardiac crescent) (Dyer and Kirby, 2009; Martinsen, 2005) (Figure 1-A). The two sides of the cardiac crescent will form endocardial heart tubes and migrate to the midline to form the primary heart tube, which will begin to beat (Martinsen, 2005) (Figure 1-B). The primary heart tube consists of an inner layer of epithelial endoderm, an outer layer of myocardium with an extracellular matrix (ECM)-rich cardiac jelly between the two layers (Markwald et al., 1977; Smith and Bader, 2007). The secondary heart field is located anterior and dorsal to the primary heart tube and will form the right ventricle, outflow tract and venous poles (Buckingham et al., 2005; Kelly et al., 2001; Mjaatvedt et al., 2001; Srivastava, 2006; Verzi et al., 2005; Waldo et al., 2001; Zaffran et al., 2004) (Figure 1-A). After the primary heart tube is completely fused, it will rightwardly loop to form the atria, atrioventricular junction and left ventricle (Manner, 2000; Snarr et al., 2008; Srivastava, 2006) (Figure 1-C). Once looping is complete, the chambers of the heart will begin to remodel and septate to form the four-chambered

Figure 1: Heart Development. The heart initially forms as a cardiac crescent around Day 15 of human development (E7.5 of mouse development) and consists of the first (primary) heart field (red) and the second heart field (blue) (A). The crescent will fuse the midline of the embryo to form the heart tube around Day 20 of human development (E8 of mouse development) (B). The heart will then loop rightward around Day 28 of human development and E9 of mouse development (C). Starting at Day 32 (mouse E10), the heart will further remodel to form the mature four chambered heart (D). FHF, first (primary) heart field; SHF, second heart field; RV, right ventricle; LV, left ventricle; RA, right atrium; LA, left atrium; V, ventricle; OT, outflow tract. Adapted from: (Bruneau, 2008)

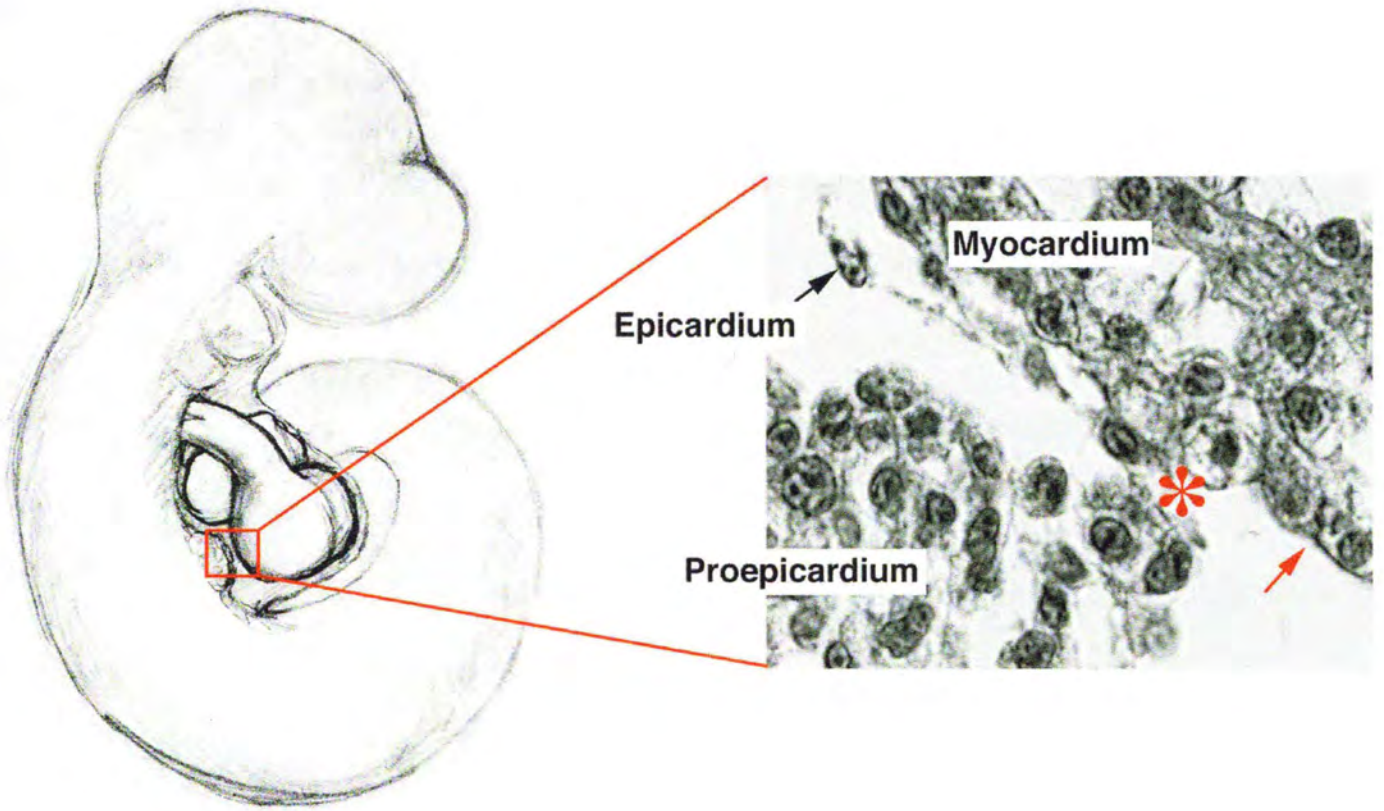


	A	B	C	D
Stage:	Cardiac crescent	Linear heart tube	Looping heart	Chamber formation
Mouse embryo day:	E7.5	E8	E9	E10
Human embryo day:	Day 15	Day 20	Day 28	Day 32
Milestones:	<ul style="list-style-type: none"> • Cardiac differentiation • Migration to midline 	<ul style="list-style-type: none"> • Heart tube formation • First heartbeat • Anterior-posterior and dorsal-ventral patterning 	<ul style="list-style-type: none"> • Early chamber formation • Looping to the right 	<ul style="list-style-type: none"> • Chamber formation • Trabeculation • Cushion formation • Outflow tract septation • Early conduction-system formation

heart (Figure 1-D). The complete four-chambered heart is made up of the primary heart field and the secondary heart field as well as from contributions from neural crest cells and epicardially-derived cells. The primary heart field contributes to the atria, atrioventricular junction and the left ventricle (Buckingham et al., 2005). The second heart field will form the outflow tract, right ventricle and parts of the venous pole (Buckingham et al., 2005).

During looping, some of the endocardial cells overlying the cardiac jelly will delaminate, migrate into the cardiac jelly and eventually form the endocardial cushions (Markwald et al., 1977; Potts et al., 1991). The endocardial cushions appear as localized swellings of the cardiac jelly in the atrioventricular junction and the outflow tract and contain extracellular matrix molecules and eventually mesenchymal cells of varying origins (Schroeder et al., 2003; Snarr et al., 2008). Part of the ventricular septum, the outflow tract septum and the valves are, in part, derived from the endocardial cushions (Eisenberg and Markwald, 1995). Neural crest cells will migrate into the developing heart and contribute to the development of the outflow tract septum, semilunar valves, the great arteries and sympathetic innervation of the heart (Hildreth et al., 2008; Hutson and Kirby, 2007; Nakamura et al., 2006; Verberne et al., 1998). The epicardium will form from cells derived from the proepicardium and cover the myocardium (Viragh and Challice, 1981) (Figure 2). Some cells from the epicardium will undergo epithelial to mesenchymal transformation (EMT) to contribute to various processes and structures in the heart including the maturation and development of the myocardium, seeding of the endocardial cushions and become endothelial and smooth muscle cells of the coronary vasculature (Dettman et al., 1998; Manner, 1999; Mikawa and Fischman, 1992; Perez-Pomares et al., 2002; Perez-Pomares et al., 1998).

Figure 2: Illustration of epicardium formation in the E9.5 mouse. The inset shows the relationship between the proepicardium and the myocardium during the early stages of epicardium formation. The asterisk indicates an area where proepicardial cells are directly interacting with the myocardium. The black arrow indicates an area of myocardium that is covered by newly formed epicardium. The red arrow indicates an area of bare myocardium.



C. Formation of the epicardium

The epicardium is an important structure in the heart because it contributes cells and signals to aid in the formation of many structures in the developing heart. Loss of the epicardium or proper epicardium function results in various heart defects including defective development of coronary vasculature and abnormal ventricular chamber development. The epicardium, the epithelial covering of the myocardium, is derived from a cell population referred to as the proepicardium (PE) (Manasek, 1969; Viragh and Challice, 1981) (Figure 2). The PE is a cluster of cells of mesenchymal and epithelial origin contained within an extracellular matrix (ECM) (Viragh and Challice, 1981). It is located on the septum transversum above the liver primordium and will form from the pericardial coelomic mesothelium (Manner, 1992; Schulte et al., 2007; Tomanek, 2005; Viragh and Challice, 1981) (Figure 2). The PE contains precursors for endothelial, smooth muscle and connective tissue cells (Mikawa and Gourdie, 1996).

During the transition from PE to epicardium, which occurs between embryonic day (E) 9.0 and E10.0 (looping of the heart) in the mouse, cells from the PE will delaminate and form vesicular-like buds (Manner et al., 2001; Mikawa and Gourdie, 1996; Viragh and Challice, 1981; Viragh et al., 1993) (Figure 2). These buds will migrate to the myocardium where they will attach and move across the surface of the myocardium, proliferate and form the epicardium (Komiyama et al., 1987; Viragh and Challice, 1981) (Figure 2). The extracellular matrix within the proepicardial buds will become part of the subepicardial space, which contains fibronectin, collagens I, IV, V and VI (Bouchey et al., 1996; Hurle et al., 1994; Kalman et al., 1995; Kim et al., 1999; Tidball, 1992), proteoglycans, laminin (Kalman et al., 1995) vitronectin, fibrillin-2 and elastin (Bouchey et al., 1996). These ECM proteins play roles in epicardium attachment, coronary vasculogenesis and possibly other roles such as signaling to the myocardium from the epicardium. Mesenchymal cells, derived from the proepicardial buds or from

the newly formed epicardium, will also occupy the subepicardial space and form epicardially-derived cells (EPDCs) (Dettman et al., 1998; Munoz-Chapuli and Hamlett, 1996; Munoz-Chapuli et al., 1994; Perez-Pomares et al., 1997, 1998; Van den Eijnde et al., 1995; Viragh et al., 1993).

The PE cells can reach the myocardium in one of two ways depending on species. In the mouse and other mammals, the PE buds will free-float through the pericardial space to the myocardium; however there is also some direct migration that will occur (Komiyama et al., 1987; Kuhn and Liebherr, 1988; Munoz-Chapuli et al., 1994). In the chick there is evidence that the PE buds migrate to the myocardium via an extracellular matrix bridge made up of fibronectin, glycoproteins and collagens (Manner et al., 2001; Nahirney et al., 2003). It has been hypothesized that mice also have this extracellular matrix bridge but this has not been shown. A recent report in mouse suggests that the PE will form microvilli that will protrude and attach to the myocardium as the main method by which PE cells reach the myocardium but that some PE budding does occur (Rodgers et al., 2008).

Epicardial cells will undergo EMT to form EPDCs that will contribute to interstitial fibroblasts, seeding of the endocardial cushions, fibroblasts of the endocardial cushions and smooth muscle cells and endothelial cells of the coronary vasculature (Dettman et al., 1998; Gittenberger-de Groot et al., 1998; Manner, 1999, 2000; Mikawa and Fischman, 1992; Mikawa and Gourdie, 1996; Perez-Pomares et al., 1997; Vrancken Peeters et al., 1999). The epicardium normally expresses RALDH2, a retinoic acid synthesizing enzyme (Duester, 2000) and Wilms' tumor 1 transcription factor (Wt1) (Little et al., 1999). As EPDCs develop into smooth muscle and endothelial cells of the coronary vasculature, RALDH2 and Wt1 will be downregulated within the cells (Perez-Pomares et al., 2002). Wt1 has previously been implicated in epicardium development with loss of Wt1 causing a failure of epicardium formation (Moore et al., 1999).

Two recent Cre-models have suggested that EPDCs will also become myocytes in the ventricular myocardium and interventricular septum (Cai et al., 2008; Zhou et al., 2008a; Zhou et al., 2008b). A $Wt1^{GFPcre/+}$ mouse was used to trace the fate of $Wt1+$ epicardial cells throughout the heart (Zhou et al., 2008a). Some of these $Wt1+$ cells differentiated into functional cardiomyocytes that were found in all four chambers of the heart as well as in the interventricular septum (Zhou et al., 2008a). These $Wt1-$ expressing cardiomyocytes also expressed GATA4 and $Nkx2-5$ (Zhou et al., 2008a). $Wt1+$ PE cells were found to arise from $Nkx2-5$ and $Isl1$ ($Isl1$)-expressing progenitor cells, indicating that PE/epicardial cells may share a developmental origin from cardiogenic progenitor cells (Chien et al., 2008; Laugwitz et al., 2008; Martin-Puig et al., 2008; Zhou et al., 2008a). A $Tbx18$ -cre has also been used to label epicardial cells and trace EPDCs in the developing heart (Cai et al., 2008). Cai et al found that $Tbx18+$ epicardial cells went to the interventricular septum and the ventricular myocardium where they became cardiomyocytes that were $Nkx2-5+$ (Cai et al., 2008). These data (Cai et al., 2008) support the findings of Zhou et al. However, there has been some debate from another group who suggests that $Tbx18$ is normally expressed in the interventricular septum and myocardium and is found in a mouse model with absent epicardium and therefore cannot be used as a marker of epicardially-derived cardiomyocytes (Christoffels et al., 2009). Further evidence supports the theory that PE/epicardial cells are derived from the same cardiogenic progenitor pool as cardiomyocytes in work from van Wijk et al. This group found through Dil tracing that PE/epicardial cells come from the same precursor pool as the inflow myocardium and that this separation of PE/epicardium from myocardium required a balance of BMP and FGF signaling (van Wijk et al., 2009). FGF2 was found to enhance epicardium formation while BMP stimulation enhanced myocardium formation (van Wijk et al., 2009). These

recent studies of EPDC cells fate suggest a new role for EPDCs as a cardiomyocyte progenitor cell population.

Cell-cell as well as cell-matrix interactions are necessary for proper epicardial EMT. For example, connexin-43, vascular cell adhesion molecule (VCAM-1) and integrin $\alpha 4$ have been previously noted to be required for epicardial EMT (Kwee et al., 1995; Li et al., 2002; Rhee et al., 2009; Yang et al., 1995). Loss of Cx43, a gap junctional protein, in the mouse results in embryos with decreased epicardial EMT as well as bubbling of the epicardium (Rhee et al., 2009). Loss of VCAM-1 or integrin $\alpha 4$ in the mouse results in embryos that have no epicardium, thus, form no EPDCs (Kwee et al., 1995; Yang et al., 1995). Erythropoietin (EPO) and retinoic acid are produced by the epicardium and are thought to signal for secretion of trophic signals that aid in myocardium development (Chen et al., 2002; Perez-Pomares et al., 2002; Stuckmann et al., 2003). EPO knockout mice have been previously reported to have a detached epicardium similar to the $RXR\alpha^{-/-}$ mouse (Wu et al., 1999). Failure to properly signal to the myocardium from the epicardium can affect myocardium development as both the EPO knockout and $RXR\alpha^{-/-}$ have hypoplastic ventricles indicating the importance of proper epicardium function. It may be that detachment of the epicardium impairs proper functioning of the epicardium. Currently, the mechanism by which the epicardium can become detached and the role this detachment plays in epicardial signaling and EMT is not fully known.

D. Mouse models of aberrant epicardium formation

Since defects in the epicardium lead to various abnormalities in the heart including hypoplastic ventricular myocardium and coronary vasculature anomalies, animal models that perturb proteins and molecules important for epicardium

development result in many of these phenotypes. A list of these mouse models is found in Table 1. Integrin $\alpha 4$ is a cell surface receptor that is involved in cell-cell and cell-matrix interactions (Hynes, 1992) and is expressed in the epicardium. Knockout of integrin $\alpha 4$ results in two possible phenotypes. The first phenotype is failure of allantois fusion early in development affecting extraembryonic circulation leading to embryonic lethality by E11 (Pinco et al., 2001; Yang et al., 1995). Other embryos fail to form an epicardium and have hypoplastic ventricular myocardium and missing coronary vasculature resulting in embryonic lethality by E14.5 (Pinco et al., 2001; Yang et al., 1995) (Figure 3). Integrin $\alpha 4$ promotes migration of proepicardial cells over the surface of the myocardium through its interaction with VCAM-1 on the surface of the myocardium. Proepicardial cells come into contact with the myocardium but will not migrate over the surface of the heart in the absence of integrin $\alpha 4$ in $\alpha 4$ -knockin-lacZ mice (Sengbusch et al., 2002). In the absence of integrin $\alpha 4$ in this mouse model, there is also decreased proepicardial cell budding, indicating a role for integrin $\alpha 4$ in proepicardial cell bud formation to initiate migration over the myocardium (Sengbusch et al., 2002). Integrin $\alpha 4$ will interact with fibronectin during proepicardial cell budding and with fibronectin and/or VCAM-1 during proepicardial cell migration over the myocardial surface to aid in formation of the epicardium (Sengbusch et al., 2002). Loss of the ability of PE cells to bind to the myocardium via an interaction between integrin $\alpha 4$ and VCAM-1 can result in failure to form an epicardium.

VCAM-1 is a cell surface protein and a ligand for integrin $\alpha 4$ that is involved in inflammatory processes and development (Kwee et al., 1995) and is expressed within the myocardium. VCAM-1 knockout mice (VCAM-1^{-/-}) are embryonic lethal and die between E10.5 and E12.5 with two different phenotypes (Kwee et al., 1995). One group of embryos did not develop extraembryonic circulation while the other group of embryos

Table 1: Knockout mice displaying an epicardial phenotype.

KO mice with Epicardium Detachment	KO mice with Epicardial Defects
RXR α	VCAM-1
Epicardial-specific ALK5	Integrin α 4
Cx43	Wt1
N-cadherin Wnt-1 Cre conditional KO	GATA4
EPO/EPO receptor	PAR3
Podoplanin	
Foxc1/c2	

Figure 3: Epicardial phenotype of the integrin $\alpha 4$ knockout mouse. A histological analysis of the integrin $\alpha 4$ knockout from E10.5 to E12.5. WT at E12.5 (A,C) has an epicardium present. KO at E12.5 (B,D) has no epicardium present. KO at E10.5 (E) has an epicardium present but is lost by E11.5 (F). The WT forms coronary vessels (G) while the KO has none present (H). A, atrium; EC, endocardial cushions; B, blood cells; Cv, coronary vessel; Ep, epicardium; M, myocardium; O, outflow tract; V, ventricle (Taken from Yang et al, 1995)

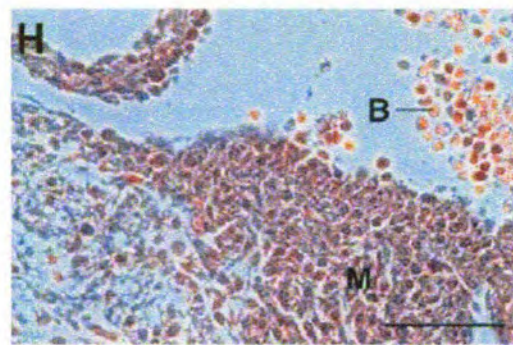
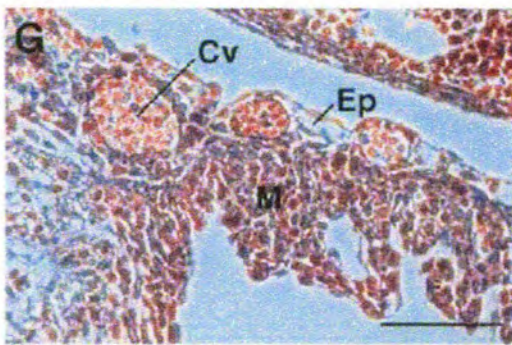
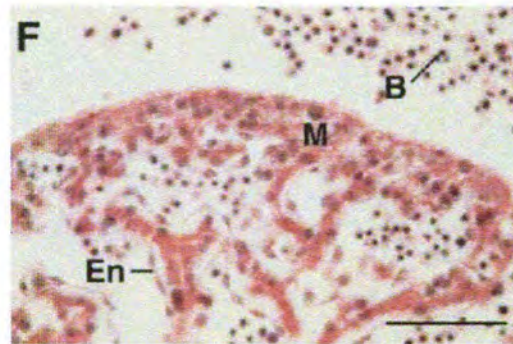
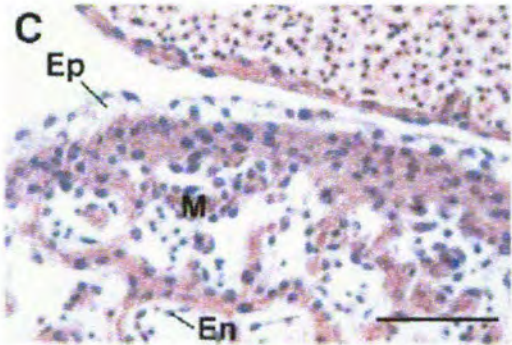
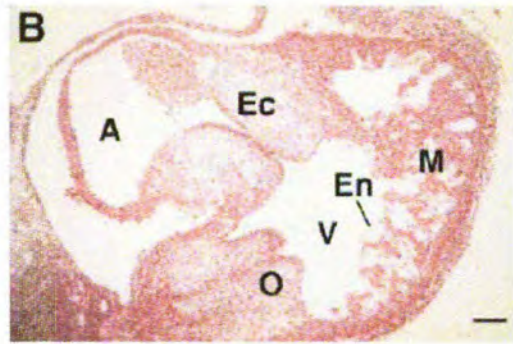
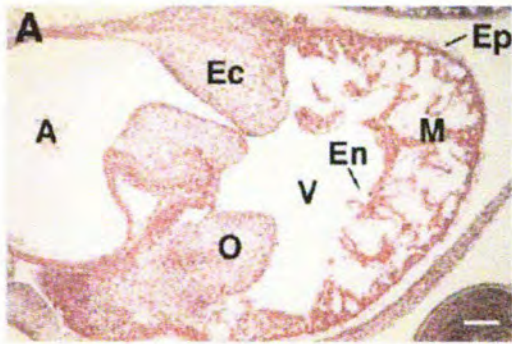
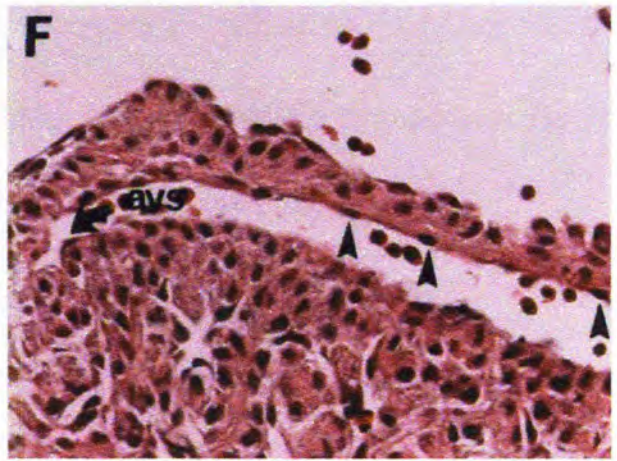
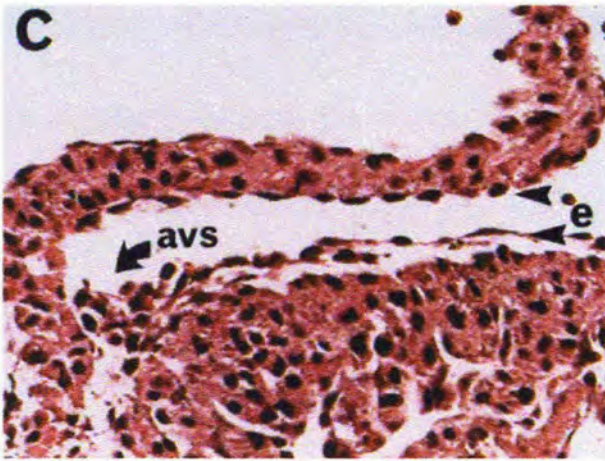
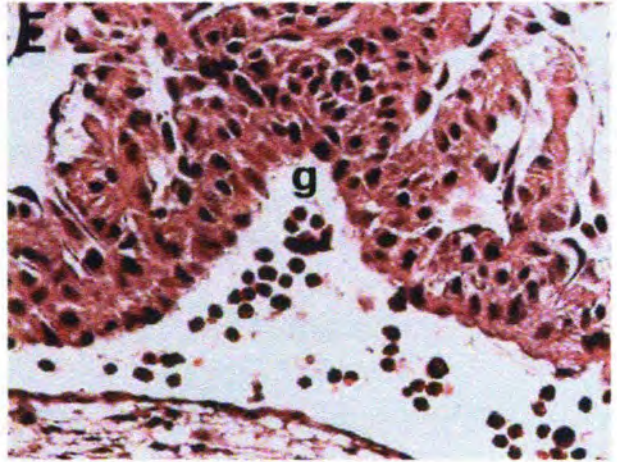
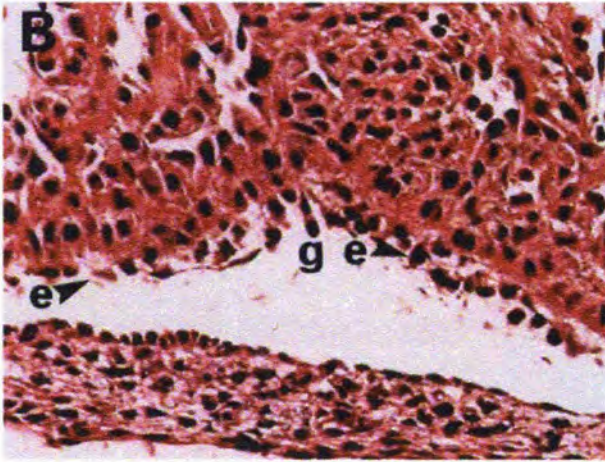
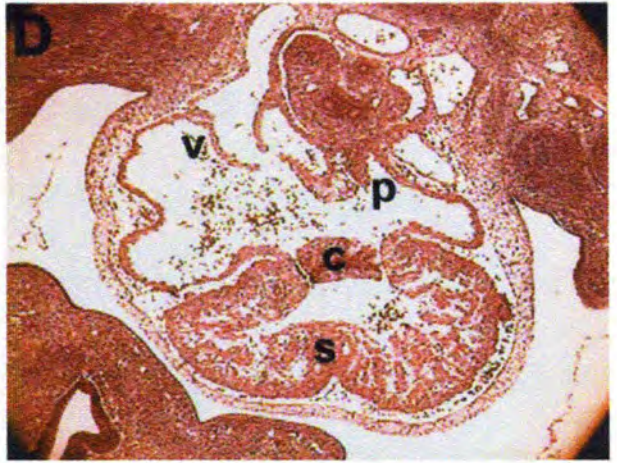
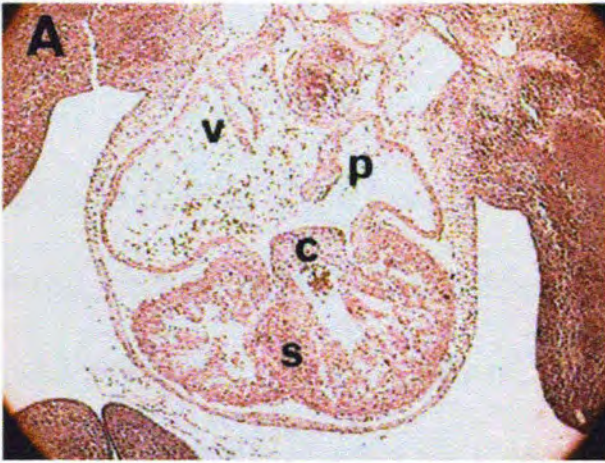


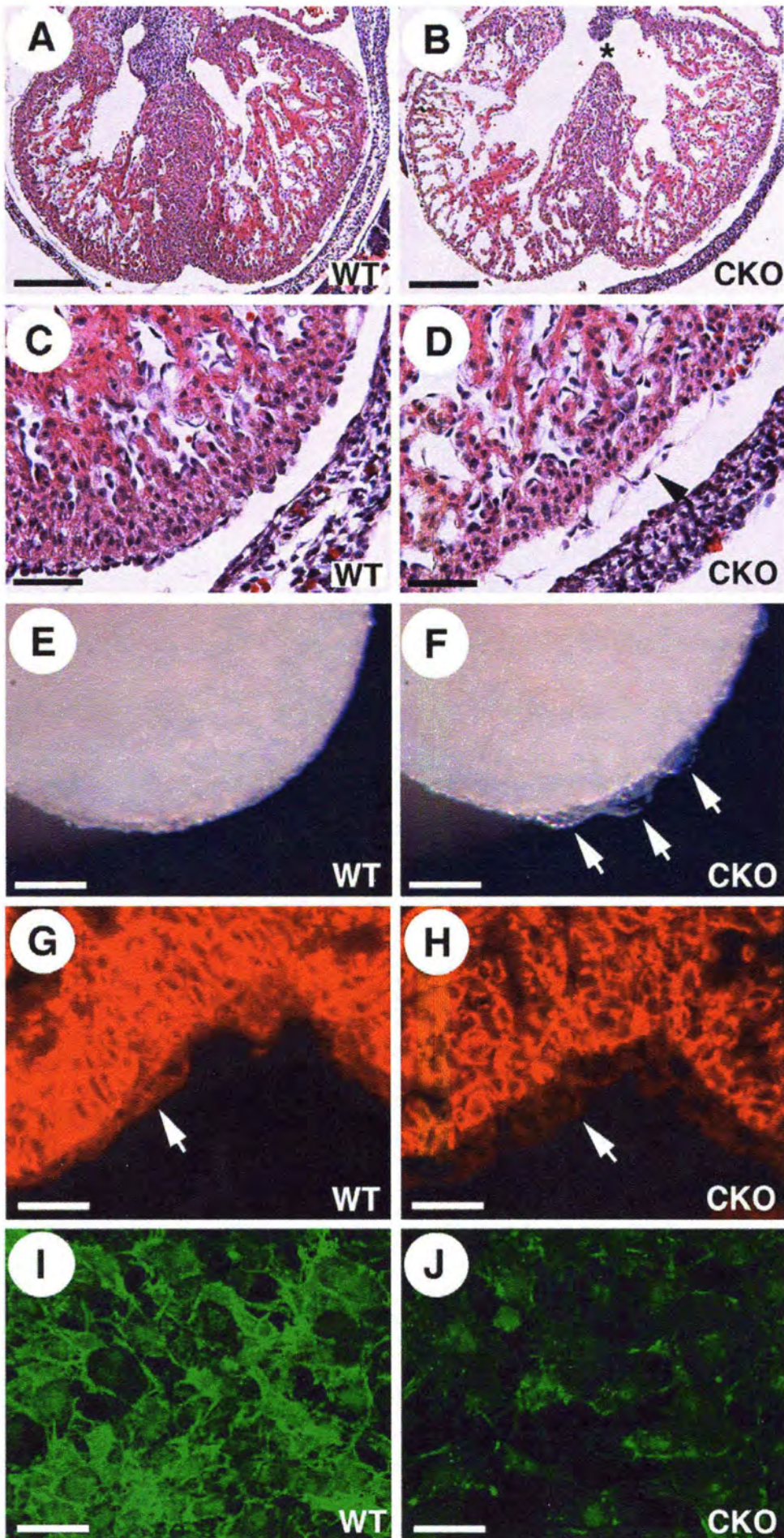
Figure 4: Epicardial phenotype of the VCAM-1 knockout mouse. The WT mouse at E11.5 (A-C) forms an epicardium (indicated by arrowheads). The KO mouse fails to form an epicardium by E11.5 (D-F). (Taken from Kwee et al, 1995)



showed various heart defects including loss of epicardium, hypoplastic ventricular myocardium and abnormal coronary vasculature (Kwee et al., 1995) (Figure 4). In the absence of VCAM-1, there is also a loss of integrin $\alpha 4$ expression in the epicardium but not in the endocardial cushions (Kwee et al., 1995). VCAM-1^{-/-} mice fail to form an epicardium by E11.5, however, a small number of epicardial cells can be seen on the atria (Kwee et al., 1995). The failure of the epicardium to form could be due to the inability of the PE buds to attach to the surface of the myocardium in the absence of VCAM-1. As seen with other models of aberrant epicardial development, there is a reduction in myocardial wall thickness and a decrease in ventricular compaction (Kwee et al., 1995) (Figure 4). The phenotype of VCAM-1^{-/-} is similar to that of integrin $\alpha 4$ ^{-/-}, which could be expected considering the two proteins are binding partners and likely involved in the same developmental processes during heart formation. VCAM-1 is expressed in the myocardium while integrin $\alpha 4$ is expressed in the epicardium, suggesting a role for each in adhesion between the epicardium and myocardium (Kwee et al., 1995; Yang et al., 1995). Alterations in the levels of either VCAM-1 or integrin $\alpha 4$ could have adverse effects on intercellular binding between these proteins potentially due to changes in the stoichiometry of these transmembrane proteins.

N-cadherin has been implicated in proper epicardial attachment. Conditional knockout (CKO) of N-cadherin specifically in the neural crest cells caused an epicardial bubbling phenotype similar to that of the RXR α ^{-/-} mouse (Luo et al., 2006) (Figure 5). It was found that Wnt1-Cre used for the conditional knockout is also active in epicardial cells resulting in decreased N-cadherin in the epicardium as well (Luo et al., 2006). In these mice, the epicardium itself remains intact but is detached from the underlying myocardium. N-cadherin is normally expressed in both the myocardium and epicardium

Figure 5: Epicardial phenotype of the N-cadherin conditional knockout mouse. The WT mouse forms a normal attached epicardium seen in H&E stained sections (A,C) and whole mount (E). The CKO mouse forms a detached epicardium seen in H&E stained sections (B,D) and whole mount (F- arrow indicates detached epicardium). Immunofluorescence for N-cadherin shows it present in the epicardium of the WT (arrow in G) and absent in the CKO (arrow in H). Epicardial explants showed N-cadherin present in the WT (I) and present at low levels in the CKO (J). (Taken from Luo et al, 2006)



and is involved in adhesion of the epicardium to the myocardium via formation of adherens junctions (Luo et al., 2006). In addition to the detached epicardium, there is also thinning of the ventricular myocardium similar to what is seen in other mice that have epicardial defects (Figure 5).

Another mouse model that fails to form an epicardium is the Wilm's Tumor 1 (Wt1) knockout mouse. Wt1 is a zinc finger transcription factor that targets genes such as those responsive to retinoic acid receptors and integrin $\alpha 4$ signaling (Kirschner et al., 2006; Little et al., 1999). Wt1 knockout mice have no epicardium, hypoplastic ventricular myocardium and improper formation of the coronary vasculature (Moore et al., 1999). This is similar to the integrin $\alpha 4$ knockout mouse so it is possible that decreased transcription of integrin $\alpha 4$ due to loss of Wt1 contributes to the phenotype of Wt1 knockout mice further pointing to the importance of integrin $\alpha 4$ and its interactions in normal epicardium formation. Embryos with an epicardial-specific knockout of Wt1 die between E16.5 and E18.5 as a result of cardiovascular failure (Martinez-Estrada et al., 2010). These embryos fail to form coronary vasculature and had an upregulation of E-cadherin and cytokeratin (indicative of epithelial phenotype) and a reduction in the mesenchymal cell markers Snail and vimentin expression, indicating a reduction of epicardial EMT (Martinez-Estrada et al., 2010). Using immortalized epicardial cells with a tamoxifen-inducible Wt1 knockout, it was found that loss of Wt1 increased E-cadherin expression, downregulated N-cadherin and decreased cell migration (Martinez-Estrada et al., 2010), indicating the importance of Wt1 in epicardial EMT.

Podoplanin is a mucin-like transmembrane glycoprotein that has been found to downregulate E-cadherin in human oral and mouse skin carcinomas leading to an upregulation of EMT (Mahtab et al., 2008; Martin-Villar et al., 2005). Loss of podoplanin produces embryos that have hypoplastic and perforated ventricular and septal

myocardium, hypoplastic atrioventricular cushions, epicardial detachment, incomplete epicardium formation and impaired coronary vasculature formation (Mahtab et al., 2008). A reduction in epicardial EMT was also found as a result of upregulation of E-cadherin (Mahtab et al., 2008), indicating the importance of the appropriate ratio of cell adhesion molecules to epicardial EMT.

GATA4 is a zinc finger transcription factor that interacts with other proteins important for heart development including Nkx2.5 (Watt et al., 2004). GATA4 knockout mice have no proepicardium and as a result lack an epicardium and have hypoplastic ventricular myocardium, disrupted looping and disrupted septation (Watt et al., 2004), suggesting a role for GATA4 more in development of the PE. Friend of GATA 2 (FOG2) is a cofactor for GATA transcription factors (Tomanek, 2005). FOG2 knockout mice have abnormal epicardial EMT resulting in hypoplastic ventricular myocardium, common atrioventricular canal and absence of coronary arteries (Tevosian et al., 2000), suggesting a role for FOG2 in transcription of genes involved in epicardial EMT.

Foxc1 and Foxc2 are forkhead/Box transcription factors that play a role in the development of the heart, especially in the formation of the outflow tract (Seo and Kume, 2006). Combination Foxc1 heterozygote and c2 knockout mice have improper formation and function of the epicardium including detachment from the myocardium, accelerated EMT, failure of outflow tract septation, hypoplasia of the outflow tract, defects in endocardial cushions and a thin myocardium (Seo and Kume, 2006). The phenotype of the Foxc1^{+/-}/c2^{-/-} mouse is quite similar to the RXR α ^{-/-} mouse with the exception of the accelerated EMT. Transforming growth factor β -2 (TGF β 2) signaling has previously been shown to be required for expression of Foxc1 in the eye during development (Ittner et al., 2005). Foxc1 has also been shown to be a TGF β 1 responsive gene and can be upregulated by TGF β 1 in several cancers (Zhou et al., 2002). Foxc2 has been shown

previously to interact with Smads to promote EMT (Fuxe et al., 2010). Since both Foxc1 and Foxc2 have been implicated in EMT, it is possible that these two transcription factors could play a role in EMT in the epicardium, possibly with TGF β 2.

PAR3 is a protein that complexes with PAR6 and atypical protein kinase C (aPKC) to establish epithelial cell polarity and has been shown to be important for epithelial cyst/bud formation (Hirose et al., 2006; Hurd et al., 2003; Joberty et al., 2000). PE cells express both integrin α 4 and GATA4 but fail to form buds to migrate to the myocardial surface, thereby failing to form an epicardium by E11.5 (Hirose et al., 2006). There were no integrin α 4-positive cells on the surface of the myocardium (indicating that no epicardial cells were present) but there was no effect on the expression of VCAM-1 in the myocardium (Hirose et al., 2006). PAR3 is important for the formation of epithelial cell junctions with loss of proper cell junctions leading to a loss of PE bud formation (Hirose et al., 2006). These results point to the importance of cell adhesion to the formation of the epicardium.

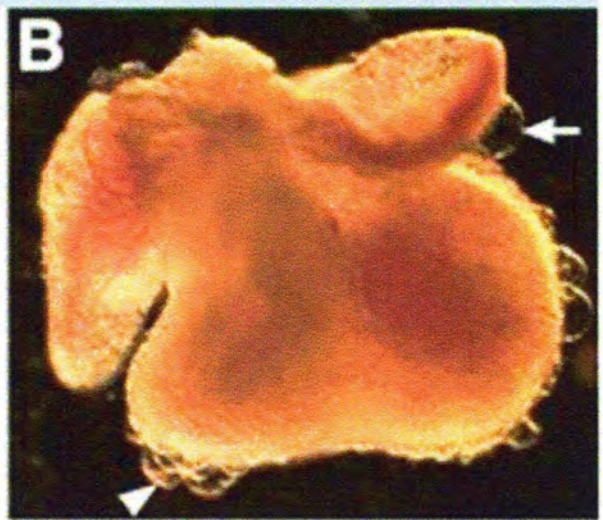
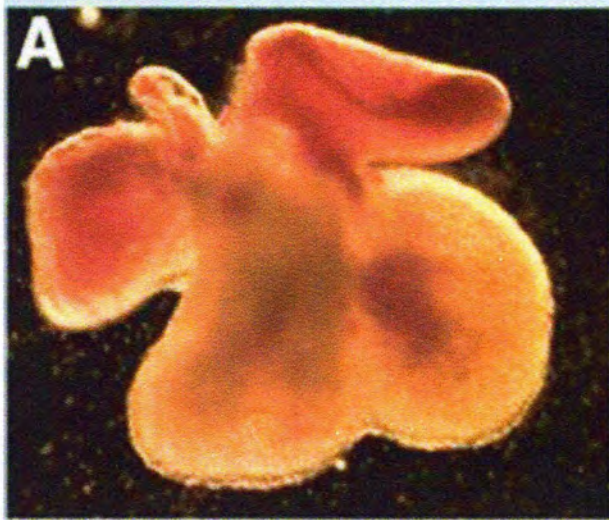
Erythropoietin (EPO) is a growth factor that is involved in various processes in the body such as endothelial cell proliferation and erythrocyte production and in heart development (Anagnostou et al., 1990; Krantz, 1991). EPO and EPO receptor knockout embryos have a detached epicardium, vascular abnormalities and a reduction in proliferating myocytes and will die from cardiac dysfunction and anemia by E13.5 (Wu et al., 1999). EPO has been shown to be a trophic factor for cardiomyocyte proliferation following its secretion from the epicardium (Stuckmann et al., 2003). EPO could play a role in regulating cell adhesion molecules since its phenotype is similar to both RXR α -/- (Jenkins et al., 2005) and N-cadherin-/- (Luo et al., 2006) mice but this is currently unknown. It has been noted previously that EPO levels are reduced in the RXR α -/- mouse and that the EPO gene is a direct target of retinoid signaling (Makita et al., 2005)

suggesting a link between $RXR\alpha^{-/-}$ phenotype and the EPO knockout phenotype. Early fetal hypoxia can cause epicardial detachment and thinning of the ventricular myocardium (Ream et al., 2008). One hypoxia induced target gene is EPO (Ream et al., 2008) suggesting the importance of EPO signaling for epicardium attachment.

Epicardial-specific knockout of $Alk5$ (TGF β type I receptor) resulted in embryos with a detached epicardium, thinning of the ventricular myocardium, decreased myocardial cell proliferation and decreased epicardial EMT (Sridurongrit et al., 2008). These embryos also have a downregulation of N-cadherin and zona occludens 1 (ZO1) (Sridurongrit et al., 2008). ZO1 is known to interact with Connexin 43 (Cx43) in formation of gap junctions (Gourdie et al., 2006). Cx43 knockout mice have outflow tract defects, coronary artery defects, epicardial bubbling similar to the $RXR\alpha^{-/-}$ mouse and defects in epicardial EMT (Rhee et al., 2009). Cx43 is known to be involved in the formation of gap junctions between cells and is necessary for the electrical conduction system of the heart. These studies point to the importance of proper epicardial cell signaling for epicardium function because decreased gap junction formation and decreased growth factor receptors can result in epicardial defects.

The $RXR\alpha^{-/-}$ mouse is a model of aberrant epicardium formation. Phenotypically this mouse displays a detachment of the epicardium from the myocardium, hypoplastic ventricular myocardium and defects in septation and outflow tract (OFT) formation (Jenkins et al., 2005; Sucov et al., 1994) (Figure 6). The $RXR\alpha^{-/-}$ mouse will be discussed further later in this chapter.

Figure 6: Epicardial phenotype of the $RXR\alpha^{-/-}$ mouse. The WT seen in whole mount (A) and H&E section (C) shows normal architecture of the epicardium. The $RXR\alpha^{-/-}$ heart seen in whole mount (B) and H&E section (D) shows a bubbling of the epicardium indicated by the arrowhead and arrow in D. The hypoplastic ventricular myocardium can also be seen in the $RXR\alpha^{-/-}$ heart section in D. (Taken from Jenkins et al, 2005)



E. Cell Adhesion

Cell-cell interactions are important to all development processes and formation and maintenance of tissues and organs. In order for the epicardium to form and function properly, appropriate cell-cell and cell-extracellular matrix adhesions need to be in place. There are several types of cell-cell junctions that can be found in an organism including tight junctions, gap junctions, desmosomes, hemidesmosomes, adherens junctions and focal adhesions. Both adherens junctions and focal adhesion complexes serve to connect the cell membrane to the actin cytoskeleton (Niessen, 2007; Wozniak et al., 2004). Desmosomes are found within epithelia and muscle and are capable of resisting shear forces that can occur in these two tissues. The components of a desmosome will connect the cell membrane with the cell cytoskeleton and one cell membrane to another cell membrane to form a strong junction (Green and Simpson, 2007). Improper functioning or formation of desmosomes has been implicated in skin blistering diseases (Has and Bruckner-Tuderman, 2006). This would indicate that proper desmosome function is necessary for adhesion since with loss of desmosomes function there is a “bubble-like” detachment, similar to the epicardium in the $RXR\alpha^{-/-}$ mouse. Cadherins are a family of cell adhesion molecules that are found mainly in adherens junctions and desmosomes (Elangbam et al., 1997) and attach the cell to the actin cytoskeleton using interactions with catenins (Wheelock and Johnson, 2003). Desmosomes in particular contain two specialized cadherins that interact with intermediate filaments (Green and Simpson, 2007). N-cadherin knockout mice have a detached epicardial phenotype (Luo et al., 2006), indicating the importance of cellular junctions in epicardial cell attachment to the myocardium.

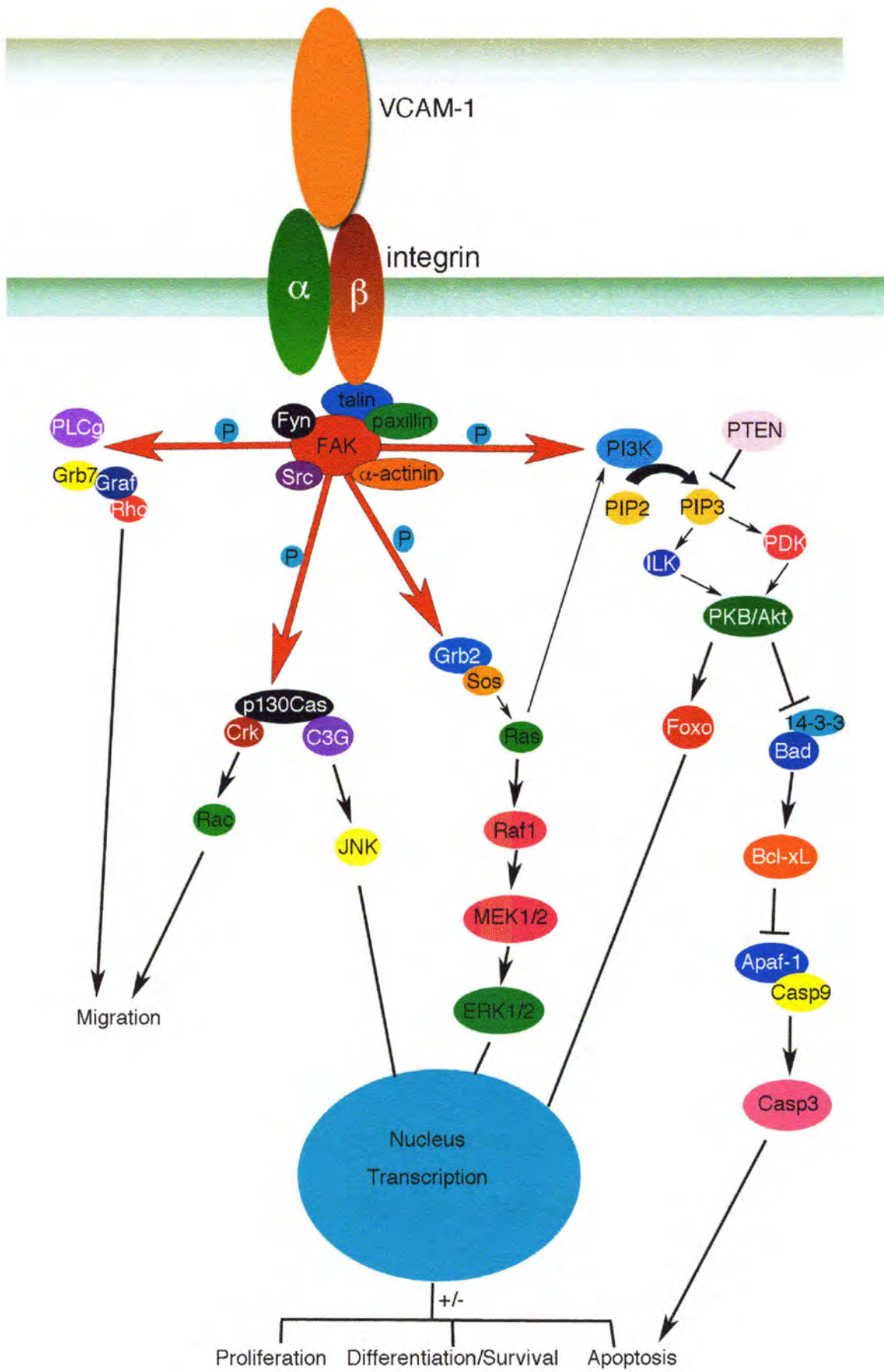
The focal adhesion complex is important for cell migration as well as transient cell adhesion. Focal adhesions bind cells to the extracellular matrix or to other cells through integrins. The focal adhesion complex consists of focal adhesion kinase (FAK),

fibronectin (FN), VCAM-1, integrins, paxillin and various other ECM proteins (Wozniak et al., 2004) (Figure 7). FAK is a tyrosine kinase that will interact directly with integrins and other proteins attracted to the focal adhesion such as paxillin (Wozniak et al., 2004) (Figure 7). Fibronectin will induce tyrosine phosphorylation of FAK following binding to integrin heterodimers (Ilic et al., 1995). Paxillin has been shown to be involved in fibronectin-dependent cell migration, as was illustrated by the loss of cell migration on fibronectin in paxillin null primary cell culture (Hagel et al., 2002). There is decreased tyrosine phosphorylation of FAK in paxillin null mice, which indicates a role for fibronectin, FAK and paxillin in cell migration (Hagel et al., 2002).

FN is an extracellular matrix glycoprotein that is expressed in the proepicardium, epithelial basement membranes, connective tissues, vessel walls and muscles of the mouse embryo and is involved in the focal adhesion complex through its binding to integrins (Hynes, 1985; Kalman et al., 1995; Peters and Hynes, 1996). FN contains a specific RGD sequence that is recognized by the fibronectin-binding integrins to mediate signaling and cell-matrix attachment (Hynes, 1992). FN^{-/-} embryos die at gastrulation as a result of defects in mesodermally-derived tissues (George et al., 1993). Epicardium formation in FN^{-/-} cannot be studied because of the early embryonic death. Previously it has been shown that FN is increased in the RXR α ^{-/-} heart and might play a role in epicardium formation (Jenkins et al., 2005).

Integrins are transmembrane receptors that aid in cell adhesion and attachment of the cell to the extracellular matrix and to neighboring cells (Hynes, 1992). Integrins are composed of α and β subunits which can form 24 different integrin heterodimers (Hynes, 2002). The integrin heterodimers α 5 β 1, α 8 β 1 and α V β 1 will bind to FN at the RGD (arginine-glycine-aspartate) sequence within the FN protein (Hynes, 2002). The heterodimer α 4 β 1 will also bind FN although it primarily binds VCAM-1, which will also

Figure 7: Signaling pathways downstream of VCAM-1 or FN binding to integrin $\alpha 4\beta 1$. This diagram illustrates the major signaling pathways that occur downstream of integrin $\alpha 4\beta 1$ binding to VCAM-1 or fibronectin. VCAM-1 binding is shown in the diagram but integrins can also bind to fibronectin and initiate signaling.



bind FN (Kwee et al., 1995) (Figure 7). Other integrin heterodimers bind different extracellular matrix molecules including laminins that do not possess RGD sequences (Hynes, 2002). After binding their particular ligand, integrins will activate signaling processes such as proliferation, cell motility, cell survival, cytoskeletal organization and transcriptional control (Hynes, 2002). Integrins are referred to as “outside-in” transducers, receiving signals from extracellular components and then sending signals within the cell (Hynes, 2002).

Integrin $\alpha 4$ and $\alpha 5$ are expressed in the proepicardium and epicardium of the mouse (Pinco et al., 2001). Integrin $\alpha 5$ knockout mice have defects in the posterior trunk, have malformed yolk sac blood vessels and display defects in embryonic blood vessels, but exhibit no heart defects (Yang et al., 1993). Integrin $\alpha 4$ knockout mice have no epicardium resulting in coronary artery and myocardial defects (Yang et al., 1995) (Figure 3). Integrin $\alpha 4$ has been shown previously to be required in EPDCs to initiate FN-mediated migration (Sengbusch et al., 2002). Inhibiting integrin $\alpha 4$ by using adenovirus expressing antisense integrin $\alpha 4$ in chick epicardial cells resulted in stimulation of EMT, increased migration and invasion of EPDCs into the underlying myocardium and inability to become smooth muscle cells in the coronary vasculature (Dettman et al., 2003). While it is known that integrin $\alpha 4$ is involved in epicardium formation, its role in maintenance of epicardium attachment and epicardium function is not entirely known. The $RXR\alpha^{-/-}$ mouse has a defect in epicardial EMT (Ruiz-Lozano and Kubalak, unpublished) hence disrupting cell adhesion could have an adverse affect on EMT.

VCAM-1 is a transmembrane protein that was originally identified for its involvement in adhesion of leukocytes expressing integrin $\alpha 4$ during the inflammatory response (Elangbam et al., 1997). The primary function of VCAM-1 is to mediate

intercellular adhesion with the integrin $\alpha 4\beta 1$ heterodimer. VCAM-1 is expressed in a number of cell types including vascular endothelial and smooth muscle cells, bone marrow cells, and myocardial cells (Rosen et al., 1992; Sheppard et al., 1994). Expression in the heart can be found in the myocardium especially in the interventricular septum and outflow tract myocardium (Kwee et al., 1995). The VCAM-1 binding partner integrin $\alpha 4$ is expressed in the epicardium and also in the endocardial cushions (Kwee et al., 1995). The VCAM-1 knockout is embryonic lethal as a result of either loss of extraembryonic circulation or heart defects including a failure to form the epicardium (Kwee et al., 1995). One study showed that VCAM-1 expression will increase in cultured cardiomyocytes and NIH3T3 cells in response to an epicardial-derived factor (serum-free conditioned media from cultured epicardial cells) (Kang and Sucov, 2005). In this same study, VCAM-1 mRNA levels were reported to be reduced in the E11.5 $RXR\alpha^{-/-}$ heart (Kang and Sucov, 2005) (Figure 13). However, a complete developmental profile of VCAM-1 in the mouse was not done. VCAM-1 is necessary for epicardium formation with loss of VCAM-1 resulting in failure to form an epicardium (Kwee et al., 1995), however, the role of VCAM1 in events following epicardium formation is unknown. In this study VCAM-1 was examined through analysis of its expression in the $RXR\alpha^{-/-}$ mouse model of aberrant epicardium formation.

F. Retinoid signaling during heart development

Retinoic acid signaling is important for a wide variety of events during vertebrate embryonic development including cell proliferation, apoptosis, cell differentiation and tissue homeostasis (Mark et al., 2006). VAD in vertebrates results in defects such as malformations of the eye, heart, respiratory system and urogenital system (Mark et al., 2006; Wilson and Warkany, 1949). Retinoic acid isoforms (all-trans retinoic acid and 9-

cis retinoic acid) are derivatives of vitamin A. Retinoids are ligands for the retinoid receptors, which when activated will translocate into the nucleus, dimerize and either activate or inhibit transcription. There are two types of retinoid receptors: retinoic acid receptors (RARs) and RXRs, with an α , β and γ subtype of each (Chambon, 1996). RARs will bind all-trans (at-RA) and 9-cis retinoic acid (9-cisRA) while RXRs will bind only 9-cisRA for activation (Chambon, 1996; Mark et al., 2006) (Figure 8). Hetero- or homodimers of retinoid receptors will control transcription of RA-target genes by binding to retinoic acid response elements (RAREs) on DNA (Chambon, 1996) (Figure 8). Once 9-cisRA or at-RA binds to the RAR/RXR heterodimer or receptor homodimer, the complex will bind to the DNA and up- or downregulate transcription (Chambon, 1996; Mark et al., 2006) (Figure 8). RARs and RXRs can also dimerize with thyroid hormone receptors, vitamin D3 receptors (Mark et al., 2006), farnesoid X receptor, peroxisome proliferator-activated receptors (PPARs) and liver X receptor (Desvergne, 2007) to initiate transcription.

Vitamin A is converted to retinol in the body and is then further metabolized to retinal and finally to at-RA and 9-cis-RA. RALDH2 is a retinoic acid-synthesizing enzyme responsible for the conversion of retinal to at-RA (Duester, 2000) (Figure 8). In chick and mouse, RALDH2 is expressed in the proepicardium and continues to be expressed in the proepicardial buds and epicardium suggesting a role for RALDH2 in epicardium development (Hoover et al., 2008a; Moss et al., 1998; Niederreither et al., 1997; Xavier-Neto et al., 2000) (Figure 9). In the chick model, epicardially-derived cells that express RALDH2 are contained within the subepicardial space and then invade the ventricular myocardium (Perez-Pomares et al., 2002). As these cells differentiate into smooth muscle and endothelial cells, RALDH2 is downregulated (Perez-Pomares et al., 2002). RALDH2 knockout mice have heart defects that include decreased cardiomyocyte proliferation and ventricular trabeculation suggesting a role for epicardial

Figure 8: Retinoid signaling and cardiovascular phenotypes resulting from knockout of pathway components. RAR, retinoic acid receptor; RXR, retinoid X receptor; RBP, retinol binding protein; RoDH, retinol dehydrogenase; CRBP, cellular retinol binding protein; RARE, retinoic acid responsive element; 9-cisRA, 9-cis retinoic acid; atRA, all-trans retinoic acid; RALDH, retinaldehyde dehydrogenase; CYP1B1, cytochrome P450 1B1; CYP26, cytochrome P450 26; CRABP, cellular retinoic acid binding protein (Adapted from Hoover et al, 2008)

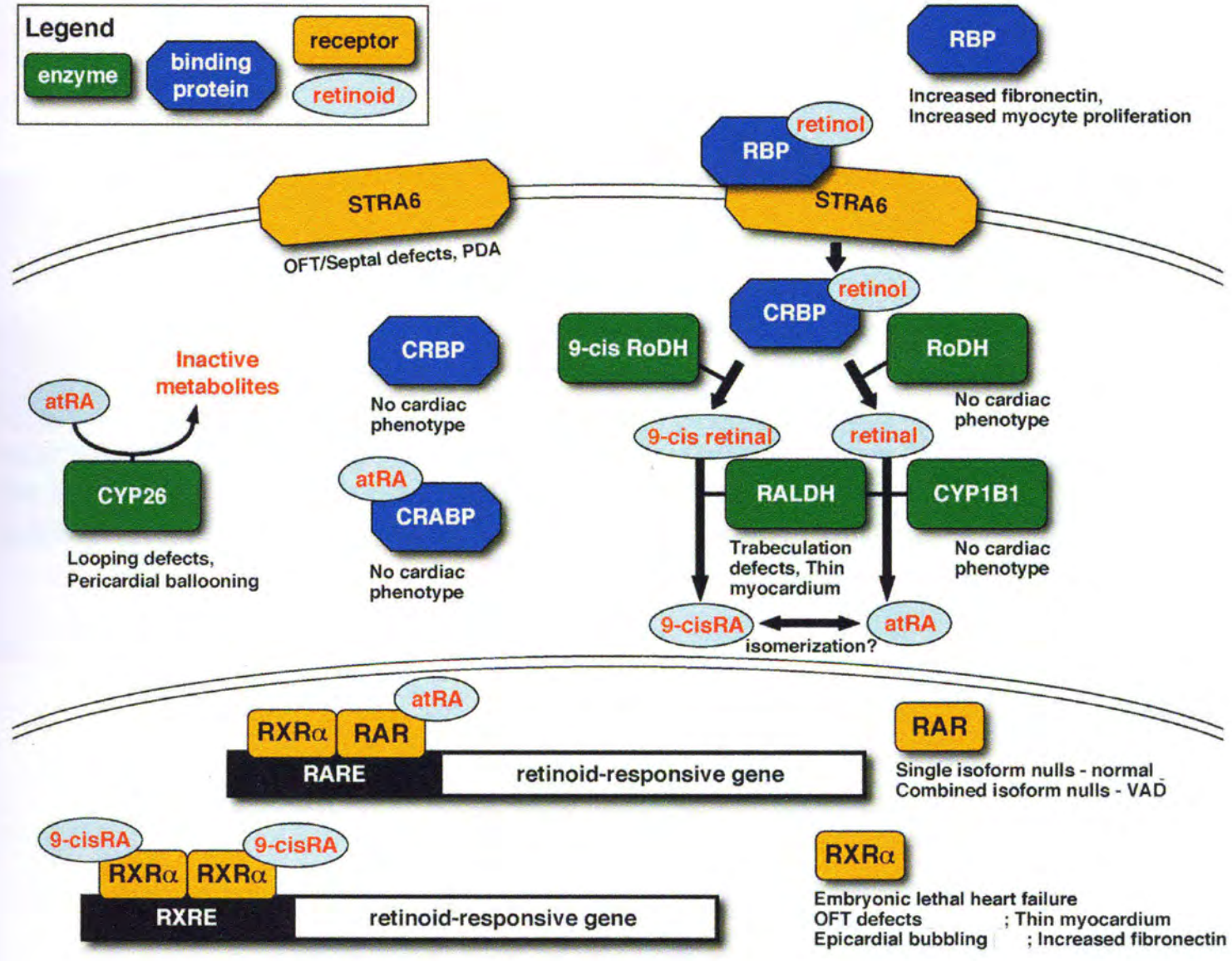
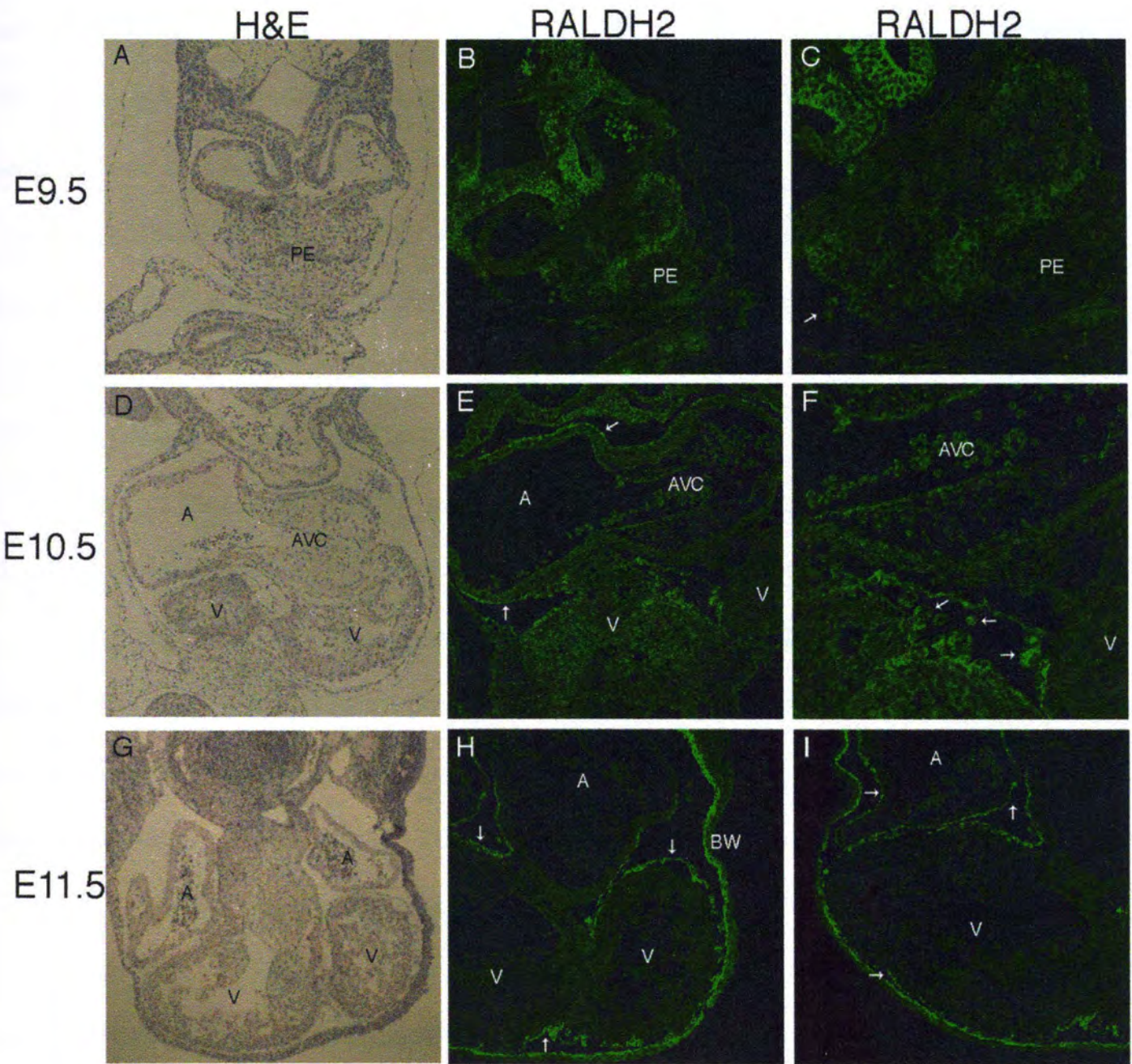


Figure 9: Immunohistochemical (IHC) analysis of RALDH2 expression in the mouse heart from E9.5-E11.5. RALDH2 expression is detected in the PE at E9.5 (B and C), in the remaining PE, PE buds and newly formed epicardium at E10.5 (E and F) and in the epicardium and body wall at E11.5 (H and I).



RALDH2 since these processes require a functional epicardium (Niederreither et al., 2001). RXR α has been shown to have a similar expression pattern to RALDH2 in avian embryos, with expression being seen in the epicardium, some subepicardial mesenchymal cells and EPDCs (Guadix et al., 2006). The similar expression patterns of RXR α and RALDH2 indicate that retinoid signaling is highly important in epicardium development and function.

Cardiac defects have been reported to be associated with several components of the retinoid pathway including RALDH2 and VAD models (mentioned above) (Figure 8). Cytochrome P450 26 (Cyp26) is responsible for converting at-RA to inactive metabolites (Figure 8). Loss of Cyp26 leads to defects in cardiac looping (Sakai et al., 2001). STRA6 is a cell surface receptor that is specific for retinol binding protein (RBP) that delivers retinol into the cell (Figure 8). Autosomal recessive mutations of STRA6 have been reported in the human population and are associated with a condition known as Matthew-Wood syndrome (Pasutto et al., 2007). The heart defects associated with this syndrome include Tetralogy of Fallot, aortic arch defects, septal defects and persistent ductus arteriosus (Pasutto et al., 2007). Defects associated with Cyp26 and STRA6 further indicate the importance of proper retinoid signaling with heart development.

Targeted deletions of several of the RARs and RXRs exist (Kastner et al., 1997; Lee et al., 1997; Luo et al., 1996; Mendelsohn et al., 1994); however, knockout of RXR α is the only single RA receptor knockout that results in cardiac malformations (Sucov et al., 1994). Combination RA receptor knockouts have a phenotype that resembles VAD (Mark et al., 2006). The RXR α ^{-/-} mouse has a thin myocardium, improper septation of the outflow tract, hypoplastic endocardial cushions, delay in epicardium formation and detached epicardium (Jenkins et al., 2005; Kubalak et al., 2002; Sucov et al., 1994). Using a floxed RXR α mouse line, RXR α has been conditionally knocked out in the

different cell lineages in the heart including the ventricular myocardium [using MLC2V-cre (Chen et al., 1998)], neural crest cells [using Pax3-cre (Ruiz-Lozano and Chien, 2003) and Wnt-1-cre (Merki et al., 2005)] and endocardial cells [using Tie2-cre (Merki et al., 2005)]. Epicardial-specific RXR α knockout (using GATA-5-cre) is the only region of the heart where specific removal of RXR α produced a cardiac phenotype that resembled the systemic RXR α -/- illustrating the importance of retinoic acid signaling within the epicardium (Mark et al., 1999; Merki et al., 2005). These mice have defects in the coronary arteries (abnormal branching), thinning of the myocardium, detachment of the epicardium and thinning of the subepicardium (Merki et al., 2005). There is also downregulation of β -catenin (Merki et al., 2005), which is known to be involved in cell adhesion through interactions with N-cadherin.

Secretion of retinoic acid and EPO from the epicardium appears to be required for cardiomyocyte proliferation (Stuckmann et al., 2003). In response to retinoic acid and requiring a functional RXR α , the fetal epicardium will secrete trophic factors, such as fibroblast growth factor 2 (FGF2), that help promote ventricular chamber morphogenesis (Chen et al., 2002; Smith and Bader, 2007) by activating the PI3K/Akt and Erk pathways to promote cell proliferation (Kang and Sucov, 2005). At this time it is not entirely known if proper epicardial cell adhesion is necessary for signaling to the myocardium but it is likely. The RXR α -/- mouse also has a loss of mitogenic signals from the epicardium as well as a reduction in the proliferative rate of ventricular cardiomyocytes (Kang and Sucov, 2005). The expression of VCAM-1 was reduced in the E11.5 RXR α -/- (Kang and Sucov, 2005), suggesting that this extracellular matrix molecule is likely regulated by retinoic acid receptor.

G. Transforming Growth Factor- β signaling

TGF β 2 is found in the proepicardium, epicardium and ventricular myocardium during heart development (Molin et al., 2003) (Figure 10) and, importantly, is elevated in the RXR α -/- mouse (Kubalak et al., 2002). TGF β 2 is a member of the TGF β superfamily of signaling proteins (Derynck and Feng, 1997) and has been shown to play a role in cardiovascular development (Harvey, 1999). Other members of this signaling family include TGF β 1, TGF β 3, bone morphogenetic proteins (BMPs) and activins (Feng and Derynck, 2005). TGF β 1 is expressed in the vascular endothelium and endocardium, particularly in the endocardium overlying the atrioventricular region and ventricular trabeculae (Molin et al., 2003) (Figure 10). TGF β 2 (Figure 10) and TGF β 3 are expressed in the epicardium, endocardial cushions and fibrous structures of the heart (Molin et al., 2003) indicating that these signaling molecules are especially relevant to epicardium formation and function.

TGF β 2 is secreted as a latent protein (as are TGF β 1 and TGF β 3), which is then proteolytically cleaved and activated (Derynck and Feng, 1997). TGF β 2 binds to the TGF β type II receptor, inducing heterodimerization with the type I receptor (Derynck and Feng, 1997) (Figure 11). The type II receptor phosphorylates the type I receptor through intrinsic serine/threonine kinase activity (Derynck and Feng, 1997). The type I receptor then phosphorylates the receptor-activated Smads (R-Smads) Smad2 and Smad3 (Derynck and Feng, 1997) (Figure 11). Once a R-Smad is activated by phosphorylation, it dimerizes with the co-Smad, Smad4, translocates into the nucleus and binds to DNA to regulate gene transcription (Figure 11). The R-Smad/Smad4 complex, once inside the nucleus, activates transcription by assembling with a nucleoprotein complex at Smad consensus DNA-binding sites (Feng and Derynck, 2005) (Figure 11). This nucleoprotein complex includes Smad-binding elements on the DNA, DNA-binding transcription factors

Figure 10: TGF β mRNA expression in the mouse heart at E9.5. TGF β 1 transcripts (B, E and H) are detected in the endocardium, dorsal mesocardium (arrow in B) and dorsal aorta. TGF β 1 mRNA was not detected in the myocardium or PE (B). TGF β 2 mRNA (C, F and I) is expressed in the myocardium, endocardium, PE (arrowhead in C) and newly formed epicardial cells (arrow in C). (Taken from Molin et al., 2003)

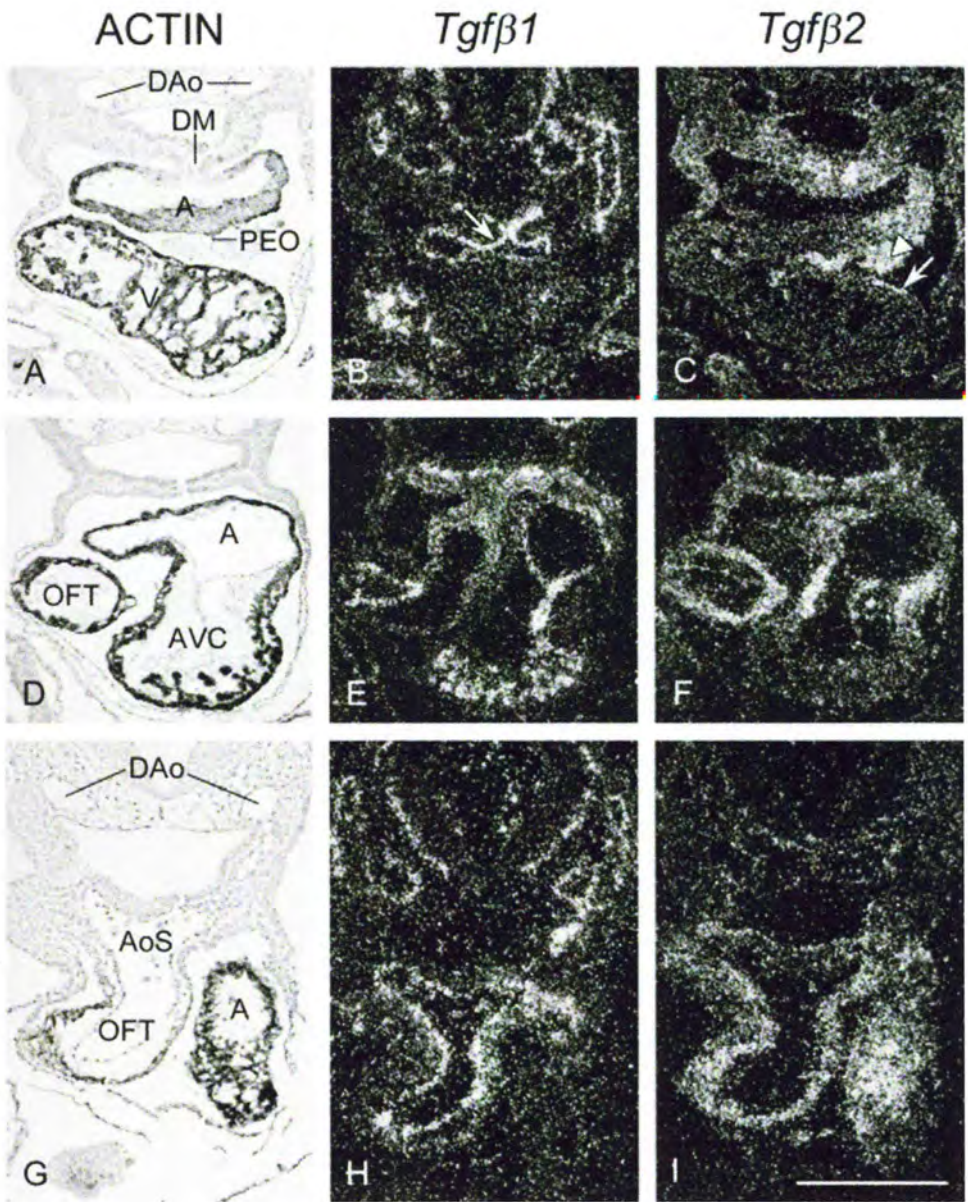
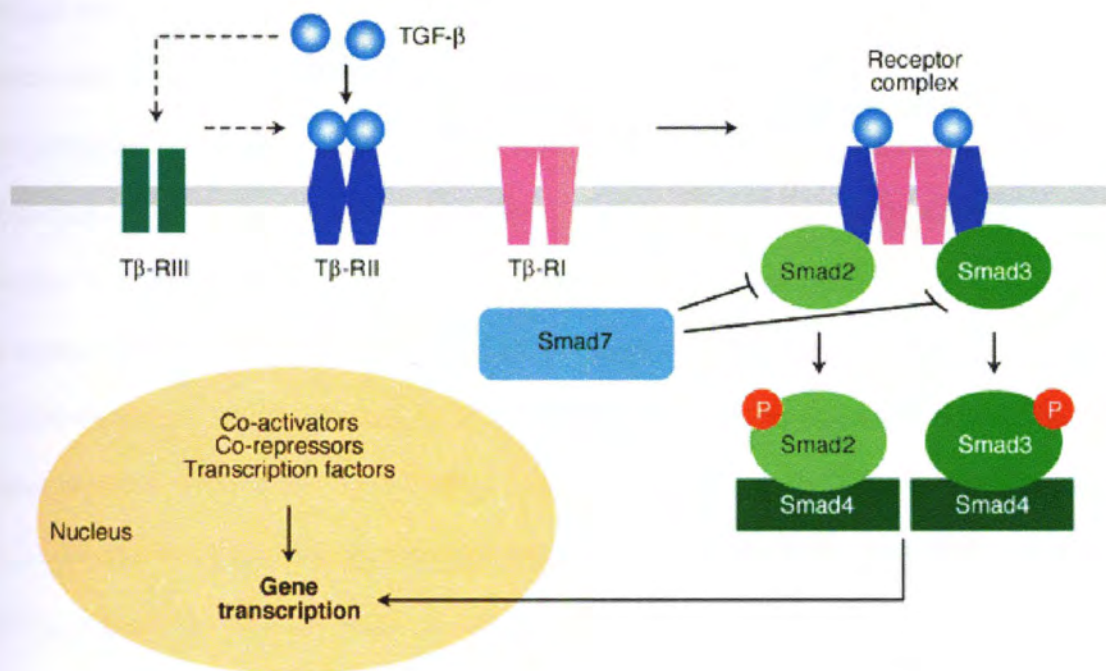


Figure 11: TGF β signaling. Diagram of the canonical TGF β signaling pathway. (adapted from Hui and Friedman, 2003)



and transcriptional coactivators (Feng and Derynck, 2005). In order to stop signaling through Smads, the inhibitory Smad, Smad7, is induced by Smad3 and serves as a negative regulator (Feng and Derynck, 2005). The inhibitory Smad7 competes with the receptor-activated Smads for receptor interaction (Moustakas et al., 2001).

Knockout of TGF β 2 results in cardiovascular defects including ventricular and outflow tract septal defects, hypoplastic ascending aorta, dual outlet right ventricle and dual inlet left ventricle (Sanford et al., 1997), but no reported epicardial defects. The mutant mice die perinatally due to respiratory distress possibly as a result of cardiovascular dysfunction (Sanford et al., 1997). TGF β 2 is the only TGF β isoform that is expressed in the proepicardium (Molin et al., 2003) (Figure 10) suggesting it may be important for development of the epicardium. TGF β 2 is also localized to the developing outflow tract and cardiomyocytes (Molin et al., 2003) (Figure 10) and is known to be an activator of EMT and possible regulator of apoptosis in endocardial cushions (Camenisch et al., 2002; Kubalak et al., 2002). At this time, no epicardial defects have been reported or observed by in TGF β 2 $^{-/-}$ mice. Interestingly, the RXR α $^{-/-}$ mouse heart has elevated TGF β 2 expression during midgestation (Kubalak et al., 2002) (Figure 12) and potentially during early heart development (Jenkins and Kubalak, unpublished data). We hypothesize that increased TGF β 2 plays a role in the abnormal epicardium formation seen in the RXR α $^{-/-}$ mouse, indicating the need to explore the TGF β 2 signaling pathway further in epicardium attachment and proper epicardium function

H. The retinoid X receptor knockout (RXR α $^{-/-}$) mouse

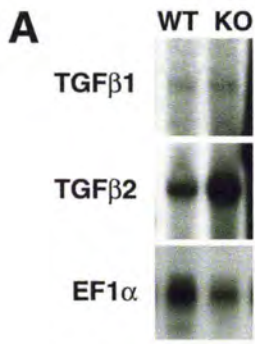
The RXR α $^{-/-}$ mouse is the only single retinoid receptor knockout to result in congenital heart disease. The RXR α $^{-/-}$ mouse has a thin myocardium, improper septation of the OFT and hypoplastic endocardial cushions and is embryonic lethal

between E13.5 and E15.5 (Gruber et al., 1996; Sucov et al., 1994). RXR α ^{-/-} mice also have an increase in apoptosis in the outflow tract and elevated TGF β 2 at midgestation (Kubalak et al., 2002) (Figure 12). In addition to its cardiac defects, the RXR α ^{-/-} mouse also has decreased liver mass as well as edema and ocular defects (Kastner et al., 1994; Sucov et al., 1994).

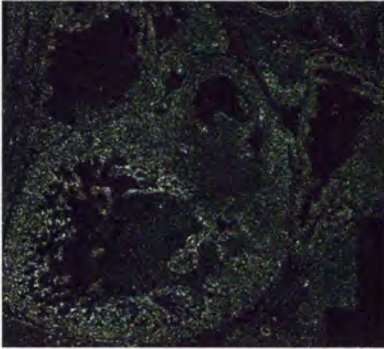
The RXR α ^{-/-} mouse has, among other cardiac defects, a defect in epicardium development (Jenkins et al., 2005) (Figure 6). Epicardium formation in the mutant is delayed and, once the epicardium forms, is detached from the myocardium (Jenkins et al., 2005). There are several areas of bare myocardium in the RXR α ^{-/-} heart up until E11.5 when the wild type mouse epicardium is fully formed (Jenkins et al., 2005). By E12.5, the RXR α ^{-/-} mouse has epicardium fully covering the heart, however, it is detached from the myocardium (Jenkins et al., 2005) (Figure 6). A decrease in VCAM-1 mRNA in the E11.5 RXR α ^{-/-} heart was also reported (Kang and Sucov, 2005) (Figure 13), indicating VCAM-1 may be important in the RXR α ^{-/-} mouse phenotype since it has previously been shown to be involved in epicardium formation (Kwee et al., 1995). However, the study by Kang and Sucov did not do a complete developmental profile of VCAM-1 in the developing heart. This detachment from the underlying myocardium may be due to an increase in subepicardial extracellular matrix production or a defect in epicardium/myocardium attachment. In this study, epicardial cell attachment will be further studied by analyzing adhesion proteins in the RXR α ^{-/-} mouse.

The phenotype of the RXR α ^{-/-} mouse heart may largely be due to improper development and functioning of the epicardium since loss of EPDCs or fewer EPDCs can lead to many of the defects seen in the RXR α ^{-/-} heart such as thinning of the myocardium. In previously published reports, the RXR α ^{-/-} mouse was shown to have

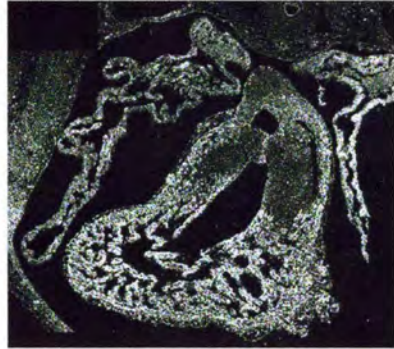
Figure 12: Elevated TGF β 2 protein and mRNA in the heart of the RXR α ^{-/-} mouse. TGF β 2 mRNA levels are elevated in the heart but not TGF β 1 in the RXR α ^{-/-} shown by RNase protection (A). Immunohistochemical analysis of E13.5 (B) and E12.5 (C) WT and RXR α ^{-/-} heart shows that TGF β 2 levels are elevated in the RXR α ^{-/-} mouse. (adapted from Kubalak et al, 2002)



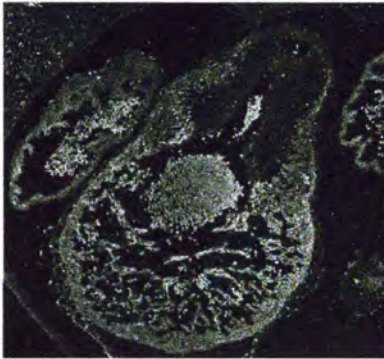
B
wildtype



RXR $\alpha^{-/-}$



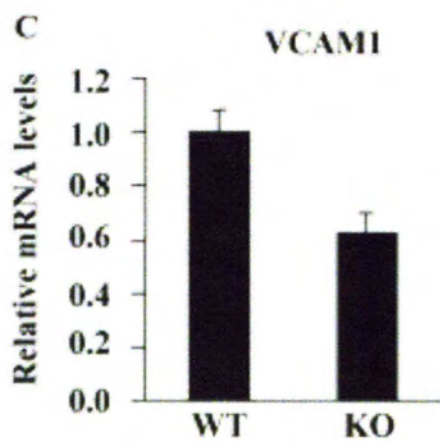
C
wildtype



RXR $\alpha^{-/-}$



Figure 13: Real time PCR analysis of VCAM-1 mRNA in the heart of the $RXR\alpha^{-/-}$ mouse at E11.5. Real time quantitative PCR shows a decreased level of VCAM-1 in the $RXR\alpha^{-/-}$ mouse heart at E11.5. (Adapted from Kang and Sucov, 2005)



increased TGF β 2 in the heart during midgestation (Kubalak et al., 2002) (Figure 12). Previous studies suggest that TGF β 2 is increased in the proepicardium using RNase protection analysis of proepicardium of WT versus RXR α ^{-/-} (Jenkins and Kubalak, unpublished). The increased TGF β 2 could be regulating proteins that are altered in the RXR α ^{-/-} mouse such as VCAM-1. RXR α ^{-/-} mice also have a reduction in GSK3 β phosphorylation (downstream of PI3K/Akt pathway) and p90rsk (downstream of Erk) phosphorylation (Kang and Sucov, 2005). Both of these pathways are known to be involved in cardiomyocyte proliferation, indicating that retinoid signaling is important for cardiomyocyte proliferation. One study showed that the RXR α ^{-/-} mouse has reduced expression of NADH-ubiquinone oxidoreductase (mitochondrial complex I), reduction in ATP content in ventricular tissue and misexpression of several genes involved in the electron transport chain (Ruiz-Lozano et al., 1998). The authors indicated that the hearts of RXR α ^{-/-} mice are energy deprived, which could contribute to embryonic lethality from impaired heart function.

Previous studies have also shown that the levels of the extracellular matrix molecule fibronectin is increased in the proepicardium, epicardium and body wall of the RXR α ^{-/-} mouse heart and thus, may play a role in the abnormal development of the mutant heart (Jenkins et al., 2005). Levels of fibronectin protein within RXR α ^{-/-} PE explants also appears to be elevated and disorganized in comparison to the fibronectin network in the wild type PE explants (Jenkins et al., 2005), which could disrupt binding with integrins. In PE explants from the RXR α ^{-/-} mouse, migration of PE-derived cells is reduced compared to wild type, which may explain the delay in epicardium formation. There is also an increase in apoptosis within the PE of the RXR α ^{-/-} mouse (Jenkins et al., 2005), which may also contribute to the delay in epicardium formation because fewer PE cells would be available to migrate to the heart.

Knockout of RXR α specifically in the epicardium results in thinning of the myocardial wall as well as defects in coronary arteriogenesis (Merki et al., 2005). The epicardial-specific RXR α knockout demonstrated that the epicardium is the only cell lineage of the heart where RXR α can be specifically knocked out and produce a phenotype illustrating the importance of retinoic acid signaling within the epicardium (Mark et al., 1999; Merki et al., 2005). These mice have defects in the coronary arteries (abnormal branching), thinning of the myocardium, detachment of the epicardium and thinning of the subepicardium (Merki et al., 2005). The coronary artery defect was not reported in the original paper describing the systemic RXR α ^{-/-} mouse (Sucov et al., 1994). In the epicardial-specific RXR α ^{-/-} mouse there is a down-regulation of FGF2, β -catenin and Wnt9b, all of which are known to be important in epicardial EMT and vasculogenesis (Merki et al., 2005). Re-expression of RXR α specifically in the myocardium for RXR α ^{-/-} hearts is unable to rescue the thin myocardium phenotype suggesting that the thinning of the myocardium is not due to loss of RXR α ^{-/-} in the myocytes (Subbarayan et al., 2000).

The cell adhesion molecule VCAM-1 has previously been shown to be required for epicardium formation (Kwee et al., 1995). VCAM-1 was altered in the RXR α ^{-/-} mouse heart with a decrease seen at E11.5 compared to the WT (Kang and Sucov, 2005). Based on its known role in epicardium formation through adhesion of the epicardium to the myocardium (Kwee et al., 1995) and in inhibiting epicardial EMT (Dokic and Dettman, 2006), it is thought that VCAM-1 could have a role in epicardium adhesion and epicardial EMT in the RXR α ^{-/-} mouse. This current study aims to analyze VCAM-1 in the RXR α ^{-/-} model of aberrant epicardium formation during E9.5-E13.5 and determine if the retinoid and/or TGF β 2 signaling pathway is responsible for its regulation.

The overall hypothesis to be tested in this dissertation is that proper expression of VCAM-1 is essential for normal cardiac morphogenesis and is regulated by TGF β 2 and/or retinoid signaling during formation of the epicardium. To address this hypothesis there are two specific aims:

Aim 1: To determine the expression pattern and levels of VCAM-1 in E9.5-E13.5 RXR α ^{-/-} versus wild type (WT) hearts.

Aim 2: To determine how TGF β 2 and/or retinoid signaling regulate VCAM-1 expression during heart and epicardium development

Chapter 2: Materials and Methods

Transgenic Mice and Embryos

RXR α ^{+/-} breeders were maintained as previously described on a C57BL6 background (Sucov et al., 1994). RXR α ^{+/-} mice were crossed to yield WT and RXR α ^{-/-} embryos to use for some experiments (immunohistochemistry, western blot, real time PCR and epicardial explants). WT mice were crossed to yield WT embryos to use for epicardial explants and whole embryo culture (WEC). Timed pregnant females were sacrificed using isofluorane followed by cervical dislocation on the appropriate embryonic day for experimentation. Embryos were staged using the day of plug as embryonic day (E) 0.5. Embryos were removed from the uterus and yolk sac then dissected according to each experiment.

Immunohistochemistry

Whole embryos (E9.0-E12.5) from RXR α ^{+/-} matings were bisected and fixed in 2% paraformaldehyde for 1 hour at room temperature (RT). A portion of the tail of each embryo was removed for genotyping. Wild type and mutant littermates were dehydrated through graded ethanols and embedded in paraffin for sectioning. The paraffin embedded tissues were sectioned at 5 μ m and mounted onto slides (Fisher Superfrost plus). A guide series of each embryo (every ninth section) was made and hemotoxylin and eosin stained to use as a reference. Slides were deparaffinized in xylenes, rehydrated in graded ethanols and washed in 1x phosphate buffered saline (PBS). Slides were blocked in a blocking solution with 1% bovine serum albumin (BSA), 0.01% Tween 20 in 1x PBS for 1 hour. Sections were incubated in primary antibody diluted in blocking solution overnight at 4°C. The primary antibodies used were rabbit anti-VCAM-

1 H276 (Santa Cruz Biotechnologies), rabbit anti-integrin α 4 (Abcam 65984) and rabbit anti-N-cadherin (Abcam 12221). The following day, sections were washed with 1x PBS, incubated in anti-rabbit secondary antibody conjugated to Alexa-488 or Alexa-594 from Molecular Probes diluted in blocking solution, for 2 hours and washed in 1x PBS. Following PBS wash, sections were nuclear stained using ToPro3 nuclear stain (Invitrogen Molecular Probes) for 10 minutes then washed. Slides were coverslipped using DABCO in PBS and a glass coverslip, sealed with nail polish (Fisher) for microscopic analysis. The fluorescently stained tissue sections were viewed on a Leica TCS SP2 AOBS confocal microscope. To compare WT and RXR α ^{-/-}, constant gain and laser settings were used throughout the analysis.

Western Blotting/Immunoblotting

Samples of whole heart were taken from wild type and mutant embryos. The genotypes of the embryos were determined by PCR following dissection as described above. Protein was extracted from single hearts in 20 μ l RIPA (20 mM Tris pH 7.5, 100 mM NaCl, 0.5% NP-40, 0.5 mM EDTA, 0.5 mM PMSF) buffer containing protease inhibitors (Complete mini, Roche) and sonicated until the tissue was disintegrated. Protein samples were centrifuged at maximum speed for 10 minutes at 4°C to pellet any cell debris. The supernatant was removed and 6x loading buffer (200 mM Tris-HCl pH 6.8, 50% glycerol, 8% SDS, 400 mM DTT, 0.4% Bromophenol blue) was added to each sample to a final concentration of 1x. Samples were heated at 95°C for 5 minutes and then loaded onto a 10% Tris-HCl gel along with Precision Plus Kaleidoscope Standard molecular weight marker (Biorad). The gel was run for 45 minutes at 60 volts (V) then for an additional 2-3 hours at 130V. Following electrophoretic separation, the gel was equilibrated in transfer buffer for 20 minutes. PVDF (GE water and processing

technology) membrane was cut to the appropriate dimension (8.5cm x 5.5cm), activated in methanol for 1 minute, washed in water for 10 minutes then equilibrated in transfer buffer for 10 minutes. Blot paper (BioRad) was cut to appropriate dimensions (9cm x 6cm) and equilibrated with transfer buffer. A Transblot semi-dry transfer cell (BioRad) was used to transfer the proteins from the gel to the PVDF membrane. Protein transfer was done at 20V for 30 minutes. Once proteins were transferred, the blot was rinsed in 1XTBST (Tris-buffered saline containing 0.01% Tween20). After washing, the blot was blocked in 5x blocking buffer (TBST with 5% dry milk) for 1 hour. Primary antibody (rabbit anti-VCAM-1 H276) was diluted to 1:500 in 1x blocking buffer and incubated with the blot overnight at 4°C. The following day, the blot was washed for 1 hour with TBST, incubated in horseradish peroxidase (HRP) conjugated anti-rabbit secondary antibody diluted 1:10,000 in 1x blocking buffer, then washed with TBST for 1 hour. The blot was incubated with West Femto (Pierce) solution per the manufacturer's recommended time and developed using autoradiography film (Hyperfilm, Amersham). Blots were stripped for probing with different antibodies using ReBlot mild solution (Millipore) as per manufacturer's recommendations. Blots were scanned for quantification of protein levels using Image J (NIH) for densitometry and normalized to β -tubulin.

Real time PCR (RT-PCR)

Intron-spanning primers were designed for each mRNA of interest and checked for specificity to the gene of choice by using BLAST on the NCBI website (<http://www.ncbi.nlm.nih.gov.ezproxy.musc.edu/BLAST/>). The intron-exon boundaries of each gene were mapped and primer sets designed to span an intron in order to verify that we were amplifying cDNA and not genomic DNA in the PCR.

Sequences of the primers were:

Integrin α 4 F: 5' CCCACAGGCCTTTATTTTCAT

Integrin α 4 R: 5' CTATCCTTGAGAGGCGATCC
VCAM-1 F: 5' CACTCTTACCTGTGCGCTGT
VCAM-1 R: 5' CTCCAGATGGTCAAAGGGAT
GAPDH F: 5' AACTTTGGCATTGTGGAAGGGCTC
GAPDH R: 5' TGGAAGAGTGGGAGTTGCTGTTGA
N-cadherin F: 5' ATGCCCAAGACAAAGAAACC
N-cadherin R: 5' CTGTGCTTGGCAAGTTGTCT
TGF β 2 F: 5' GCTTTGGATGCTGCCTACTGCTT
TGF β 2 R: 5' TGTACAGGCTGAGGACTTTGGTGT

RNA was isolated from whole hearts of RXR α ^{-/-} and wild type mice using RNA Stat60 (Tel-Test, Inc) per manufacturer's recommendations. The amount of RNA was quantified by UV absorbance at 260nm. Complementary DNA (cDNA) was made from 1 μ g RNA samples using M-MLV reverse transcriptase (Promega) and Oligo dT (Gibco). Real time reverse transcriptase (RT) PCR was performed using SYBR green (BioRad) per manufacturer's protocol using the BioRad iCycler. All reactions were performed in triplicate. Relative mRNA levels in each sample were determined based on differences between the cycle thresholds (Ct) for each amplicon. The delta Ct was determined by subtracting the Ct value of the GAPDH from the Ct value of the gene of interest. The fold change between WT and RXR α ^{-/-} was determined using the delta delta Ct method (Scheffe et al., 2006).

Transmission Electron microscopy (TEM)

Embryos fixed in 2% glutaraldehyde were sent to the Instrumentation Resource Facility at the University of South Carolina School of Medicine in Columbia, SC where Dr. Robert Price's lab performed the TEM analysis. Images were analyzed in

collaboration with Dr. Price to look for differences in cellular junctional complexes between the epicardium and myocardium of the E10.5 WT and RXR α ^{-/-}.

In silico promoter analysis

The VCAM-1 promoter sequence was obtained from the NCBI database (Accession number: U42327) and analyzed using the Transcription Element Search System (TESS) program (<http://www.cbil.upenn.edu/cgi-bin/tess/tess>). Smad binding elements and retinoid binding sites were also searched for manually within the promoter to ensure that all possible sites were identified.

Rat epicardial (REC) cells

Rat epicardial (REC) cells were obtained from Dr Robert Gourdie at the Medical University of South Carolina in Charleston, SC and were maintained as described (Wada et al., 2003). The cells were grown in media consisting of Dulbecco's Modified Eagle Medium (DMEM 4.5 g/L, Gibco) supplemented with 10% fetal bovine serum (Gibco), penicillin-streptomycin and L-glutamine at 37°C and 5% CO₂. Cells were passaged using 0.05% trypsin EDTA (Gibco) at 37°C and then plated according to the specific experimental protocol being used. REC cells were used for chromatin immunoprecipitation and VCAM-1-luciferase analysis.

Chromatin immunoprecipitation (ChIP)

REC cells (100,000 cells) were seeded onto 35 mm dishes and grown until 90% confluent. Each dish of cells was fixed with 37% formaldehyde to covalently crosslink proteins to the DNA. ChIP was performed using the EZ ChIP kit from Millipore per the manufacturer's instructions. Briefly, chromatin was harvested from the cells by adding of SDS lysis buffer (Millipore), scraping cells into an eppendorf tube and pelleting the cells.

DNA was sheared by sonication 4-5 times in a water bath sonicator containing ice until DNA was sheared to fragments of 200-1000 basepairs (approximately 5 minutes). DNA was analyzed on an agarose gel to assure the proper shearing of the DNA. Sheared DNA was diluted in Dilution Buffer (Millipore) to a 1:10 DNA:buffer ratio.

Protein G Agarose (Millipore) was added to the diluted sheared DNA and incubated for 1 hour at 4°C to remove proteins and DNA that may bind non-specifically to the Protein G agarose later in the procedure. Samples were centrifuged at low speed (1000g) and the pellet was discarded. Ten μ l of each supernatant was saved to use as the "input" sample. One milligram of the immunoprecipitating antibody was added to each sample and incubated overnight at 4°C with rotation. Immunoprecipitating antibodies used were anti-RNA polymerase (positive control-Millipore), RXR α (D-20, Santa Cruz) and Smad4 (Santa Cruz). The negative control had normal mouse IgG added instead of an antibody.

Protein G agarose was then added to each sample and incubated for 1 hour. Samples were centrifuged at low speed and supernatant removed and discarded. The agarose beads were first washed in low salt (Millipore) then high salt (Millipore) then LiCl buffers (Millipore) followed by TE buffer. Samples were eluted in elution buffer (Millipore) and crosslinked proteins were separated with 5M NaCl. Samples were incubated with RNase A, 0.5M EDTA, 1M Tris-HCl and Proteinase K and then purified using the DNA purification system in the EZ ChIP kit (Millipore). DNA that was crosslinked to RXR α or Smad4 will coprecipitate with the chromatin complex and can then be analyzed using PCR.

A PCR reaction using primers to the VCAM-1 promoter or the GAPDH promoter (as a positive control) was performed to determine if portions of the VCAM-1 promoter DNA were bound by RXR α or Smad4. The PCR reaction consisted of a 95°C

denaturation cycle for 5 minutes followed by 30 cycles of denaturation at 95°C for 1 minute, annealing at 60°C for 1 minute and extension at 72°C for 1 minute. A final extension at 72°C was done for 10 minutes. PCR samples were run on a 2.5% agarose gel containing ethidium bromide. DNA bands were visualized using a gel imager.

ChIP primers were as follows (Figure 14, highlighted in red):

VCAM-1 ChIP F: TCCTGTCATCCAGCAATGGGTCAA

VCAM-1 ChIP R: AACTGCCAACAGTGTGTGTGTGTG

GAPDH ChIP F: CTGAGCAGACCGGTGTCACATC

GAPDH ChIP R: GAGGACTTTGGGAACGACTGAG

TGFβ2 and 9-cisRA treatments

Lyophilized TGFβ2 (R&D Systems) was reconstituted in diluent (4 mM HCl in 0.1% BSA) at a 10ng/μl concentration. Lyophilized 9-cisRA (MP Biomedicals) was reconstituted in DMSO at a concentration of 100 mM. Most treatments were done in serum-free DMEM to eliminate the variability from growth factors contained within serum. The appropriate amount of TGFβ2 and/or 9-cisRA was added to serum-free DMEM depending on experiment (concentrations used are listed with each experiment) and then added to cells in culture. In the case of whole embryo culture and luciferase assays, the appropriate amount of TGFβ2 and/or 9-cisRA was added directly to the culture medium. Concentrations used of each varied depending on the experiment.

Figure 14: Regulatory elements contained within the mouse VCAM-1 promoter region . 5' portion of the sequence of the mouse VCAM-1 promoter (accession number: U42327) with putative and defined regulatory sites highlighted. Smad-binding elements are highlighted in yellow. Retinoid elements are highlighted in blue. The TATA box is in purple upstream of the start site indicated by the black arrow. E box sequences are highlighted in green. CHIP primers used are highlighted in red.

-1894 gatctacata gccacggaga gttcttttagc tatatgtag agtagtggtt cttaaacgag gaaggatttg acctgtgga atccacaaa tagtTTTTT
-1794 tttcacttc tctgtttagt gtaactattct ctttctctga taggaattat ttctccactc acttgggtga gaactgatac caaataagat gaTTTgcat
-1694 gatccaagta gttatttatt ttttaagtgtc aaTGGCAtgg attaacattt tcttaccatgc ctttgatcta tggagaaggt gagaatcagt agggggtaG
-1594 ctataactctc cttttatgac atgacattgt tgaggctctc tagatgacat gccagctaata gtcacgacac cctgggatatg tctgcatagc cctaaatat
-1494 atccctcaac ttccctttta taacttgctc tcagtgggag ccacatgtat tctcaagagg gaattcagaa gTCTctctg ccaggttggg goagttggcg
-1394 actgtgggTCT caactgatag cttttgtcca atgacatgat actgttaatt ttacatgtgc ccagatGTC gggaaactata ctttcttctg ggaattattt
-1294 ttttctctGAC cttttgacatt atgaactaca ttacagtatt tgaacgtttc tcttctagat tttaaacatc tagaagatgc tgcaggtttt atagtcgta
-1194 tatataaac cattatatat atatatatat atatatatat atatatatat atatatatat atggaataga aacaactatg aataagaact agtctggcc
-1094 atgcagggaa ctgataatgc catgtgggag gTaaacccac atgtgtataa taacaggaa gggctattcc ggtttcttcc tcatgggcaa gcaatttgca
-994 aggacatggg ctatgcatgt gtaTGGCActa cagaggcatt taTGAActt aattgaGTC ttcaaaaagt catttccactg ggagtgaaa ataataataa
-894 aaaaatggtt gtcaattcat ctctaaagc taatctgttt acatattcaa ttggacttgt ggctaaataa tgcagccaaa gaaatccacc acaaaaattt
-794 agcTGGCaga tcccatttt tagcgttcaa gTCCgcaaa TGGTCTCTG catccagcaa TGGCCTAG ggcTGGGGC ttgtcaaaca aaagaaaaa
-694 taattccctt cattctgcat caacgtcctt tcatttacta ctccagaaa ttatttcagg gaggtttttt ttttgcataa aatcactta tgaataaaag
-594 agtataaaaa taagaactac tgactacat tctaaaagag tgactcatga taTGGGTca ataaaaaca ataaaggata ttttctttt ttgttgaaa
-494 gagaacaatt tttattttt aaattgcaa tgcatttctt aatgaagaaa agtcagtggt tatttactga gtgatctctg TCTttgcctg tcacacacac
-394 acacacacac acacacacac acacacacac actgTGGGca gTctattt gcaatcactt tttcaggaga gatagccctt tgggagctga agTcaggaa
-294 aagccagaga tttatatact tggaaagtgc gtgtttccca ggactcagaa tgacttcagc ccagaaagca gctgaagggg ttaacgtggg gacttgctg
-194 gctgtcagtt aaacttttc cctgctctg ggtttccctt tgaaggattt tccctccgc totctagca gTCTccttTATAagagcTCTcttctatt
-94 cactcacacc agcccgctg cgtttggagg ctgaacactt ttccTGGCca cttttTGGTGGCcaaa gaaggctttg aagcagTCTctt ttgaaatgcc
6 tgtgaagatg gtcgctGTC tgggagctc aacggtactt tggatactgt ttgcaTCTG taagttcctg acctattca cacatctaca gcttctggtg
106 tactacagag ctttgcata agagccagta ttctgacaga gctggggagc gattttctt ccactgtcaa atgagtaatt tggattatat cggtagtgg

Whole embryo culture (WEC)

WEC was performed as previously described (Hertig et al., 1999). Embryos at E11.5 were removed from the uterus then dissected to leave the embryo attached to the placenta and yolk sac via the two pairs of umbilical vessels. The embryos were placed into roller culture bottles containing pre-equilibrated 50% DMEM and 50% immediately centrifuged rat serum (ICRS) and cultured at 37°C with 95% O₂ and 5% CO₂. Following a 1 hour pre-equilibration period, TGFβ₂ (10ng/ml), 9-cisRA (100nM), diluent or TGFβ₂ (10ng/ml)+9-cisRA (100nM) was added directly to the culture medium. Embryos were grown in culture for 12 to 18 hours. After treatment, embryos were fixed in 2% paraformaldehyde for 1 hour at RT, embedded in paraffin and sectioned at 7μm to analyze epicardial and ventricular phenotypes (using H&E staining) and immunohistochemical analysis. Immunohistochemical analysis was performed as described above using antibodies for VCAM-1 and α4 integrin.

Epicardial explant culture

Ventricles were dissected from E11.5 or older embryos with removal of the atria, outflow tract and atrioventricular cushions. The ventricles were cut in half so that each half included part of the right and left ventricle (i.e. bisected in the coronal plane). The ventricular pieces were placed epicardium side down on a fibronectin-coated 4-chamber glass slide (Nunc). Enough media was removed to create a meniscus to hold the ventricular pieces in place to allow the epicardium to attach to the FN-coated glass slide overnight. The following day, fresh media was added to each well and the myocardium was carefully removed from the epicardium leaving a lawn of epicardial cells attached to the slide. The following day, explants were treated with TGFβ₂ (10ng/ml), 9-cisRA (100nM), diluent or TGFβ₂ (10ng/ml)+9-cisRA (100nM) in serum-free media for 24

hours. Epicardial explants were then fixed for 10 minutes with 2% paraformaldehyde and rinsed with PBS following treatment. Explants were then immunostained for rat anti-VCAM-1 M/K2 (Santa Cruz) by first incubating in blocking buffer containing 1x PBS with 1% BSA and 0.3% Triton X-100 for 2 hours. Anti-VCAM-1 M/K2 was diluted 1:50 in 1% BSA in 1x PBS and incubated overnight at 4°C. The following day, the slides were washed with 1x PBS 3 times for 5 minutes each. Goat anti-rat secondary antibody conjugated to Alexa488 (Molecular Probes) was diluted in 1x PBS at a 1:100 concentration and incubated with the slides for 2 hours at room temperature. The slides were washed with 1x PBS and coverslipped using Vectashield mounting media containing DAPI nuclear stain (Vector Laboratories, Inc, Burlingame, CA). Explants were viewed and photographed on a Zeiss AXIO M2 fluorescent microscope. Quantification was performed using ImageJ software and the mean gray value for representative cells from each explant was found. Images were converted to gray scale and the antibody staining was seen as white pixels. The mean gray value represents the intensity of white pixels present in the sample, with a higher mean gray value indicating a higher level of expression. Statistics were calculated using a paired T-test.

VCAM-1-luciferase plasmid

Several attempts to generate the reported VCAM-1 promoter were made following the published protocol from Hosking et al. (2004) while simultaneously respectfully asking the authors to obtain an aliquot from the same lab (Dr. Muscat, Australia). After a long process of clearing the Material Transfer Agreement and Dr Muscat tracking down the plasmid for us (many months had passed) the plasmid was finally shipped to us. The plasmid contains the full-length VCAM-1 promoter inserted into the pGL2B-basic (pGL2B-Promega), which contains a luciferase reporter gene and ampicillin resistance gene (Figure 15). This plasmid is promoter-less until a promoter is

inserted into it indicating that any expression of luciferase seen is due to activation of the inserted promoter (i.e. VCAM-1).

The primers used to make the VCAM-1 luciferase plasmid (VC1889) were as follows (Hosking et al., 2004) and were also used to verify plasmid identity via PCR and direct sequencing:

1895 VCAM: GCCGGTACCGATCTACATAGCCACGGAGAG

19 VCAM: CGACCATCTTCACAGGCATTT

1887 KPN1 VCAM: CGGGGTACCATAGCCACGGAGAGTTCTT

1XHO1 VCAM: GCCCTCGAGTTCAAGTCTCTGCTTCAAAGCC

GLprimer 1: TGTATCTTATGGTACTGTAAGT

GLprimer 2: CTTTATGTTTTTGGCGTCTTCCA

These primers were used to verify that we had the correct plasmid (Figure 16) following amplification of the plasmid using *Escherichia coli* (*E. coli*). We also performed a restriction digest using KpnI and XhoI to remove the VCAM-1 promoter insert from the plasmid as another means of plasmid identity verification.

The plasmid was eluted from the filter paper in a 1.5 ml eppendorf tube containing 100 μ l of sterile filtered 1x PBS. The filter paper was incubated in 1x PBS overnight at 4°C. The CMV-Renilla luciferase plasmid was obtained from Promega and was used as an internal transfection efficiency control to normalize the luciferase data. Empty pGL2B-basic plasmid was used as a negative control. All plasmid DNA was transformed into OneShot Mach1 chemically competent *E. coli* cells (Invitrogen) per manufacturer's protocol. Transformed bacteria cells were grown on LB agar plates containing ampicillin at 37°C. Single colonies were selected and grown in small cultures for MiniPrep (Qiagen) to verify that we had the correct plasmids. When the plasmids were confirmed by sequencing, PCR and restriction digest, we grew the transformed bacteria in a large culture (500 ml) for MaxiPrep (Qiagen) to obtain a large amount of

Figure 15: Diagram of the mouse VCAM-1 promoter luciferase plasmid. A schematic diagram of the 1889 base pair portion of the mouse VCAM-1 promoter construct cloned into the pGLBasic luciferase reporter plasmid. Luc, luciferase reporter gene; F1 ori, origin of replication; Amp, ampicillin resistance gene. (Hosking et al., 2004)

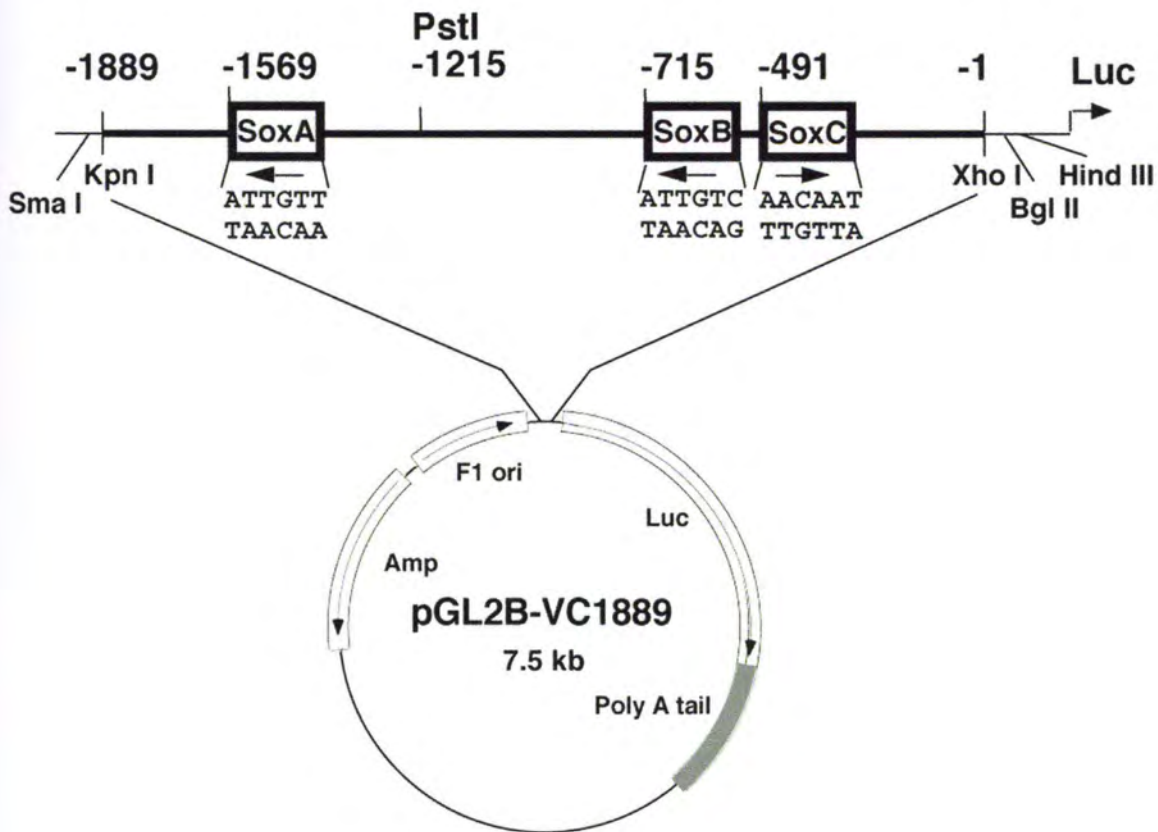
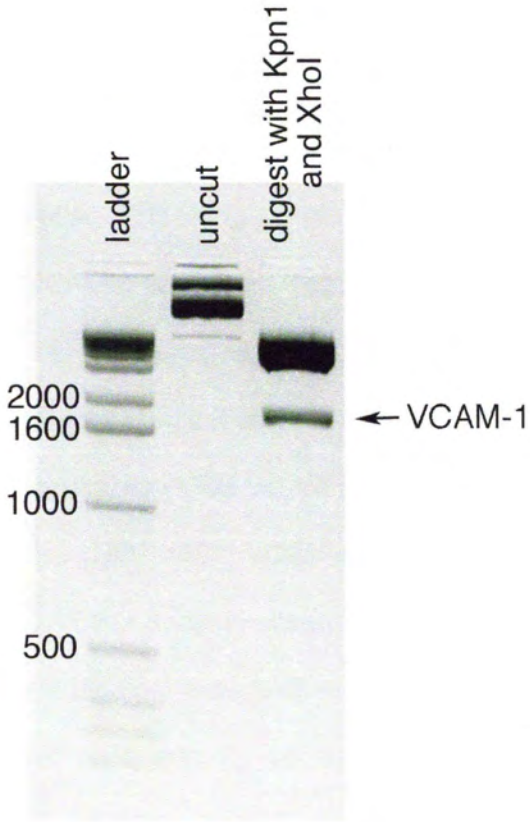
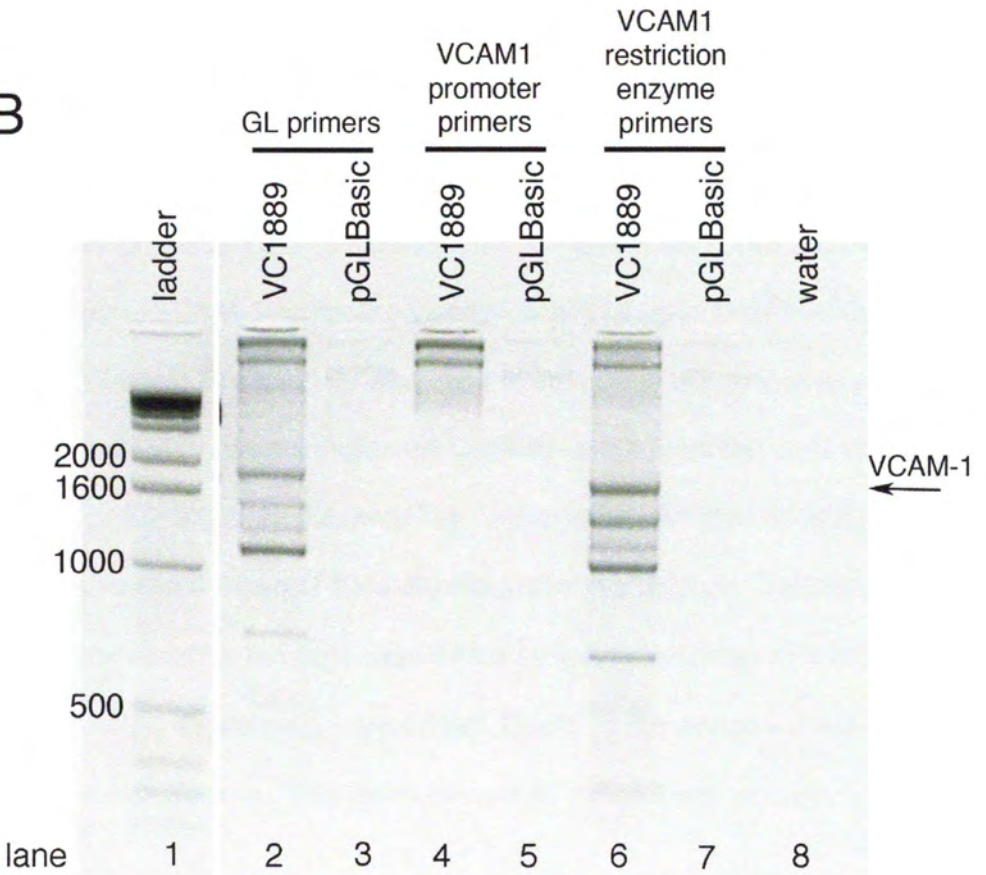


Figure 16: VC1889 plasmid restriction digest and VCAM-1 promoter PCR. A. The VC1889 luciferase plasmid was digested (lane 3) to verify the plasmid integrity. Digest with Kpn1 and Xho1 releases the VCAM-1 promoter element, which is 1889 basepairs. B. PCR with the GL primers (plasmid-specific, lane 2) and VCAM-1 restriction enzyme primers (specific to the inserted VCAM-1 plasmid, lane 6) also confirm a band at approximately 1889 basepairs. The empty plasmid (pGLBasic, lanes 3, 5 and 7) shows no bands from the PCR indicating that the VCAM-1 promoter is not present. PCR with the VCAM-1 primers is negative for the presence of the 1889 basepair product (lane 4), which is expected. In order to insert the VCAM-1 promoter sequence into the plasmid, restriction enzyme sites were inserted on the ends of the VCAM-1 promoter where these primers (VCAM1 promoter primers) would normally bind.

A



B



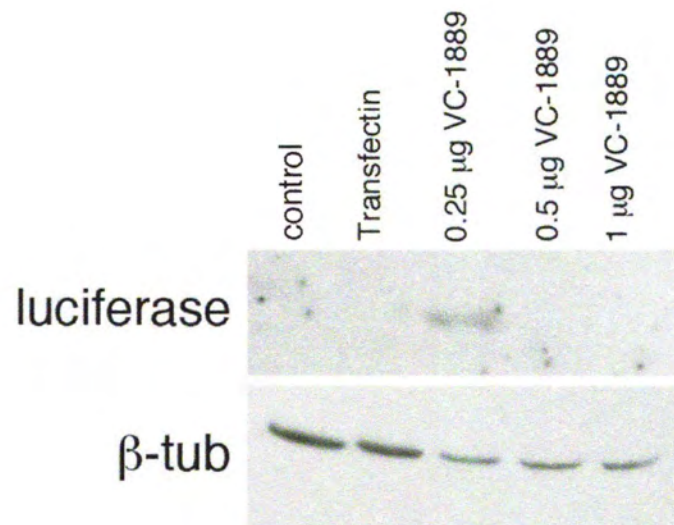
plasmid for transfection. Both the MiniPrep and MaxiPrep were performed via the manufacturer's recommendations.

In order to confirm that we had the correct VCAM-1-luciferase plasmid we performed a restriction digest at 37°C using the restriction enzymes Kpn1 (NEB) and Xho1 (NEB) to cut out the VCAM-1 promoter. The digest was run on a 2% agarose gel and can be seen in Figure 16. We also used PCR analysis to confirm that we had the correct plasmid using the primers above that were specific to the plasmid (GL primers), the promoter without restriction sites (1895 VCAM and 19 VCAM) and the promoter containing the restriction sites (1887 KPN1 VCAM and 1XHO1 VCAM) (Figure 16). The primers 1895 VCAM and 19 VCAM should not have produced a band if the restriction sites used for cloning into the plasmid were present, which can be seen in Figure 16. Sequencing was also used to verify that we had the correct plasmid. The VCAM-1-luciferase and CMV-Renilla luciferase plasmids were then used for assays.

VCAM-1-Luciferase analysis

Following passaging, 35 mm dishes were seeded with 100,000 REC cells. The dishes were grown to 75% confluency prior to transfection. The cells were transfected with 0.25 µg of VCAM-1-luciferase plasmid and 0.25 µg of CMV-Renilla luciferase plasmid. Western blot analysis was used to determine the optimal amount of plasmid to use for transfection using a luciferase antibody to measure the production of luciferase (Figure 17). For experiments, negative control cells were transfected with 0.25 µg of pGL2B-basic and 0.25 µg of CMV-Renilla luciferase plasmid. Twenty-four hours following transfection, the cells were treated with the indicated concentrations of TGFβ2 and/or 9-cisRA. Treatments were added directly to the dishes without changing the media from transfection. Twenty-four hours following treatment, the cells were

Figure 17: Western blot of luciferase protein following transfection with VC1889. Detergent extracts of REC cells transfected with different concentrations (0.25 μ g, 0.5 μ g and 1 μ g) of VC1889 plasmid were assayed for the presence of luciferase protein in order to determine the appropriate concentration to use for experiments. The 0.25 μ g transfection (lane 3) is the only one that produced luciferase and thus was the concentration used for experiments. Lanes 1 and 2 were negative controls.



harvested using Passive Lysis Buffer (Millipore) diluted to 1x concentration. Each dish was washed with 1x PBS, followed by addition of 200 μ l of 1x Passive Lysis Buffer. Each dish was scraped with a cell scraper and the buffer was transferred to a 1.5 ml eppendorf tube. Each sample was subjected to one freeze-thaw cycle prior to assaying for luciferase activity. Luciferase activity was analyzed using the DualGlo luciferase assay kit (Promega) per the manufacturer's recommendations using a luminometer. Each experiment was performed in triplicate. Statistics were calculated using a paired T-test between each treatment group.

Chapter 3: Results and Discussion

A. Expression patterns of VCAM-1 in $RXR\alpha^{-/-}$ at E9.5 and E10.5 are similar to WT

The expression of VCAM-1 was assessed using immunohistochemical analysis of paraffin embedded sections of WT and $RXR\alpha^{-/-}$ embryos. At E9.5, VCAM-1 protein was expressed throughout the myocardium (Figure 18). VCAM-1 was expressed in the PE but at levels lower than those seen in the atrial and ventricular myocardium in both WT and $RXR\alpha^{-/-}$ (Figure 18). Expression of VCAM-1 was also seen in budding PE cells as well as migrating PE cells moving to the myocardial surface in both the WT and $RXR\alpha^{-/-}$ (Figure 18). There were no detectable differences seen in the expression patterns of VCAM-1 between WT and $RXR\alpha^{-/-}$ in any area of the heart at E9.5. Previous studies by others have shown that VCAM-1 is expressed in the PE and myocardium at this stage of mouse development (Yang et al., 1995) hence our results in the WT are consistent with other published results. No differences in expression of integrin $\alpha 4$ between WT and $RXR\alpha^{-/-}$ were observed (Figure 19 and Jenkins and Kubalak, unpublished). Both VCAM-1 and integrin $\alpha 4$ are necessary for PE bud formation as well as initial PE cell attachment to the myocardium for epicardium formation. Since the epicardium will form in the $RXR\alpha^{-/-}$ mouse heart, it is not surprising for VCAM-1 and integrin $\alpha 4$ levels to be similar between WT and $RXR\alpha^{-/-}$. TGF $\beta 2$ is expressed in the PE (Molin et al., 2003) and TGF $\beta 2$ mRNA is elevated in $RXR\alpha^{-/-}$ PE (Jenkins and Kubalak, unpublished). At this age the signaling from TGF $\beta 2$ may not be elevated enough to affect VCAM-1 levels. However, no quantitative studies of VCAM-1 expression at E9.5 have been performed (i.e. real time PCR or western blot).

At E10.5, VCAM-1 was expressed throughout the atrial and ventricular myocardium and can be found in body wall of both the WT and $RXR\alpha^{-/-}$. VCAM-1 expression was not observed in the endocardium of WT and $RXR\alpha^{-/-}$ or in the epicardium of the WT (Figure 20), which is consistent with the current established expression pattern of VCAM-1 in the heart (Yang et al., 1995). There were few epicardial cells present on the myocardium in the $RXR\alpha^{-/-}$ heart as is common with this mouse due to the delay in epicardium formation (Jenkins et al., 2005) and there was no expression of VCAM-1 in the few epicardial cells present (Figure 20). Upon gross examination of the embryos at E10.5, there were no detectable differences in the histological phenotype of the hearts between WT and $RXR\alpha^{-/-}$ mice. At E10.5 in development, the $RXR\alpha^{-/-}$ mouse heart begins to exhibit phenotypic differences from the WT, with delayed epicardium formation observed and fewer PE buds present. A change in VCAM-1 could decrease PE bud formation, which would result in a delay in epicardium formation. Since analysis of VCAM-1 has only been done through immunohistochemistry at this age and at E9.5, it could be that there are some slight differences in VCAM-1 not observable through this method. Small changes in protein levels in embryonic development can have large consequences to the embryo. It is possible that a slight increase or decrease in VCAM-1 is present but cannot be found from our current experimental analysis.

Figure 18: IHC analysis of VCAM-1 expression at E9.5 in the WT and $RXR\alpha^{-/-}$ mouse heart. VCAM-1 expression (green) is seen in the PE, PE buds and ventricular myocardium in hearts from both WT (B and C) and $RXR\alpha^{-/-}$ (E and F). No histological abnormalities were apparent in the hearts of E9.5 $RXR\alpha^{-/-}$ (D) as compared to the WT (A). The arrow indicates PE buds that are migrating to the surface of the myocardium. Atr, atrium; Vent, ventricle; PE, proepicardium. Green- VCAM-1; Blue- ToPro3 nuclear stain. Images are representative of two experiments (2 litters) each having immunostained sections from the hearts of one WT and one $RXR\alpha^{-/-}$ embryo from the same litter.

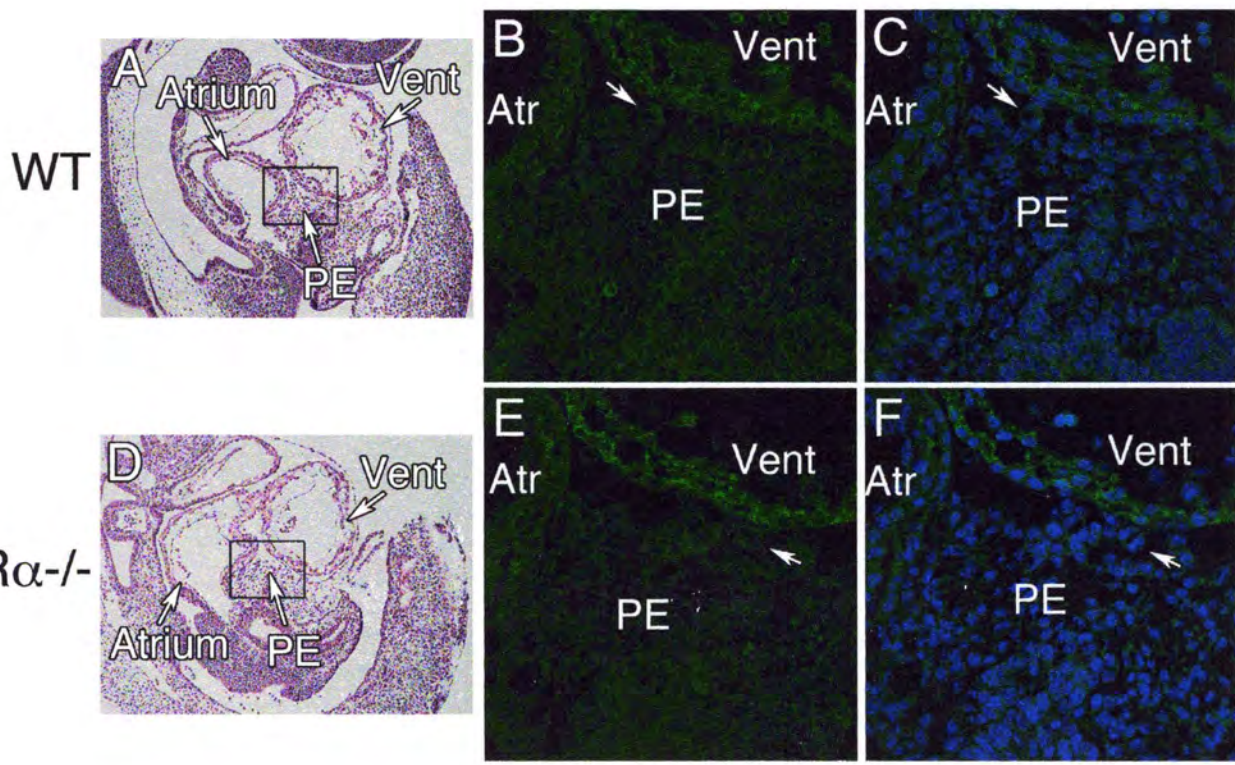
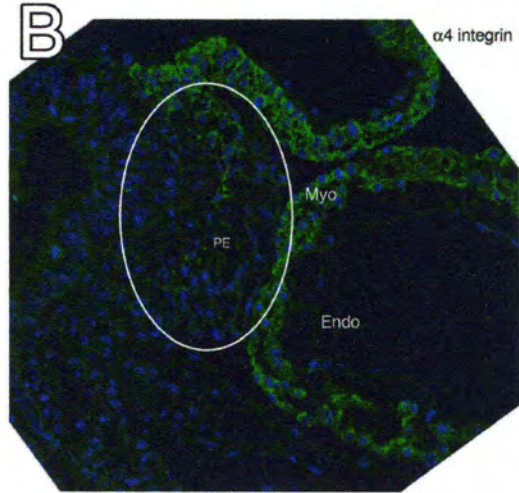
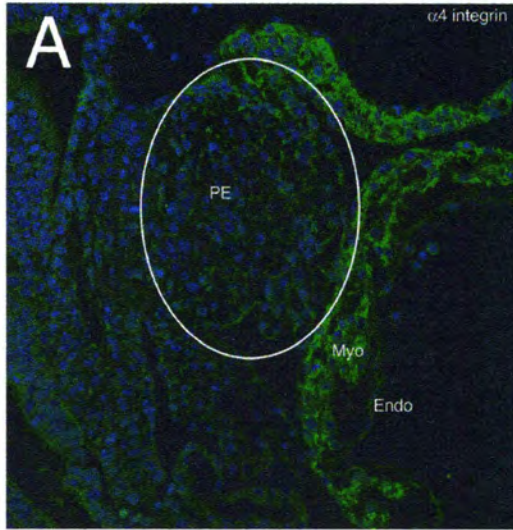


Figure 19: IHC analysis of integrin $\alpha 4$ subunit expression at E9.5 and E10.5 in the WT and $RXR\alpha^{-/-}$ mouse heart. Integrin $\alpha 4$ subunits expression (green) is seen in the PE and myocardium of the WT (A) and $RXR\alpha^{-/-}$ (B) at E9.5. Integrin $\alpha 4$ expression is seen in the epicardium and myocardium of the WT (C) and $RXR\alpha^{-/-}$ (D) at E10.5. BW, body wall; PE, proepicardium; Myo, myocardium; Endo, endocardium; Epi, epicardium. Green- integrin $\alpha 4$; Blue- ToPro3 nuclear stain. Images are representative of two experiments (2 litters from each stage) each having immunostained sections from the hearts of one WT and one $RXR\alpha^{-/-}$ embryo from the same litter.

WT

RXR $\alpha^{-/-}$

E9.5



E10.5

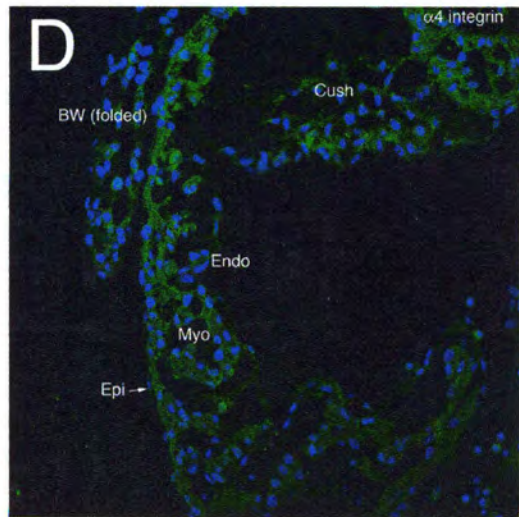
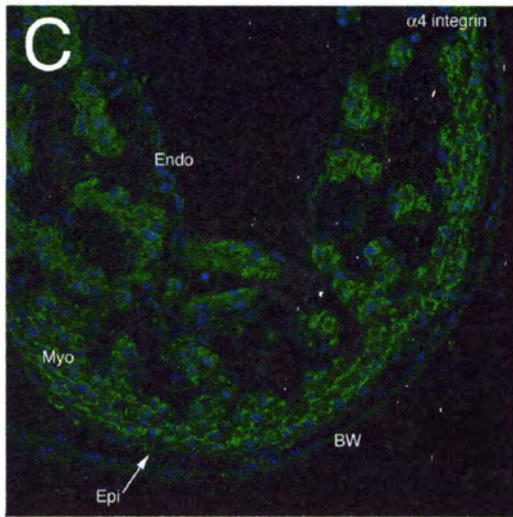
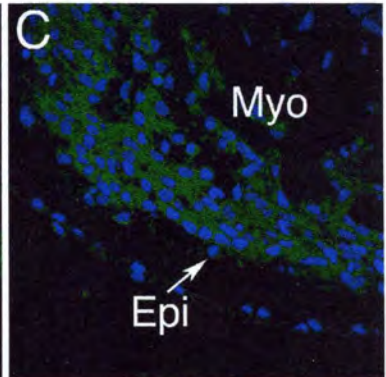
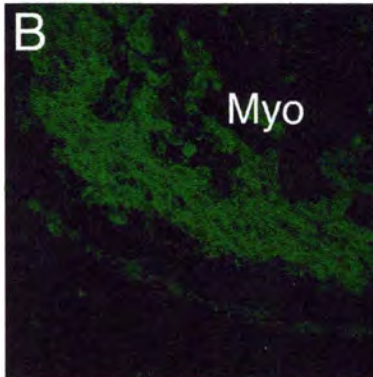
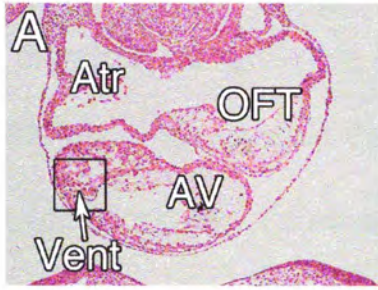
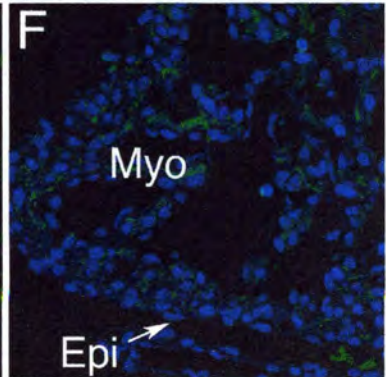
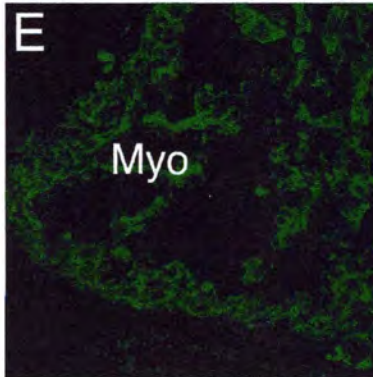
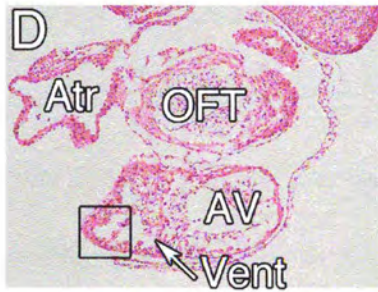


Figure 20: IHC analysis of VCAM-1 expression at E10.5 in the WT and $RXR\alpha^{-/-}$ mouse heart. VCAM-1 (green) is expressed in the myocardium and body wall in both the WT (B and C) and $RXR\alpha^{-/-}$ (E and F). The ventricular myocardium in the $RXR\alpha^{-/-}$ mouse heart is thinner (D) than the ventricular myocardium in the WT (A). Boxed area in A is found in panels B and C. Boxed area in D is found in E and F. Myo, myocardium; Epi, epicardium; Atr, atrium; OFT, outflow tract; AV, atrioventricular junction; Vent, ventricle. Green- VCAM-1; Blue- ToPro3 nuclear stain. Images are representative of two experiments (2 litters) each having immunostained sections from the hearts of one WT and one $RXR\alpha^{-/-}$ embryo from the same litter.

WT



RXR α ^{-/-}



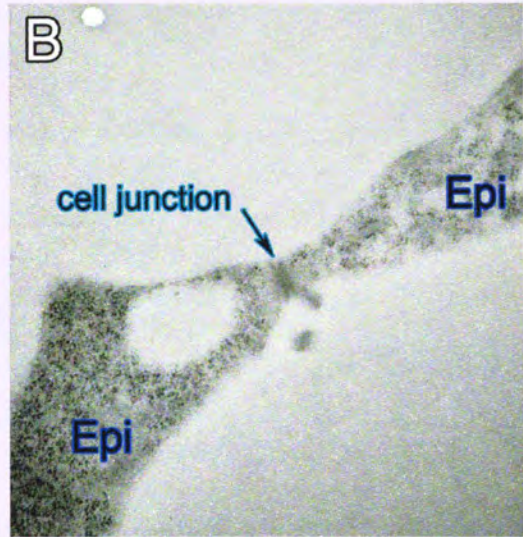
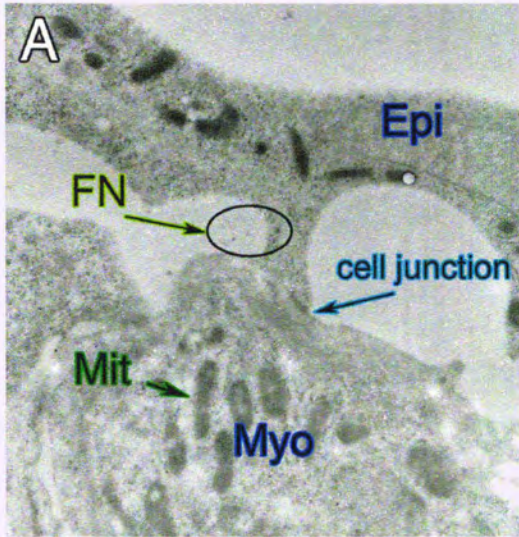
B. TEM of WT and RXR α -/- hearts at E10.5

From previous studies of the RXR α -/- mouse, there is a delay in formation of the epicardium in the RXR α -/- mouse (approximately 0.5-1.0 day later than WT) and, once formed, will be detached from the myocardium at E12.5 when the epicardium is normally closely associated with the underlying myocardium. Clearly, there must be an initial attachment of proepicardial buds that allows the epicardium to form in the mutant. This is in contrast to what was found in the integrin α 4 and VCAM-1 KOs where a lack of attachment prevents the formation of the epicardium (Kwee et al., 1995; Yang et al., 1995). In the RXR α -/- mouse heart there are a few areas of the myocardium where proepicardial cells do attach. However, since there are large areas where the epicardium is not attached, intercellular junctions were examined at the ultrastructural level. TEM analysis was used to examine cell junctions in more detail. In the RXR α -/- mouse heart, cellular junctions were harder to find between myocytes and epicardial cells as shown in Figure 21. However, cell junctions between adjacent epicardial cells were readily visible, therefore defects in detachment are most likely between epicardium and myocardium and not between adjacent epicardial cells (Figure 21). This is not surprising because there is a complete epicardium that forms in the RXR α -/- mouse heart, indicating that the epicardial cells will attach to each other however fail to remain attached to the myocardium.

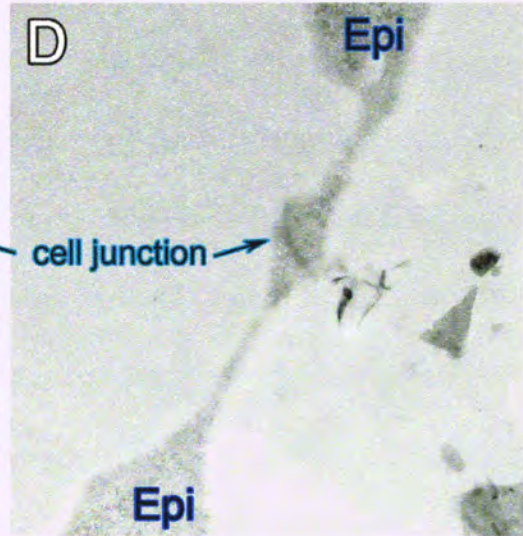
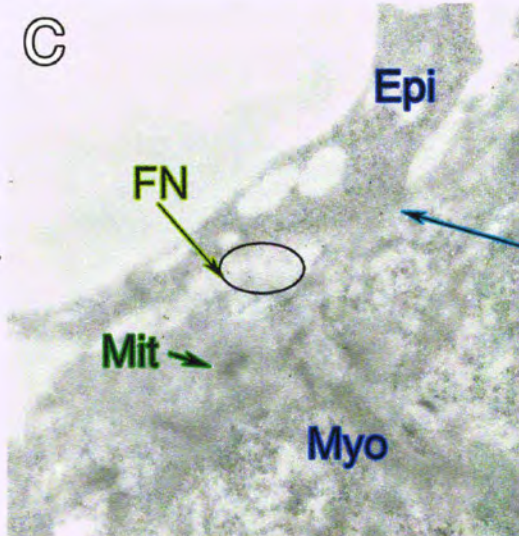
Also evident in the micrographs of the RXR α -/- mouse heart was the decrease in visible mitochondria as well as free ribosomes (Figure 21). This is also not surprising because it has been previously reported that the RXR α -/- mice have metabolic deficiencies in addition to heart defects (Ruiz-Lozano et al., 1998). Data from this paper, however, reported an increased density of mitochondria per cell possibly as a feedback mechanism responding to the decreased metabolic state (Ruiz-Lozano et al., 1998).

Figure 21: Immunogold TEM analysis of epicardium/myocardium junctions in E10.5 WT and $RXR\alpha^{-/-}$ mouse hearts. The WT epicardium/myocardium junction (A) has a visible cell junction and immunogold-labelled FN (black dots) present in the subepicardial space. The epicardial cell junction also has a well-defined junction (B). The $RXR\alpha^{-/-}$ epicardium/myocardium junction has a less well-defined cell junction (C) than the WT (A). Immunogold-labelled FN is also present in the subepicardial space (black dots in C). The cell junction between epicardial cells is well defined (D). Epi, epicardium; Myo, myocardium; FN, fibronectin; Mit, mitochondria

WT
E10.5



RXR α ^{-/-}
E10.5



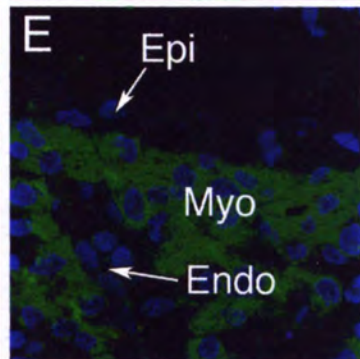
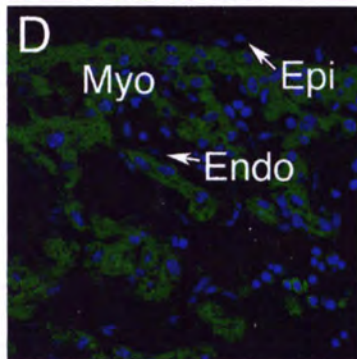
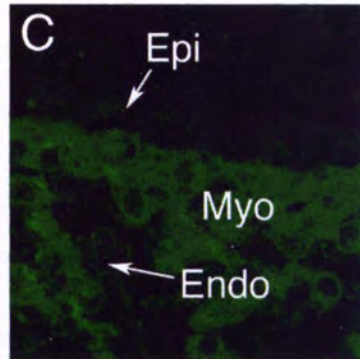
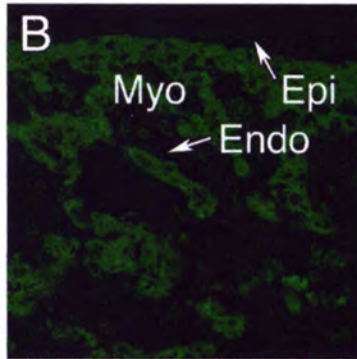
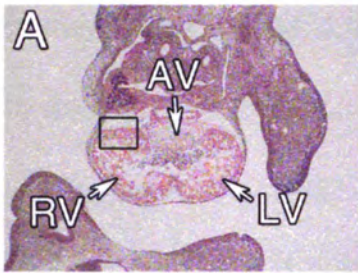
This observation in E12.5 embryos was not statistically significant (Ruiz-Lozano et al., 1998). It is possible that from E10.5 (fewer mitochondria) to E13.5 (more mitochondria) the heart is trying to make up for the metabolic deficiencies by producing more mitochondria. However, since metabolic deficiencies still exist at E13.5, the increase in mitochondria does not completely restore function.

C. VCAM-1 is misexpressed in the epicardium of the $RXR\alpha^{-/-}$ mouse heart at E11.5

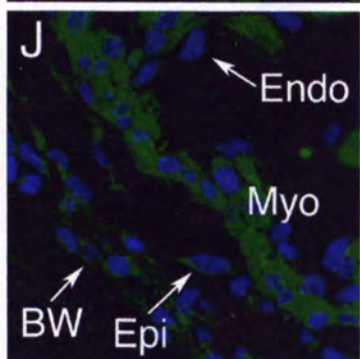
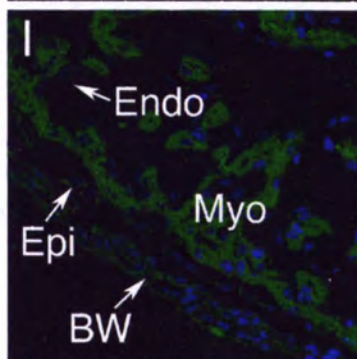
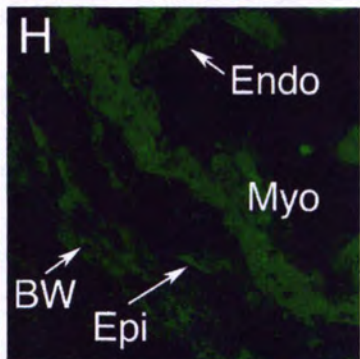
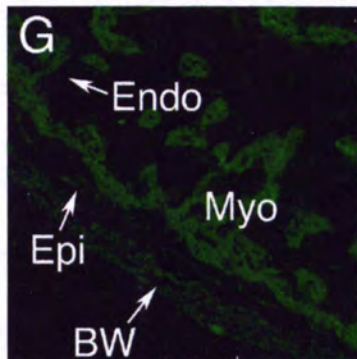
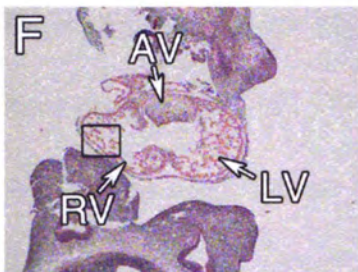
Examining embryos just prior to full epicardial attachment at E11.5, VCAM-1 was expressed throughout the atrial and ventricular myocardium and not in the endocardium of both the WT and $RXR\alpha^{-/-}$ as shown by immunohistochemistry (Figure 22). VCAM-1 was not expressed in the epicardium of the WT but was, however, expressed in the epicardium of the $RXR\alpha^{-/-}$ mouse (Figure 22). Others have shown that VCAM-1 is not expressed in the epicardium and is expressed only in the myocardium of the heart (Kwee et al, 1995). Expression of VCAM-1 in the epicardium has not been reported previously in any mouse model and represents a novel finding in heart development. Currently the role of misexpression of VCAM-1 in the epicardium of the $RXR\alpha^{-/-}$ mouse is not known but it is speculated that it could adversely affect cell-cell adhesion between the epicardium and myocardium as well as interfere with epicardial EMT. Indeed, the $RXR\alpha^{-/-}$ mouse has been previously reported to have fewer epicardial-derived cells in the heart (Merki et al., 2005) and VCAM-1 has been shown to negatively affect EMT (Dokic and Dettman, 2006). Together, these results suggest that VCAM-1 may play a role not only in the apparent defective cell adhesion found in the mutant but also the blunted EMT observed in the $RXR\alpha^{-/-}$ mouse epicardium (Ruiz-Lozano and Kubalak, unpublished), which will be discussed further in Chapter 4.

Figure 22: IHC analysis of VCAM-1 expression in hearts of E11.5 in the WT and $RXR\alpha^{-/-}$ mice. The WT mouse has expression of VCAM-1 in the myocardium but not in the endocardium or epicardium (B-E). The $RXR\alpha^{-/-}$ mouse heart has expression of VCAM-1 in the myocardium and also in the epicardium (G-J). AV, atrioventricular junction; RV, right ventricle; LV, left ventricle; Myo, myocardium; Endo, endocardium; Epi, epicardium; BW, body wall. Green- VCAM-1; Blue- ToPro3 nuclear stain. Images are representative of three experiments (3 litters) each having immunostained sections from the hearts of one WT and one $RXR\alpha^{-/-}$ embryo from the same litter.

WT



RXR α ^{-/-}



In order to get a more quantitative measure of VCAM-1 levels, real time PCR analysis of RNA from E11.5 whole hearts was performed. An increase in VCAM-1 mRNA was observed at E11.5 in the $RXR\alpha^{-/-}$ mouse heart compared to the WT (Figure 23). However, when protein levels of VCAM-1 were analyzed using Western blot analysis of E11.5 whole hearts, no differences were found between WT and $RXR\alpha^{-/-}$ (Figure 24). The increased VCAM-1 mRNA might not have been translated into protein at the time of the assay. In the $RXR\alpha^{-/-}$ mouse heart there is an increase in MLC2a mRNA observed (Dyson et al., 1995) without an increase in protein level (Kubalak et al., 2002) so it is plausible that VCAM-1 mRNA could be increased without an increase in protein. The misexpressed VCAM-1 protein at E11.5 appeared to be localized to the epicardium and was perhaps not significant enough to detect in whole heart. At this time it is not entirely known what the consequence are of having VCAM-1 expression in the epicardium. Altering the normal expression pattern of a cellular adhesion molecule might have a negative impact on epicardial cell adhesion or may have more significant effect on epicardium function such affecting epicardial EMT. VCAM-1 has been shown to negatively affect epicardial EMT (Dokic and Dettman, 2006). Soluble VCAM-1 treatments increased the association of E-cadherin and β -catenin in cellular junctions thereby decreasing epicardial EMT (Dokic and Dettman, 2006). So it is possible that misexpressed VCAM-1 in the epicardium is strengthening epicardial cell adhesion and decreasing EMT.

No apparent differences in integrin α 4 protein were seen from immunohistochemical analysis (Figure 25) between E11.5 WT and $RXR\alpha^{-/-}$. However preliminary studies using real time PCR analysis suggested there may be an increase in integrin α 4 mRNA in the $RXR\alpha^{-/-}$ mouse heart in comparison to the WT heart (Figure

Figure 23: Real time PCR analysis of VCAM-1 mRNA in hearts of E11.5 in WT and $RXR\alpha^{-/-}$ mice. Levels of mRNA are represented as a fold change from WT using the comparative Ct method. The mRNA from E11.5 $RXR\alpha^{-/-}$ whole heart have approximately 2.75 fold higher level of VCAM-1 mRNA as compared to the average of the WT samples. The error bar represents \pm standard error of the mean (SEM). The plotted values are mean fold change from the WT values. This experiment was performed in triplicate on two pairs of WT and $RXR\alpha^{-/-}$ whole hearts.

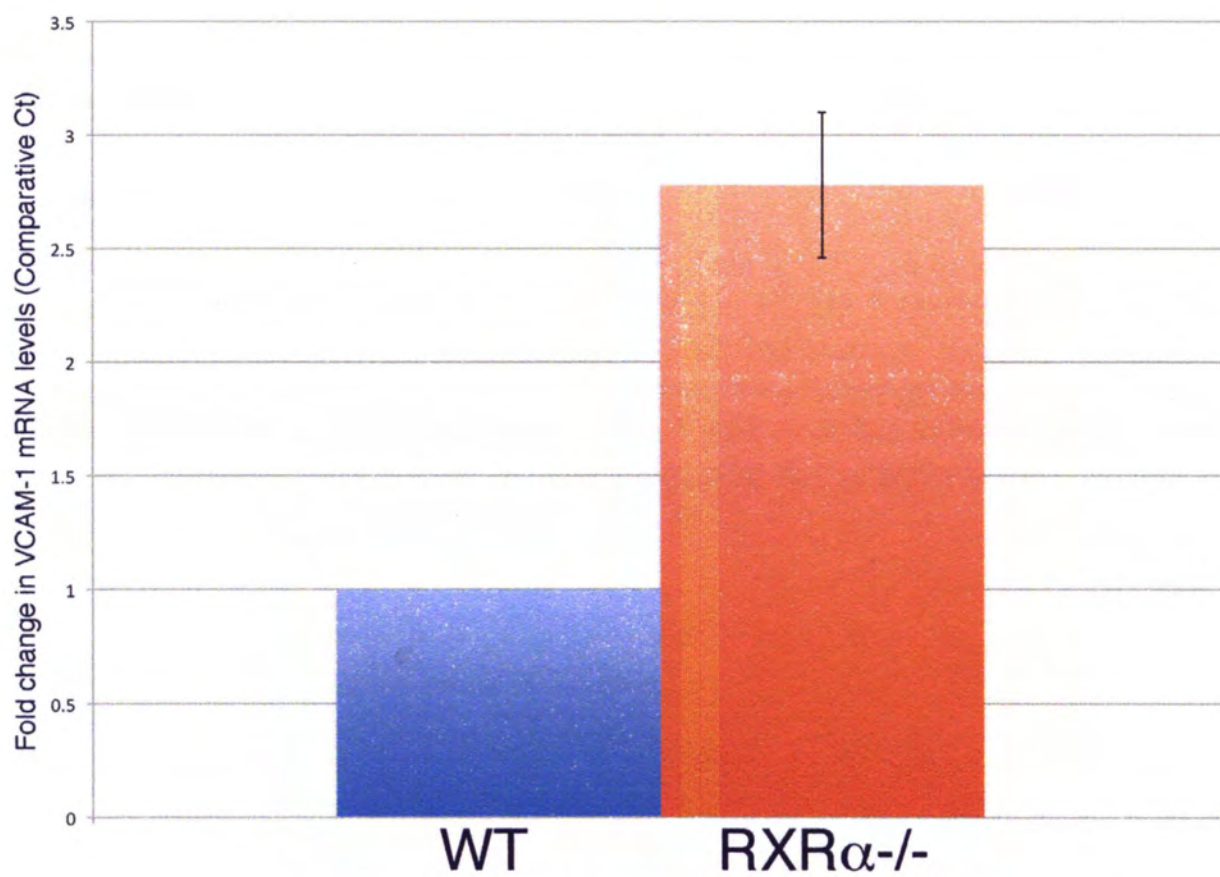


Figure 24: Western blot analysis of VCAM-1 protein in E11.5 in WT and RXR α ^{-/-} hearts. There was no statistically significant difference in VCAM-1 protein levels between WT and RXR α ^{-/-}. Protein levels are represented as fold change from the average of the WT samples. The plotted values represent the mean fold change from WT of three experiments performed on a WT and RXR α ^{-/-} pair from the same litter (3 litters total). The error bar represents \pm SEM. A representative blot is shown.

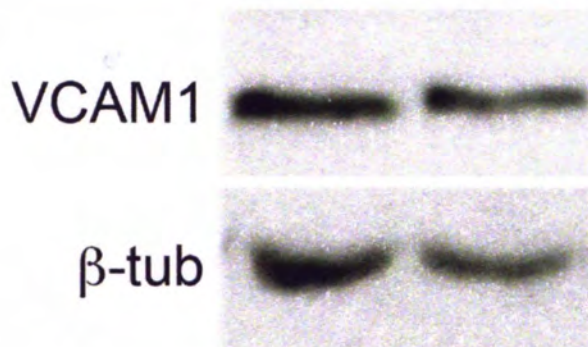
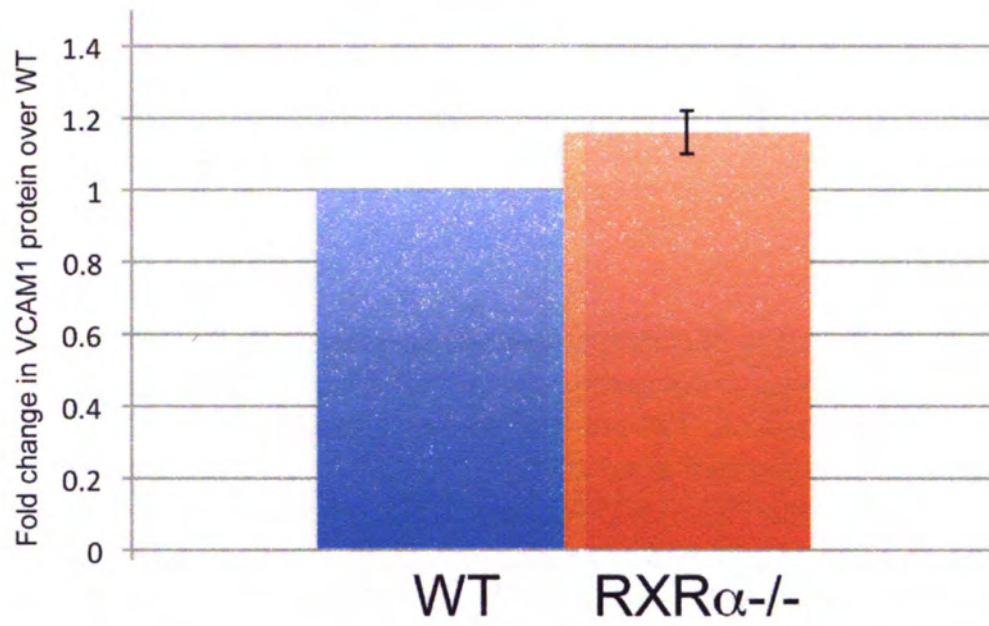


Figure 25: IHC analysis of integrin $\alpha 4$ subunit expression in E11.5 and E12.5 in the WT and $RXR\alpha^{-/-}$ hearts. Integrin $\alpha 4$ subunit expression is immunologically detected in the myocardium, epicardium and body wall of both the WT (A) and $RXR\alpha^{-/-}$ (B) at E11.5 with no apparent differences. At E12.5, integrin $\alpha 4$ is expressed in the epicardium, myocardium and body wall of the WT (C) and $RXR\alpha^{-/-}$ (D) with no apparent expression differences in levels or pattern. Myo, myocardium; BW, body wall; Epi, epicardium; Endo, endocardium. Green- integrin $\alpha 4$; Blue- ToPro3 nuclear stain. Images are representative of two experiments (2 litters) each having immunostained sections from the hearts of one WT and one $RXR\alpha^{-/-}$ embryo from the same litter.

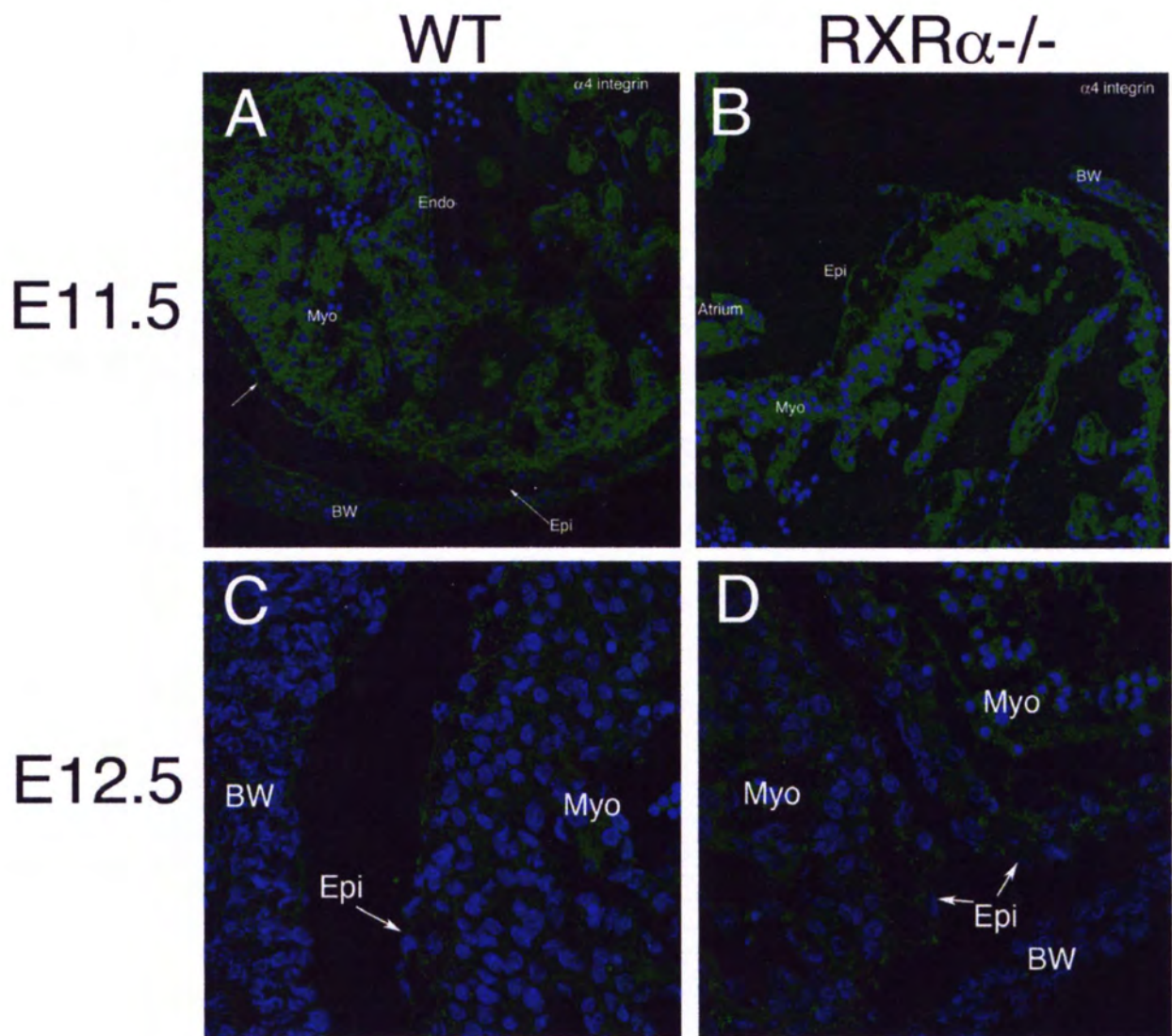
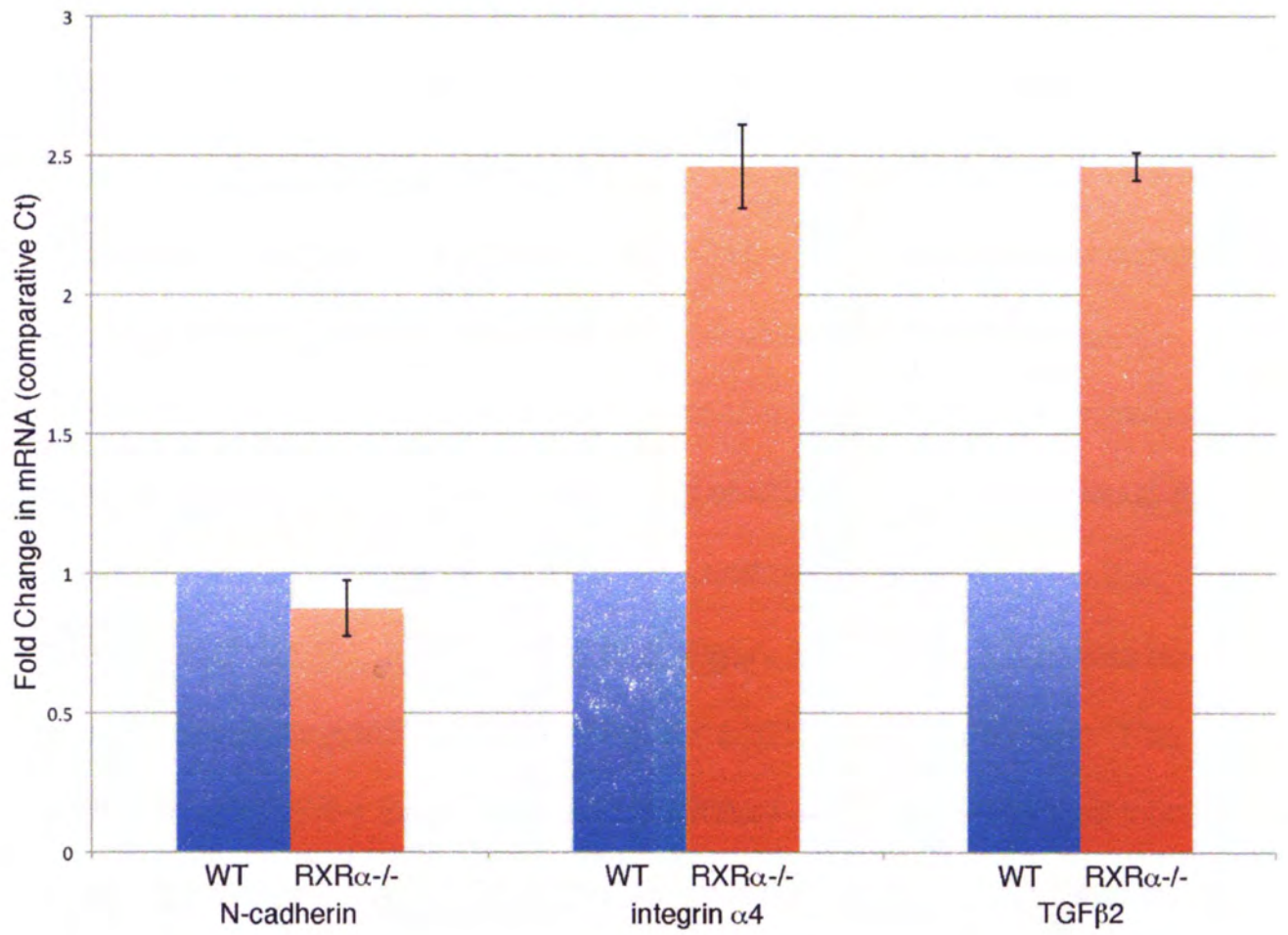


Figure 26: Real time PCR analysis of N-cadherin, integrin α 4 subunit and TGF β 2 at E11.5 in the WT and RXR α ^{-/-} heart. All mRNA levels are represented as a fold change from the WT using the comparative Ct method. N-cadherin is no different between WT and RXR α ^{-/-}. Integrin α 4 appears to have higher mRNA levels in the RXR α ^{-/-} mouse heart than the WT. TGF β 2 mRNA levels are higher in the RXR α ^{-/-} mouse heart than in the WT. This experiment was performed in triplicate on one WT and one RXR α ^{-/-} each from the same litter. Error bars represent the range of values for the triplicates.



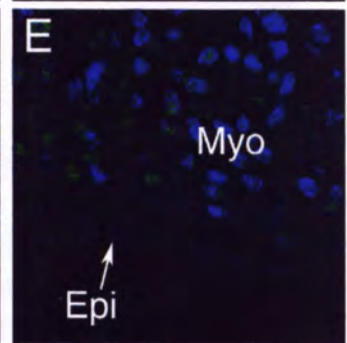
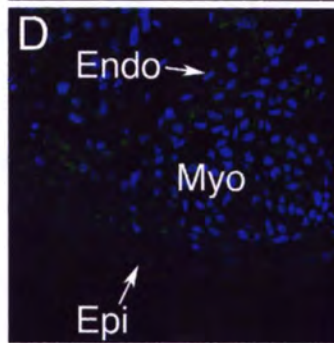
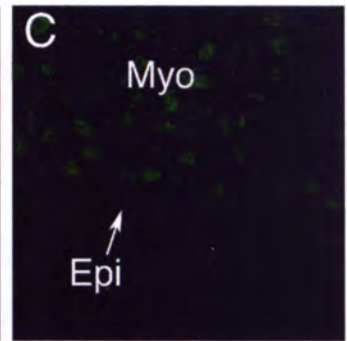
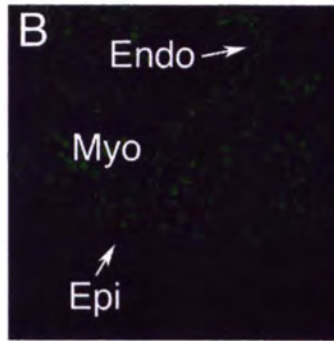
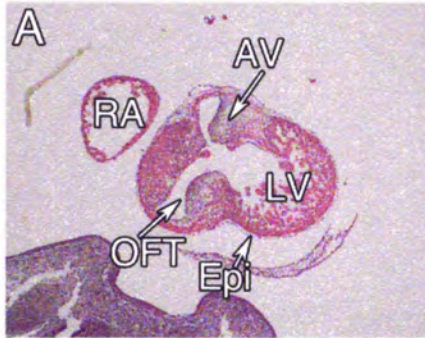
26). No difference in the mRNA expression of N-cadherin was seen between E11.5 WT and RXR α ^{-/-} (Figure 26). Increased TGF β 2 mRNA was found in the RXR α ^{-/-} mouse heart in comparison to the WT which served as a positive control and is consistent with our previous finding of increased TGF β 2 mRNA in the RXR α ^{-/-} heart during midgestation (Kubalak et al., 2002). This preliminary real time experiment (n=1) would need to be repeated prior to drawing any major conclusions from these results.

D. VCAM-1 expression is increased in RXR α ^{-/-} hearts at E12.5 and E13.5

At E12.5, the epicardium is normally in close association with the myocardium. EMT is altered in the RXR α ^{-/-} epicardium, as shown from previous studies with this mouse model (Ruiz-Lozano and Kubalak, unpublished), so it is possible that the disassociation of the epicardium from the myocardium (i.e., epicardial bubbling) is negatively impacting EMT. Relatively low levels of VCAM-1 were expressed in the E12.5 myocardium of both the WT and RXR α ^{-/-} and none was detected in the endocardium at E12.5 (Figure 27) or at E13.5 (Figure 28). VCAM-1 was also not expressed in the endocardial cushions of the AV or OFT (data not shown). The misexpression of VCAM-1 found in the E11.5 RXR α ^{-/-} epicardium was also found in the E12.5 and E13.5 RXR α ^{-/-} epicardium. No VCAM-1 expression was seen in the WT epicardium at either age (Figures 27 and 28). Analysis of VCAM-1 mRNA expression using real time PCR showed that VCAM-1 mRNA was elevated in the RXR α ^{-/-} heart at both E12.5 (Figure 29) and E13.5 (Figure 30) in comparison to the WT. When protein levels in the E12.5 and E13.5 WT and RXR α ^{-/-} heart were analyzed using Western blot analysis, higher levels of VCAM-1 protein were seen at both E12.5 (Figure 31) and E13.5 (Figure 32) RXR α ^{-/-} than in WT. At E11.5, the epicardium is normally dissociated

Figure 27: IHC analysis of VCAM-1 expression at E12.5 in the WT and $\text{RXR}\alpha^{-/-}$ heart. VCAM-1 is expressed in the myocardium but not the epicardium or endocardium of the WT heart (B-E). VCAM-1 is expressed in the myocardium at higher levels in the $\text{RXR}\alpha^{-/-}$ mouse (G-J) than the WT. VCAM-1 is also expressed in the epicardium in the $\text{RXR}\alpha^{-/-}$ mouse (G-J). H&E sections of the WT (A) and $\text{RXR}\alpha^{-/-}$ (F). Bubbling of the epicardium can be seen in the $\text{RXR}\alpha^{-/-}$ mouse (G-J). RA, right atrium; OFT, outflow tract; AV, atrioventricular junction; LV, left ventricle; RV, right ventricle; Epi, epicardium; Myo, myocardium; Endo, endocardium. Green- VCAM-1; Blue- ToPro3 nuclear stain. Images are representative of three experiments (3 litters) each having immunostained sections from the hearts of one WT and one $\text{RXR}\alpha^{-/-}$ embryo from the same litter.

WT



RXR α ^{-/-}

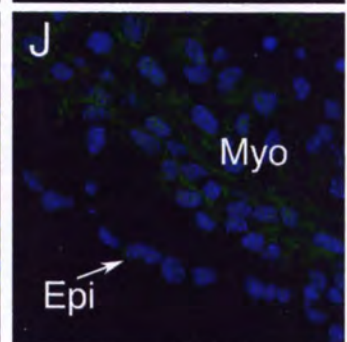
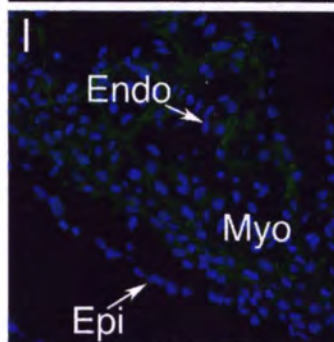
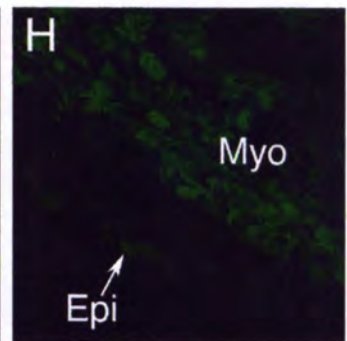
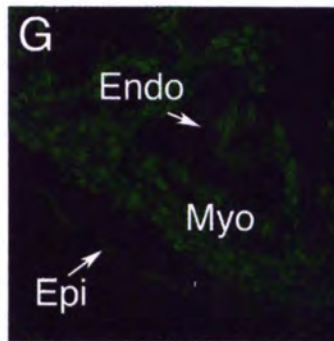
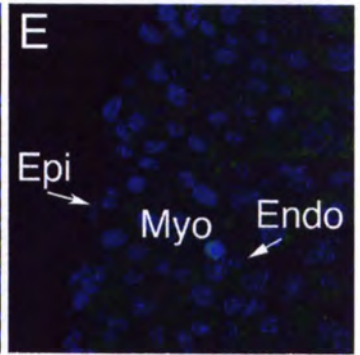
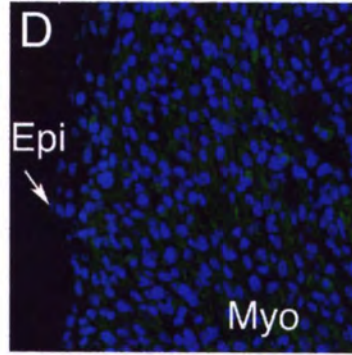
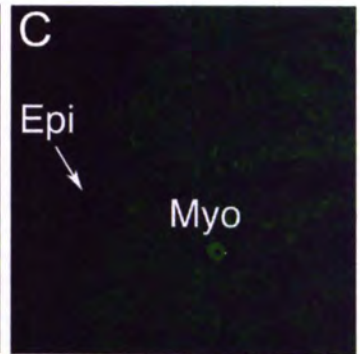
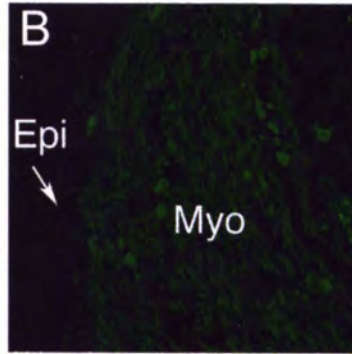
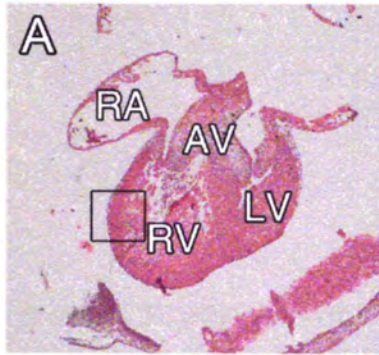


Figure 28: IHC analysis of VCAM-1 expression at E13.5 in the WT and $RXR\alpha^{-/-}$ heart. VCAM-1 is expressed in the myocardium but not the epicardium or endocardium of the WT heart (B-E). VCAM-1 is expressed in the myocardium at higher levels in the $RXR\alpha^{-/-}$ mouse (G-J) than the WT. VCAM-1 is also expressed in the epicardium in the $RXR\alpha^{-/-}$ mouse (G-J). H&E sections of the WT (A) and $RXR\alpha^{-/-}$ (F). Bubbling of the epicardium can be seen in the $RXR\alpha^{-/-}$ mouse (G-J). RA, right atrium; LA, left atrium; AV, atrioventricular junction; LV, left ventricle; RV, right ventricle; Epi, epicardium; Myo, myocardium; Endo, endocardium. Green- VCAM-1; Blue- ToPro3 nuclear stain. Images are representative of three experiments (3 litters) each having immunostained sections from the hearts of one WT and one $RXR\alpha^{-/-}$ embryo from the same litter.

WT



RXR α ^{-/-}

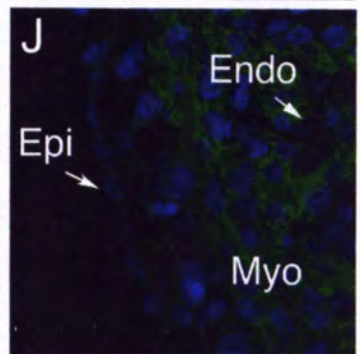
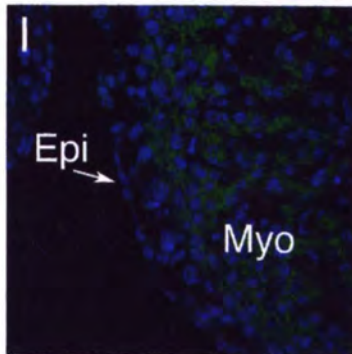
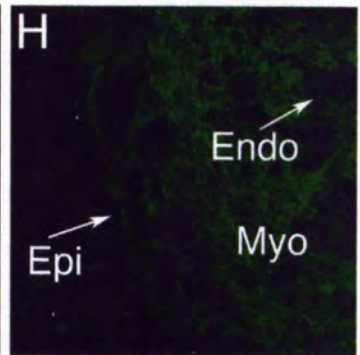
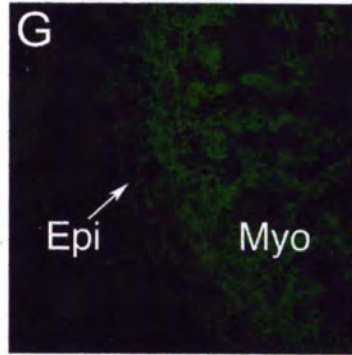
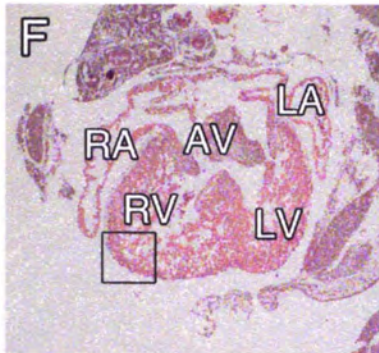


Figure 29: Real time PCR analysis of VCAM-1 mRNA at E12.5 in WT and RXR α ^{-/-} heart. VCAM-1 mRNA levels are almost 5-fold higher in the RXR α ^{-/-} mouse heart than in the WT. Values are expressed as a fold difference from WT using the comparative Ct method. The error bar represents \pm standard error of the mean (SEM). The plotted values are mean fold change from the WT values. This experiment was performed in triplicate on two pairs of WT and RXR α ^{-/-} whole hearts.

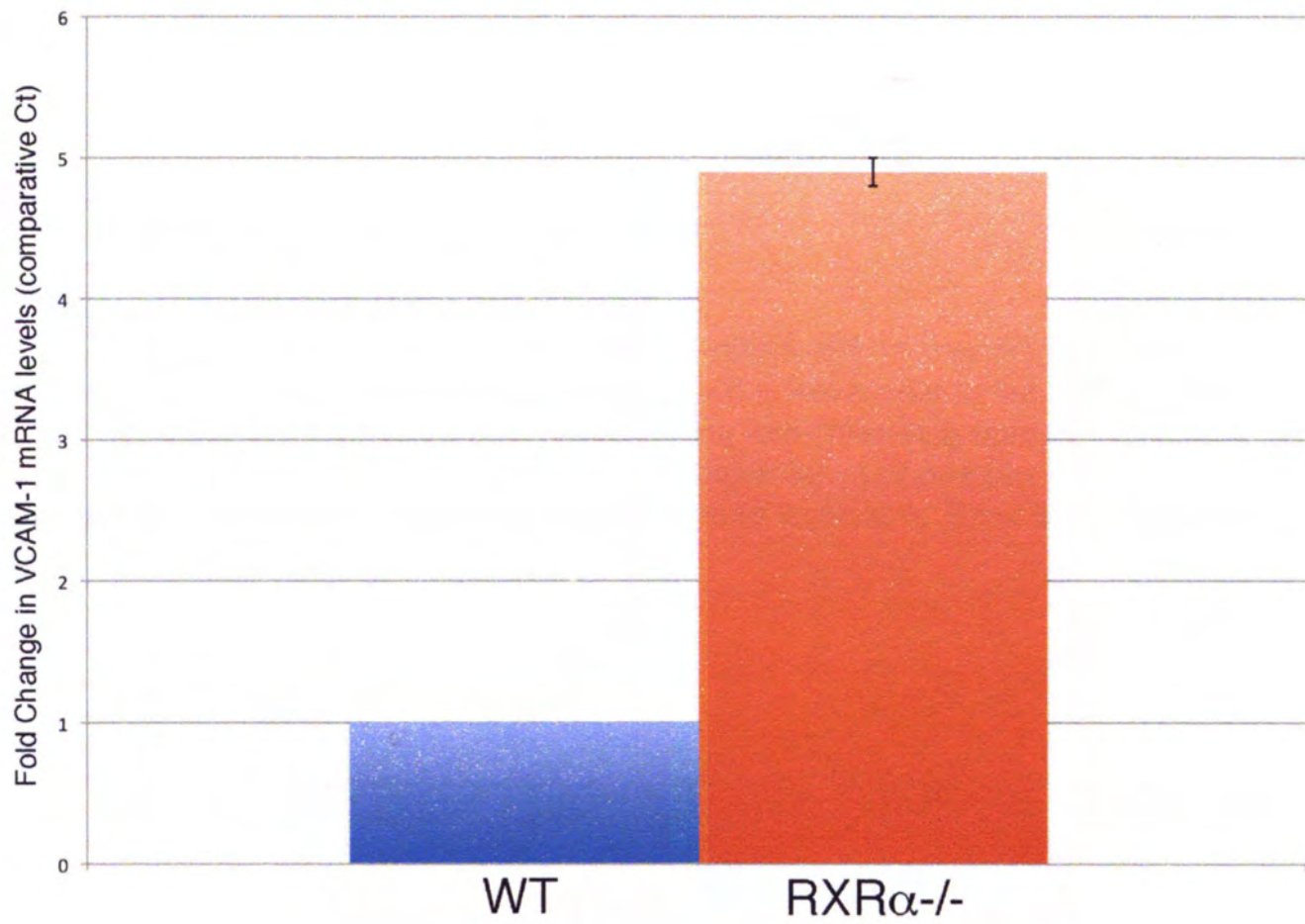


Figure 30: Real time PCR analysis of VCAM-1 mRNA at E13.5 in WT and RXR α ^{-/-} heart. VCAM-1 mRNA levels are approximately 8.5-fold higher in the RXR α ^{-/-} mouse heart than in the WT. Values are expressed as a fold difference from WT using the comparative Ct method. This experiment is representative of one pair of WT and RXR α ^{-/-} whole heart mRNA samples performed with three replicates. Error bars represent the \pm SEM of the triplicates

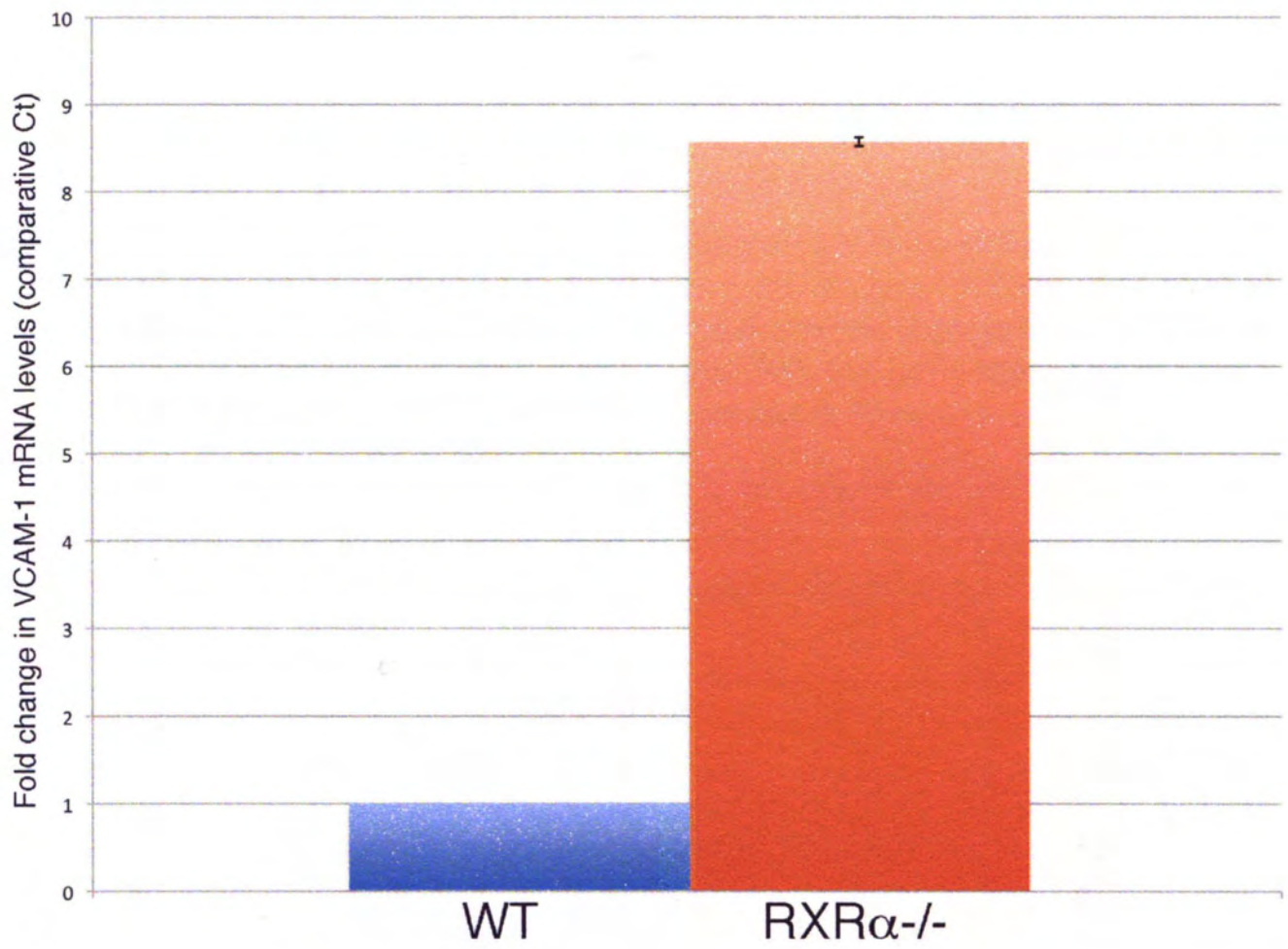
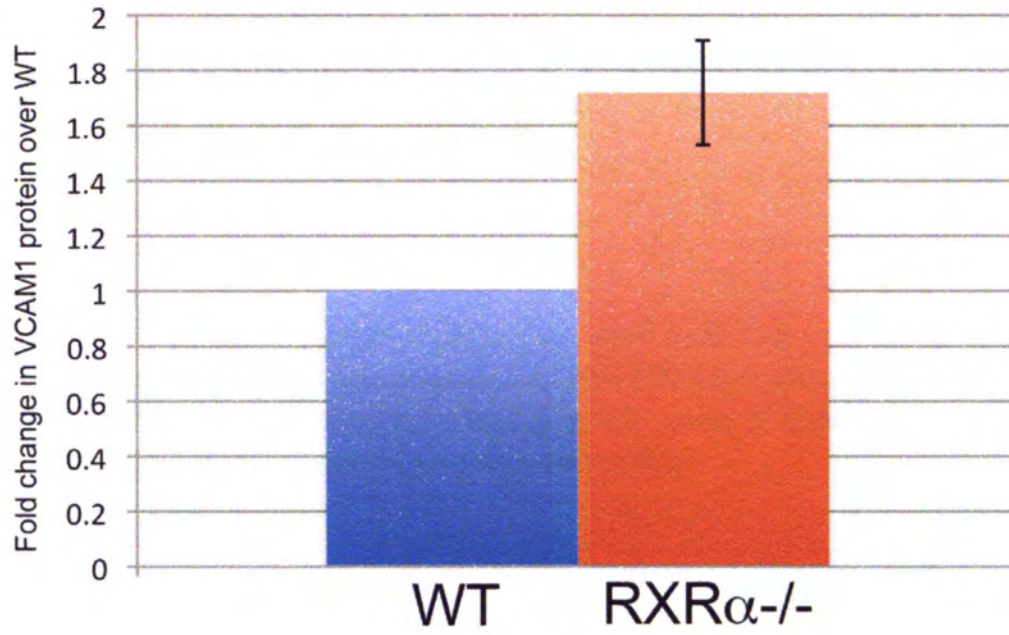


Figure 31: Western blot analysis VCAM-1 protein at E12.5 in the WT and RXR α ^{-/-} heart. VCAM-1 protein levels are elevated in the RXR α ^{-/-} mouse heart in comparison to the WT whole heart. The plotted values represent the mean fold change from WT of three experiments performed on a WT and RXR α ^{-/-} pair from the same litter (3 litters total). The error bar represents \pm SEM. A representative blot is shown.



VCAM1

β -tub

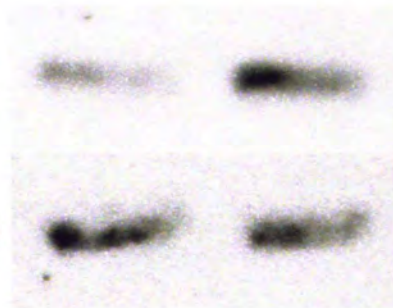


Figure 32: Western blot analysis of VCAM-1 protein at E13.5 in the WT and RXR α ^{-/-} hearts. VCAM-1 protein levels are elevated in the RXR α ^{-/-} mouse heart in comparison to the WT whole heart. The graph shows the quantification of the western blot performed on one WT and one RXR α ^{-/-} each from the same litter.

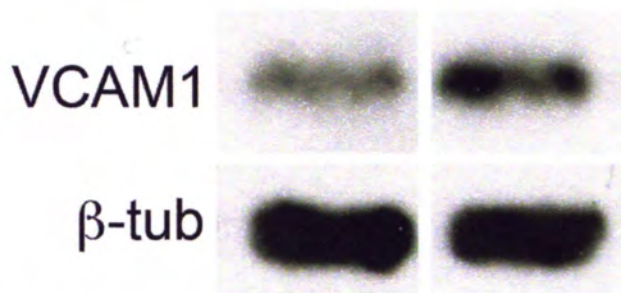
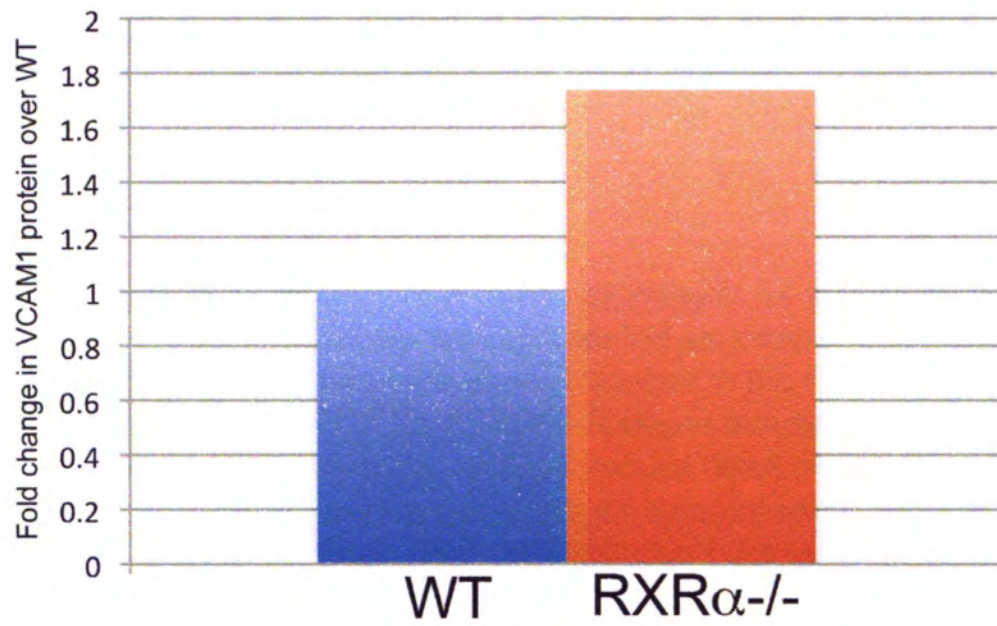
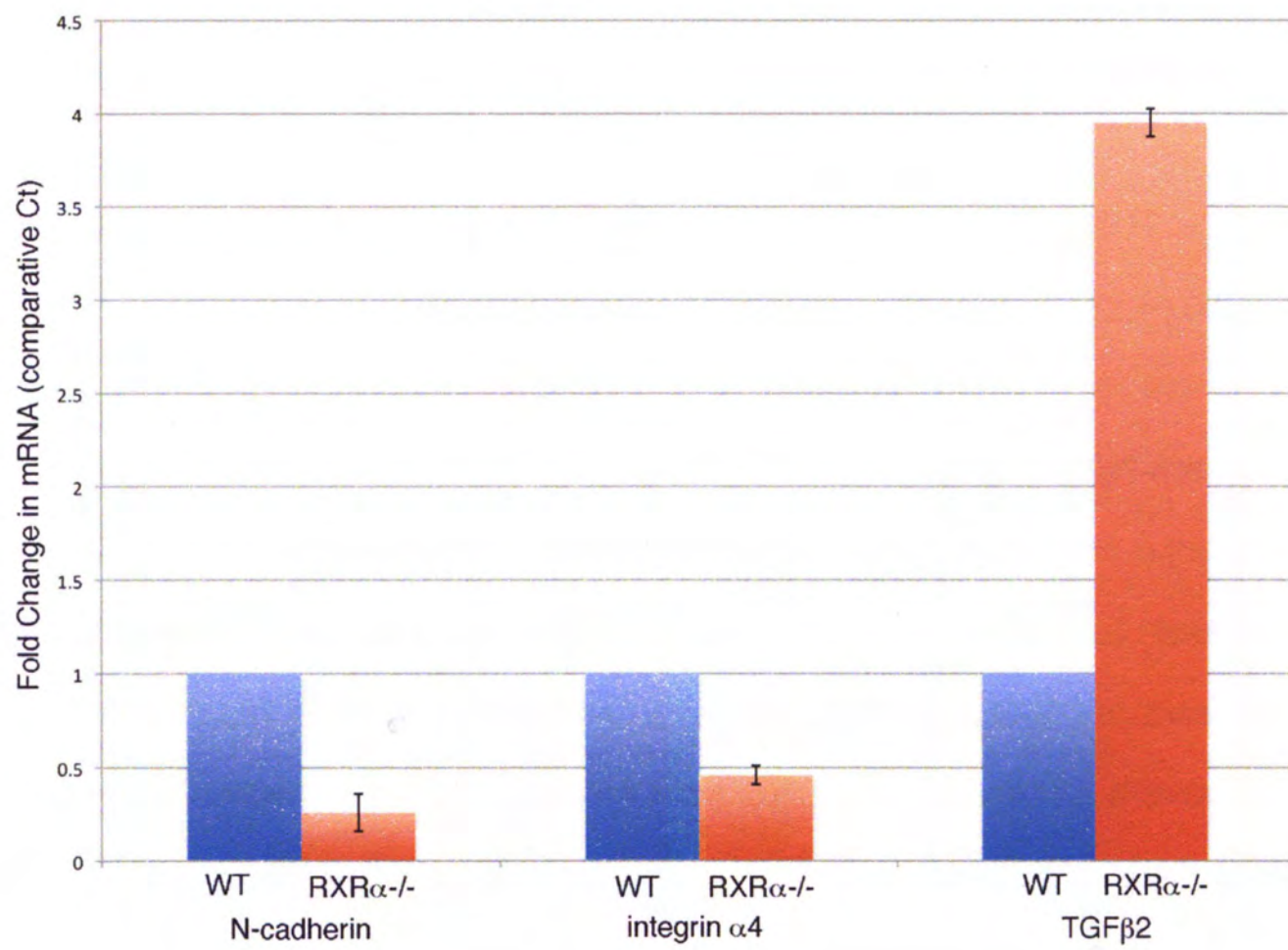


Figure 33: Real time PCR analysis of N-cadherin, integrin α 4 and TGF β 2 in E12.5 WT and RXR α ^{-/-} heart. All mRNA levels are represented as a fold change from the WT using the comparative Ct method. N-cadherin is lower in the RXR α ^{-/-} mouse heart than WT. Integrin α 4 has lower mRNA levels in the RXR α ^{-/-} mouse heart than the WT. TGF β 2 mRNA levels are higher in the RXR α ^{-/-} mouse heart than in the WT. The plotted values are the means of the triplicates from the experiment using one WT and one RXR α ^{-/-} heart from the same litter. Error bars represent the range of values for the triplicates.



from the myocardium in the WT heart. However, at E12.5 the epicardium is normally attached and closely associated with the myocardium. From E11.5 to E12.5 there is an increase in VCAM-1 protein that occurs suggesting that VCAM-1 could play a role in this detached epicardial phenotype. Epicardial EMT is also occurring at E12.5 when VCAM-1 protein is increased so VCAM-1 may play a role in inhibiting epicardial EMT. The $RXR\alpha^{-/-}$ mouse has decreased epicardial EMT (Ruiz-Lozano and Kubalak, unpublished) and VCAM-1 has been shown to negatively affect epicardial EMT (Dokic and Dettman, 2006).

No differences were observed in integrin $\alpha 4$ protein expression at E12.5 (Figure 25) or E13.5 in preliminary experiments (data not shown). When mRNA levels of integrin $\alpha 4$ at E12.5 were examined, a lower level of integrin $\alpha 4$ mRNA was seen in the $RXR\alpha^{-/-}$ mouse heart than in the WT (Figure 33). This is in contrast to what was observed at E11.5 where there appeared to be a higher level of integrin $\alpha 4$ in the $RXR\alpha^{-/-}$ heart in comparison to the WT. The result at E12.5 will need to be repeated prior to making any definitive conclusions. When N-cadherin was analyzed, there was a lower level of mRNA in the $RXR\alpha^{-/-}$ mouse heart than in the WT at E12.5 (Figure 33). At E11.5 there was a slight decrease in N-cadherin mRNA in the $RXR\alpha^{-/-}$ heart (Figure 26). The N-cadherin knockout is known to have a detached epicardium (Luo et al., 2006). However, before any conclusions can be made on the role of N-cadherin in the phenotype of the $RXR\alpha^{-/-}$ mouse, real time experiments would need to be repeated and protein levels would also need to be examined. Levels of TGF $\beta 2$ mRNA were examined as a positive control and an increase in TGF $\beta 2$ mRNA was found in the $RXR\alpha^{-/-}$ heart (Figure 33), which is consistent with our findings at midgestation (Kubalak et al., 2002).

E. Epicardial explants from E13.5 RXR α ^{-/-} have a higher level of VCAM-1 than WT

In order to provide further evidence that there was indeed aberrant expression of VCAM-1 in the epicardium of the RXR α ^{-/-} mouse, epicardial explants were grown in culture from a WT and RXR α ^{-/-} heart. The ventricular pieces were placed epicardium side down on a FN-coated glass slide as described in Chapter 2 and, after removing myocardial tissue, allowed to grow for 2 days prior to fixation with 2% paraformaldehyde. The explants were then immunostained for VCAM-1. In both the WT and RXR α ^{-/-} explants, epicardial cells expressed VCAM-1 (Figure 34). However, levels of VCAM-1 were higher in the RXR α ^{-/-} epicardial cells than in the WT. The higher levels present in the RXR α ^{-/-} cells is consistent with our previous findings that VCAM-1 is misexpressed in the epicardium prior to explant culture. The RXR α ^{-/-} epicardial explants were already expressing VCAM-1 prior to being explants and, therefore, retain higher levels of VCAM-1 in culture. The expression of VCAM-1 in the WT epicardial explants was surprising since VCAM-1 is not typically expressed in the epicardium. This expression would indicate that epicardial cells are intrinsically capable of expressing VCAM-1 but do not under normal physiological conditions. When the epicardial cells are placed into an artificial culture system, the signaling that typically occurs in the epicardium could be altered resulting in VCAM-1 expression. Epicardial explants are grown on FN-coated slides. Since binding of FN by integrin α 4 can induce several signaling cascades, excess FN/integrin α 4 binding could induce signaling changes that induce VCAM-1 expression.

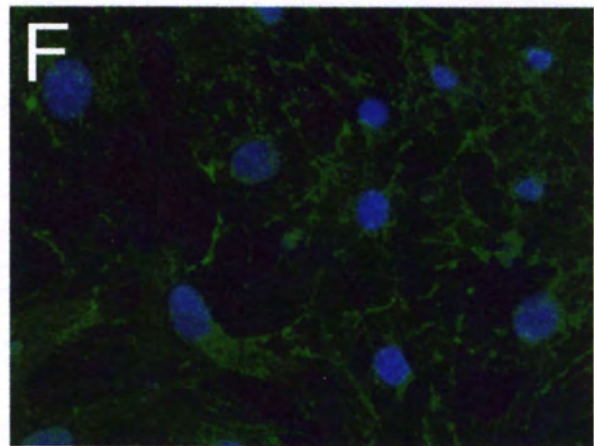
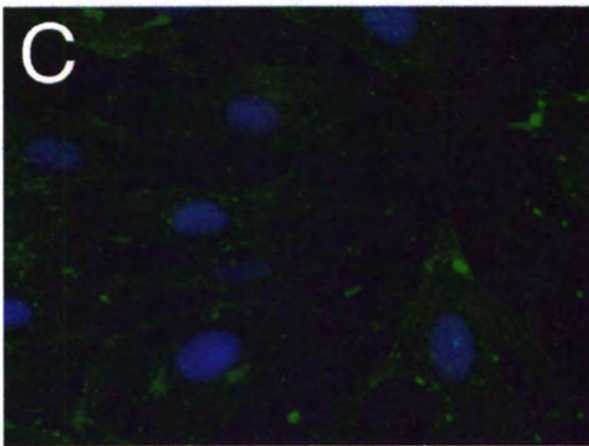
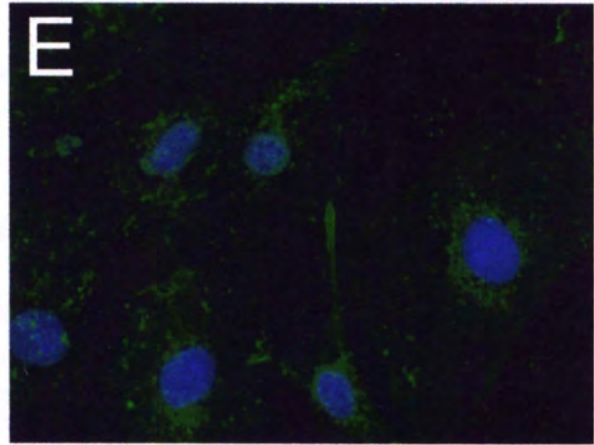
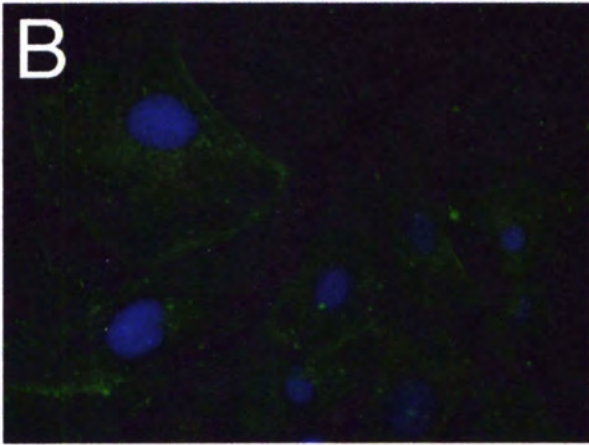
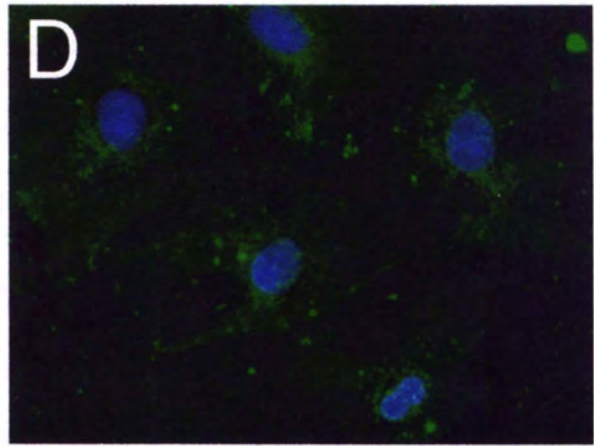
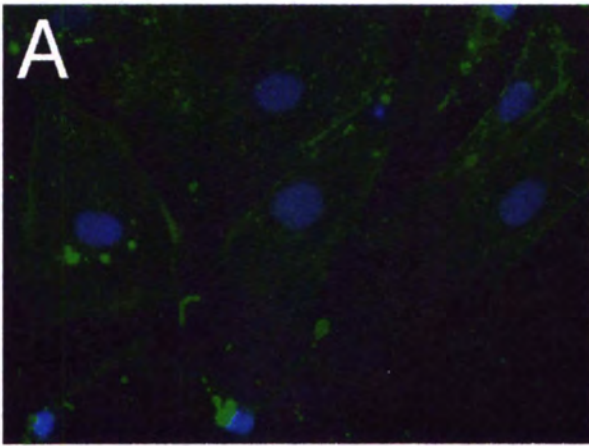
F. Smad and retinoid elements are located within the VCAM-1 promoter

The VCAM-1 promoter sequence was analyzed using the Transcription Element Search System (TESS) (<http://www.cbil.upenn.edu/cgi-bin/tess/tess>) to locate putative

Figure 34: IHC analysis of VCAM-1 protein expression in E13.5 RXR α ^{-/-} epicardial explants than WT. Epicardial explants from RXR α ^{-/-} had a higher level of VCAM-1 (D-F) than the WT (A-C). Green- VCAM-1; Blue- Dapi nuclear stain. This experiment was performed on epicardial explants from one WT and one RXR α ^{-/-} mouse from the same litter.

WT

RXR α -/-

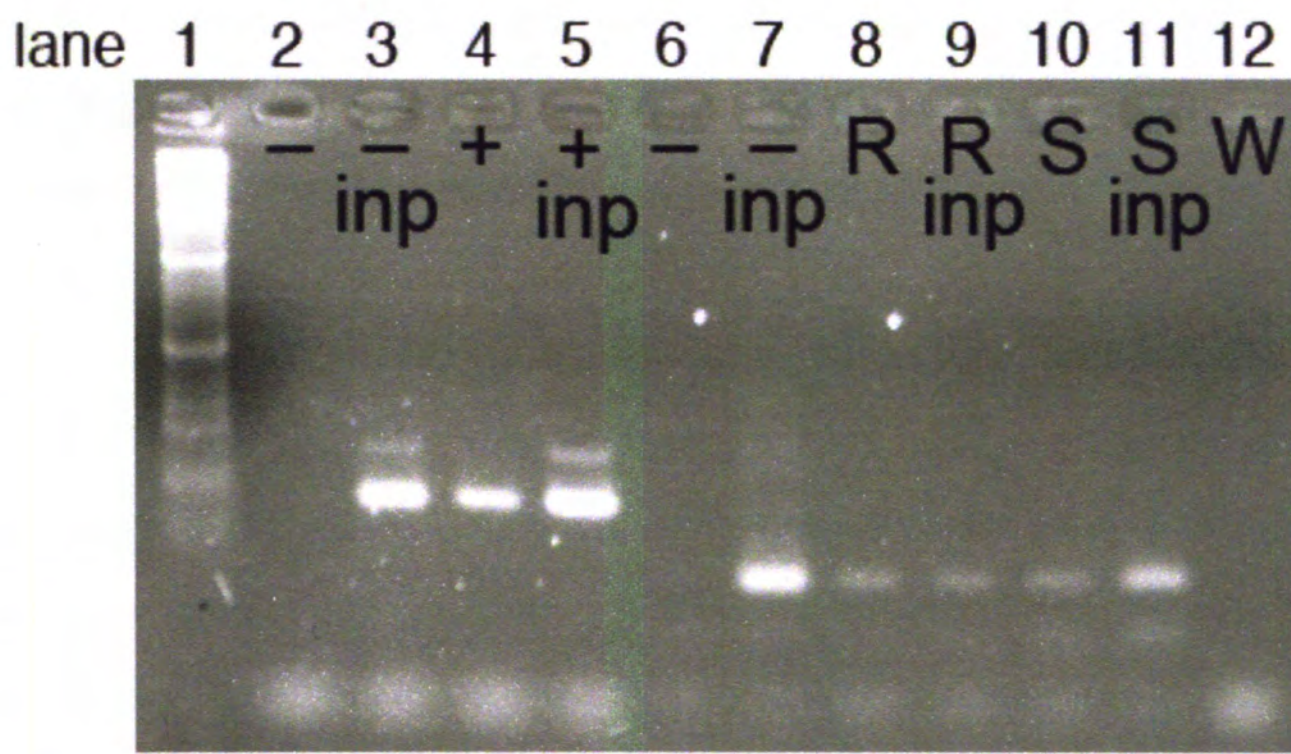


binding sites for RXR α and Smads to determine if the retinoid and/or TGF β 2 signaling pathways might regulate VCAM-1. This was followed by a manual search throughout the sequence using the consensus sequence for the binding sites. From this search several Smad binding elements (SBEs) and retinoid responsive elements were located in the VCAM-1 promoter (Figure 14). One of the pairs of retinoid elements is in a DR6 direct repeat configuration for binding of a RAR/RXR heterodimer (Figure 14). Both 9-cisRA and at-RA are predicted to activate this heterodimer. There are several retinoid elements present on the promoter that are not paired with another retinoid element (Figure 14). These elements on the promoter might be used as binding sites for any of the other receptors that RXR α is known to heterodimerize with including the vitamin D receptor, thyroid hormone receptor and PPARs.

G. RXR α and Smad4 will bind to the VCAM-1 promoter

Since potential Smad and retinoid elements have been located on the VCAM-1 promoter, we wanted to determine if it was possible for RXR α or Smads to bind to the VCAM-1 promoter. CHIP analysis was used to determine if either RXR α or Smad4 were capable of binding to the VCAM-1 promoter. In order for either RXR α or Smads to directly regulate VCAM-1 expression, they must be able to bind to the promoter. This would also validate the in silico promoter analysis which suggests that there are binding sites for both RXR α and Smads. The negative control (no immunoprecipitating antibody) was negative for bands from the VCAM-1 PCR (Figure 35, lane 6) and control PCR for the GAPDH promoter (Figure 35, lane 2). The positive control for immunoprecipitation was the RNA polymerase antibody followed by PCR for the GAPDH promoter (Figure 35, lane 4).

Figure 35: Chromatin immunoprecipitation analysis showing that RXR α and Smad4 bind to the VCAM-1 promoter. Chromatin immunoprecipitation shows RXR α and Smad4 binding to VCAM-1 promoter. ChIP using the negative control (no antibody) shows no amplicons corresponding to GAPDH in the control PCR (lane 2) or for VCAM-1 promoter (lane 6). RNA polymerase immunoprecipitating antibody followed by PCR for GAPDH was used as a positive control (lane 4). The VCAM-1 promoter band is observed in the samples using RXR α immunoprecipitating antibody (lane 8) and Smad4 immunoprecipitating antibody (lane 10). The input samples contain genomic DNA that was added to the immunoprecipitating antibody for the experiment (lanes 3, 5, 7, 9, 11) and were positive controls. Lane 1 is a 1 kilobase ladder and lane 12 is a no DNA control performed to confirm specificity of the PCR reaction.



RXR α was found to be capable of interacting with the VCAM-1 promoter. The RXR α antibody bound to RXR α located on DNA fragments of the VCAM-1 promoter and immunoprecipitated the VCAM-1 promoter as was indicated by the band seen following PCR with the VCAM-1 promoter primers (Figure 35, lane 8). No band would have been present following PCR if RXR α did not immunoprecipitate the VCAM-1 promoter. The DNA that was used in the experiments (the input- inp) also showed a band for the VCAM-1 PCR as was to be expected because it was the positive control containing all genomic DNA (Figure 35, lane 9). Currently, it is not known which of the retinoid sites RXR α is binding to or if RXR α is binding as a homodimer (RXR α /RXR α) or a heterodimer with another retinoid receptor or related receptor (RARs, other RXRs, Vitamin D, PPAR).

Smad4 was capable of binding to the VCAM-1 promoter as was indicated by the band seen in PCR for the VCAM-1 promoter (Figure 35, lane 10). The input sample also had a band from the VCAM-1 PCR (Figure 35, lane 11). Since Smad4 is a common Smad shared by multiple pathways, binding would indicate activation by any of the TGF β isoforms, activin or BMPs. Our hypothesis is that TGF β 2 is primarily responsible for activation of VCAM-1 given that there is an increase in TGF β 2 in the RXR α -/- heart coupled with an increase in VCAM-1. The following sets of experiments tested the hypothesis that TGF β 2 could increase the expression of VCAM-1. In order to determine which retinoid or Smad binding sites are responsible for regulating the VCAM-1 promoter, mutational analysis of the promoter would need to be performed.

H. TGF β 2 causes epicardial bubbling and induces VCAM-1 expression the epicardium

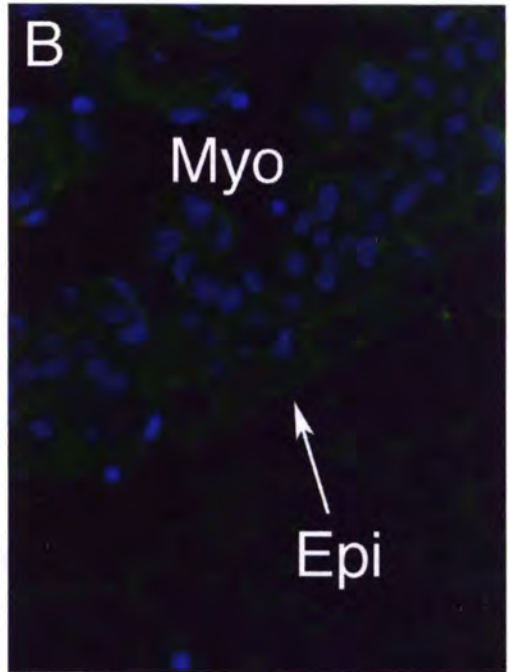
Embryos at E11.5 were grown in whole embryo culture and subjected to TGF β 2 (10 ng/ml) or 9-cisRA (100nM) treatments. Both TGF β 2 and 9-cisRA treatments were used because the CHIP and in silico promoter analyses indicated that RXR α and Smad4 could both bind to the VCAM-1 promoter. Treatments to activate TGF β 2 and/or retinoid signaling will help determine which pathway is likely responsible for the increase in VCAM-1 seen in the RXR α -/- heart since both pathways are altered in the mutant.

No gross histological differences were observed between any of the 12 hour treated embryos (Figure 36). All embryos displayed a detached epicardium and similar thickness of the ventricular myocardium. The embryos were treated for 12 hours beginning at E11.5 in development so when the culture was stopped, the age of the embryos was around E12. At E12 of in vivo development it is normal to have a somewhat detached epicardium because it is not normally fully attached until E12.5. Another possible reason that there were no gross differences between control and treated embryonic hearts after 12 hours of culture is that the embryos were not in culture long enough for differences to develop.

When the embryos were treated for 18 hours, histological analysis showed that the epicardium was attached in the diluent control (Figure 37). However, TGF β 2 treated embryos displayed a detached epicardium in various regions of the heart. There appeared to be no histological difference in the ventricular myocardium in each treatment (Figure 37). One issue that exists with the 18 hour culture is that this time frame represents the limits that whole mouse embryos can be cultured. Thus, the integrity of the embryos may become compromised once they reach the E12.0-12.5 age.

Figure 36: IHC analysis of VCAM-1 expression following TGF β 2 treatment in 12 hour whole embryo culture. There appears to be no phenotypical difference between diluent (A) and TGF β 2 treatment (C) in the H&E stained paraffin sections. There are higher levels of VCAM-1 in the TGF β 2-treated embryos (D) than in the diluent (B). VCAM-1 is expressed in the myocardium and epicardium of both the diluent (B) and TGF β 2-treated (D). Green- VCAM-1; Blue- Dapi nuclear stain. Myo, myocardium; Epi, epicardium. Images are representative of two experiments (2 embryos of each treatment) each having immunostained sections from the hearts of one diluent and one TGF β 2 treated embryo.

Diluent



TGFβ2

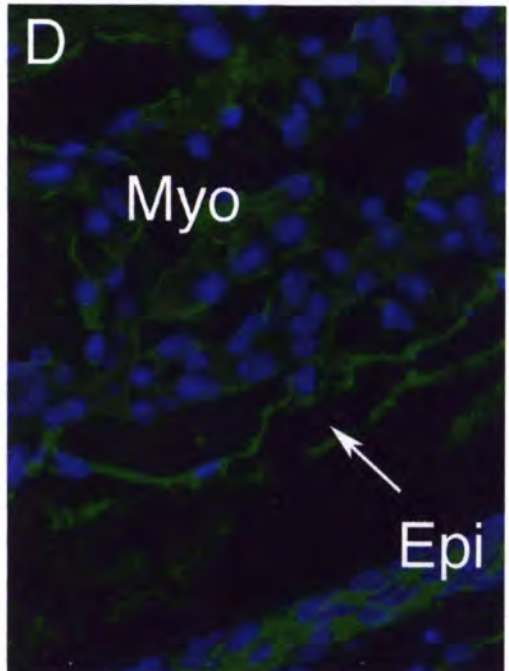
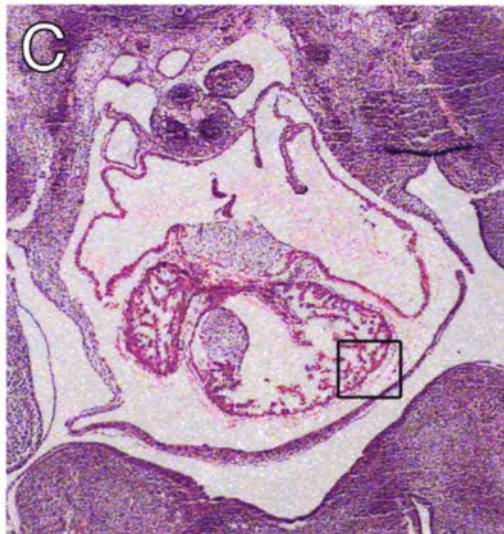
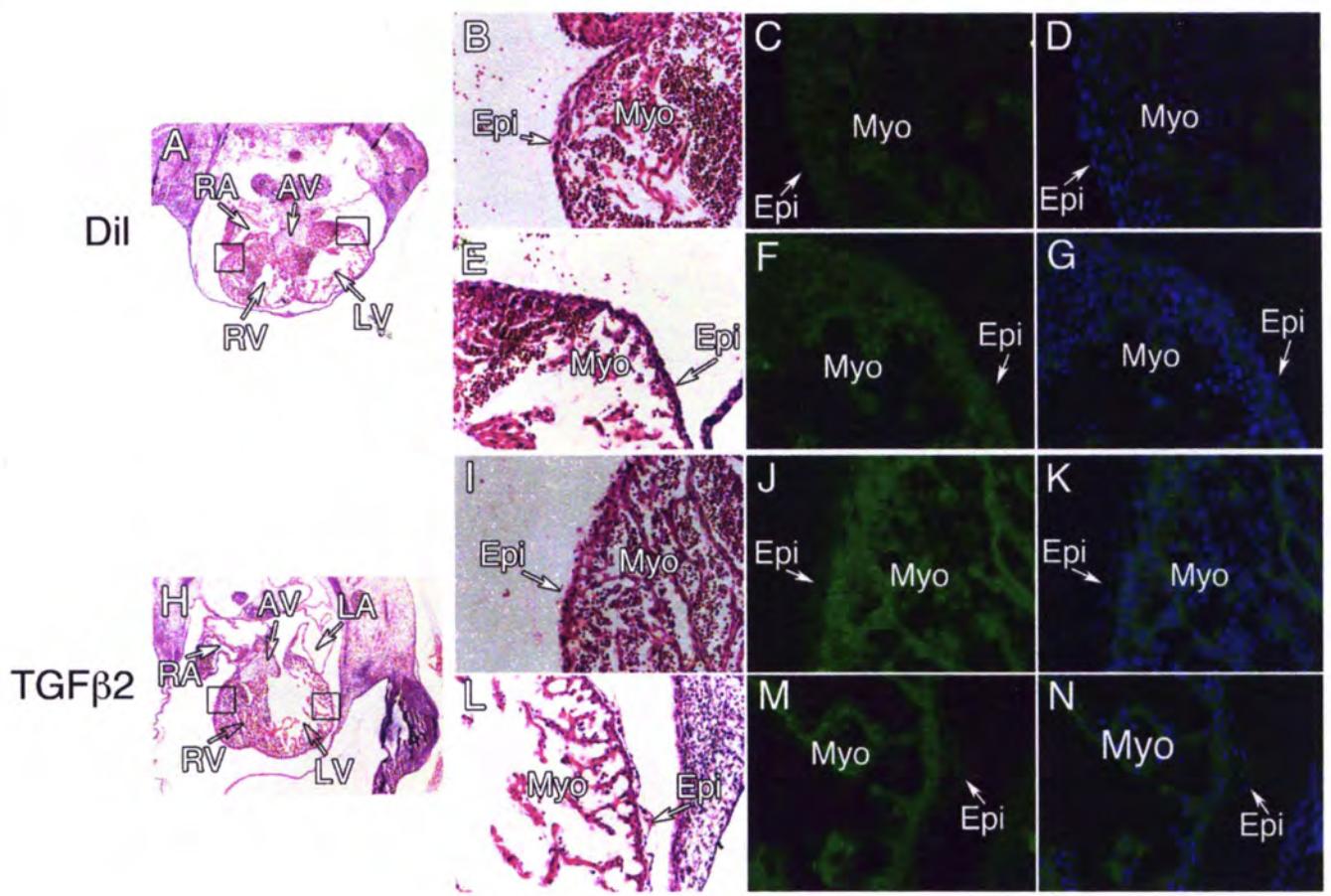


Figure 37: IHC analysis showing that VCAM-1 expression increases and the epicardium detaches following 18 hours of TGF β 2 treatment in whole embryo culture. VCAM-1 is expressed in the myocardium of the diluent treated embryo (C, D, F, G) and the TGF β 2-treated embryo (J, K, M, N). VCAM-1 is not expressed in the epicardium of the diluent-treated embryo (C, D, F, G) but is expressed in the epicardium of the TGF β 2-treated embryo (J, K, M, N). The diluent-treated embryo has an attached epicardium (A, B, E) but the TGF β 2-treated embryo has a detached epicardium (H, I, L). Images are representative of one experiment (one set of treatments) with immunostained sections from the hearts of one diluent and one TGF β 2 treated embryo.



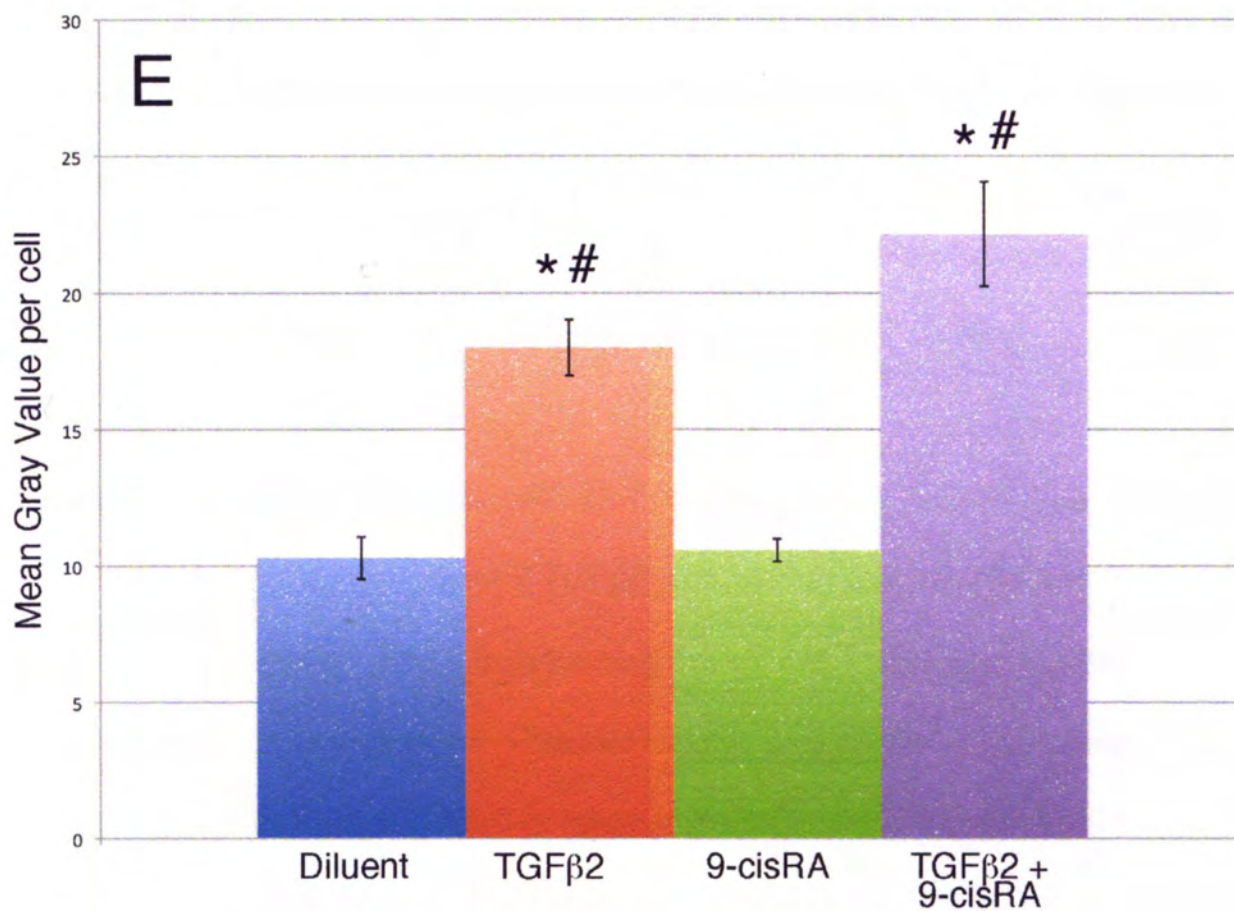
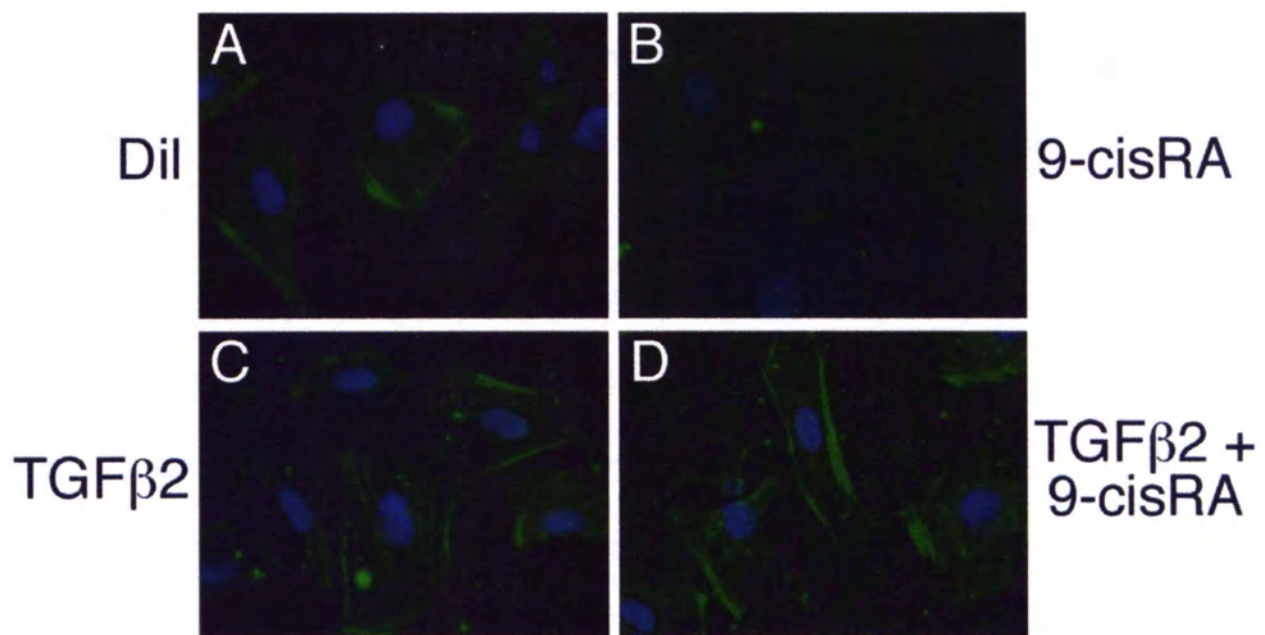
This likely negatively affects the tissue integrity and may in turn alter the expression profiles of several proteins due to the beginning stages of cell death.

In the 12 hour treated embryos, immunohistochemical analysis showed a misexpression of VCAM-1 in the epicardium in both the diluent and TGF β 2 embryos (Figure 36). However, there was a much higher level of VCAM-1 expression in the TGF β 2 treated embryos than in the diluent treated embryos (Figure 36). VCAM-1 was also localized to the myocardium in both the diluent and TGF β 2 treated embryos (Figure 36). The TGF β 2-treated embryos also had much higher levels of VCAM-1 in the myocardium than the diluent-treated embryos (Figure 36). In the 18 hour treated embryos, no expression of VCAM-1 was observed in the epicardium of the diluent treated (Figure 37). However, expression of VCAM-1 was seen in the epicardium of TGF β 2 treated embryos (Figure 37). These data would suggest that in the RXR α ^{-/-} mouse, the increase in TGF β 2 is at least in part responsible for the epicardial phenotype and the increase in VCAM-1. These results suggest that TGF β 2 is capable of upregulating VCAM-1 in vivo.

I. TGF β 2 treatment increases VCAM-1 expression in E11.5 epicardial explants

Epicardial explants from WT mice were grown in culture for 48 hours and then treated with TGF β 2 (10 ng/ml) and/or 9-cisRA (100nM) to determine what effect treatment had on VCAM-1 expression in epicardial cells grown in culture. The diluent control exhibited expression of VCAM-1, which is an interesting finding since WT cells do not normally express VCAM-1 in vivo (Figure 38). This suggests that placing the epicardial cells into an artificial culture system stimulated the expression of VCAM-1. Explanations for this were discussed in section E.

Figure 38: TGF β 2 treatment of epicardial explant cultures results in increased VCAM-1 expression. WT epicardial explants were treated with diluent, TGF β 2, 9-cisRA and TGF β 2+9-cisRA for 24 hours. VCAM-1 was expressed in all of the explants. However, there is great expression of VCAM-1 in the TGF β 2 (C) and TGF β 2+9-cisRA (D) treatments than in diluent (A) and 9-cisRA (B). These data were quantified in E using ImageJ. There is a statistically significant difference between diluent and TGF β 2 (*), diluent and TGF β 2+9-cisRA (*), 9-cisRA and TGF β 2 (#), and 9-cisRA and TGF β 2+9-cisRA (#). There is no statistical significance between diluent and 9-cisRA treatment or between TGF β 2 and TGF β 2+9-cisRA treatment. A representative immunohistochemical staining is shown in A-D. The plotted values in E are the mean gray value of pixels per cell of 3 independent experiments each having a diluent, TGF β 2, 9-cisRA and TGF β 2+9-cisRA treatment.



Treatment with TGF β 2 either alone or with 9-cisRA induced expression of VCAM-1 over that of either diluent or 9-cisRA alone (Figure 38). These data would indicate that TGF β 2 can directly stimulate expression of VCAM-1 and that addition of 9-cisRA to the TGF β 2 treatment has no additive effect on expression (Figure 38). The immunohistochemical data was quantified using ImageJ. Quantification of the immunohistochemical data confirmed what was seen in the immunohistochemical staining. Statistical significance was calculated using paired T-tests to compare each treatment. The differences seen between the diluent, TGF β 2 and TGF β 2 + 9-cisRA are statistically significant. The differences found between 9-cisRA, TGF β 2 and TGF β 2 + 9-cisRA are also statistically significant. There was no statistical significance between diluent and 9-cisRA indicating that 9-cisRA has little to no effect on VCAM-1 expression elevation. This finding would suggest that the retinoid binding elements on the promoter are not functional, not responsive to 9-cisRA (not an RXR) or that the concentration of 9-cisRA used did not induce receptor activation. The retinoid binding elements could be RXR heterodimer sites meaning that the ligand for the RXR heterodimer partner would also need to be present to activate transcription through RXR binding.

J. VCAM-1-luc activity increases with TGF β 2 treatment

In order to further determine if TGF β 2 was having a direct effect on VCAM-1 expression, an expression plasmid containing the VCAM-1 promoter upstream of a luciferase reporter gene was used. Plasmid identity was confirmed by performing a restriction digest with XhoI and KpnI to remove the VCAM-1 promoter from the plasmid and also by direct sequencing of the plasmid. When transcription factor binding activates the VCAM-1 promoter, luciferase will be produced and can be quantified using a luminometer. Luminescence gives a quantifiable response of the VCAM-1 promoter to

TGF β 2 treatment instead of a more qualitative measure used previously with explants and WEC.

Rat epicardial cells were used to analyze the VCAM-1 promoter element and were grown as described in Chapter 2 until reaching approximately 75% confluency. Once the appropriate confluency was reached, the cells were transfected with the VCAM-1-luc plasmid (VC1889) and the CMV-Renilla-luc plasmid (control for normalization). Following 24 hours of transfection, treatments were added to each 35 mm dish directly into the culture medium. The cells were treated with TGF β 2 (10 ng/mL) and/or 9-cisRA (100 nM). Following the 24 hours of treatment, the cells were harvested and subjected to a luciferase assay to determine luciferase activity. Each sample was assayed for both Firefly luciferase (VCAM-1-luc) and Renilla luciferase (CMV-Renilla-luc). The VCAM-1-luc data were then normalized to CMV-Renilla-luc to account for differences in transfection efficiency. The fold-change from the diluent treatment of VCAM-1-luc was calculated for each treatment to compare between experiments. All statistics were calculated from the raw data using paired T-tests to compare between each treatment.

Treatment with TGF β 2 resulted in a higher level of VCAM-1-luciferase activity than treatment with diluent, which was statistically significant ($p < 0.05$) (Figure 39). There was no statistically significant difference in VCAM-1-luc activity between 9-cisRA treatment and diluent or between either TGF β 2 treatment (Figure 39). This would indicate that RA signaling is not responsible for increasing transcription of VCAM-1. It is possible that the retinoid sites present on the promoter could be heterodimer sites for RXR α to bind with another receptor (Vitamin D, PPAR) indicating that the other receptor in the heterodimer needs to be activated to elicit an effect on VCAM-1. Further studies with other treatments to activate those receptors are required to address this.

Figure 39: TGF β 2 treatment of cells transfected with the VC1889 luciferase expression plasmid increases VCAM-1-driven luciferase expression. REC cells were transfected with the VC1889 plasmid and CMV-Renilla luciferase control plasmid. Following treatment, cells were harvested and assayed for luciferase expression. The firefly luciferase (VC1889) was normalized to the CMV-Renilla luciferase values. The normalized values were then expressed as a fold change from diluent. There is a statistically significant difference between diluent and TGF β 2 (*), diluent and TGF β 2+9-cisRA (*), 9-cisRA and TGF β 2 (#), and 9-cisRA and TGF β 2+9-cisRA (#). There is no statistical significance between diluent and 9-cisRA treatment. These results represent 8 independent experiments performed in triplicate. The plotted values are the mean fold change from the diluent values. Error bars represent \pm SEM.

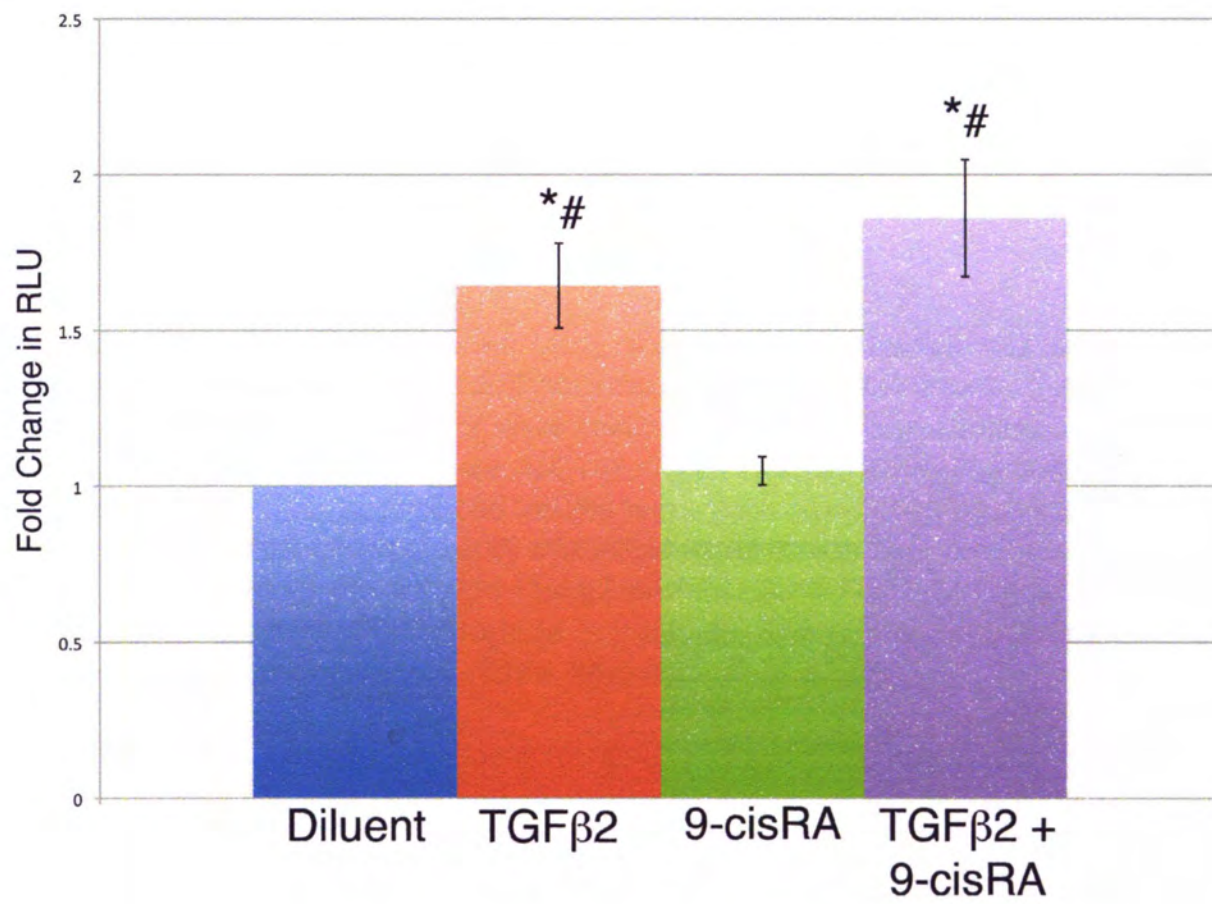
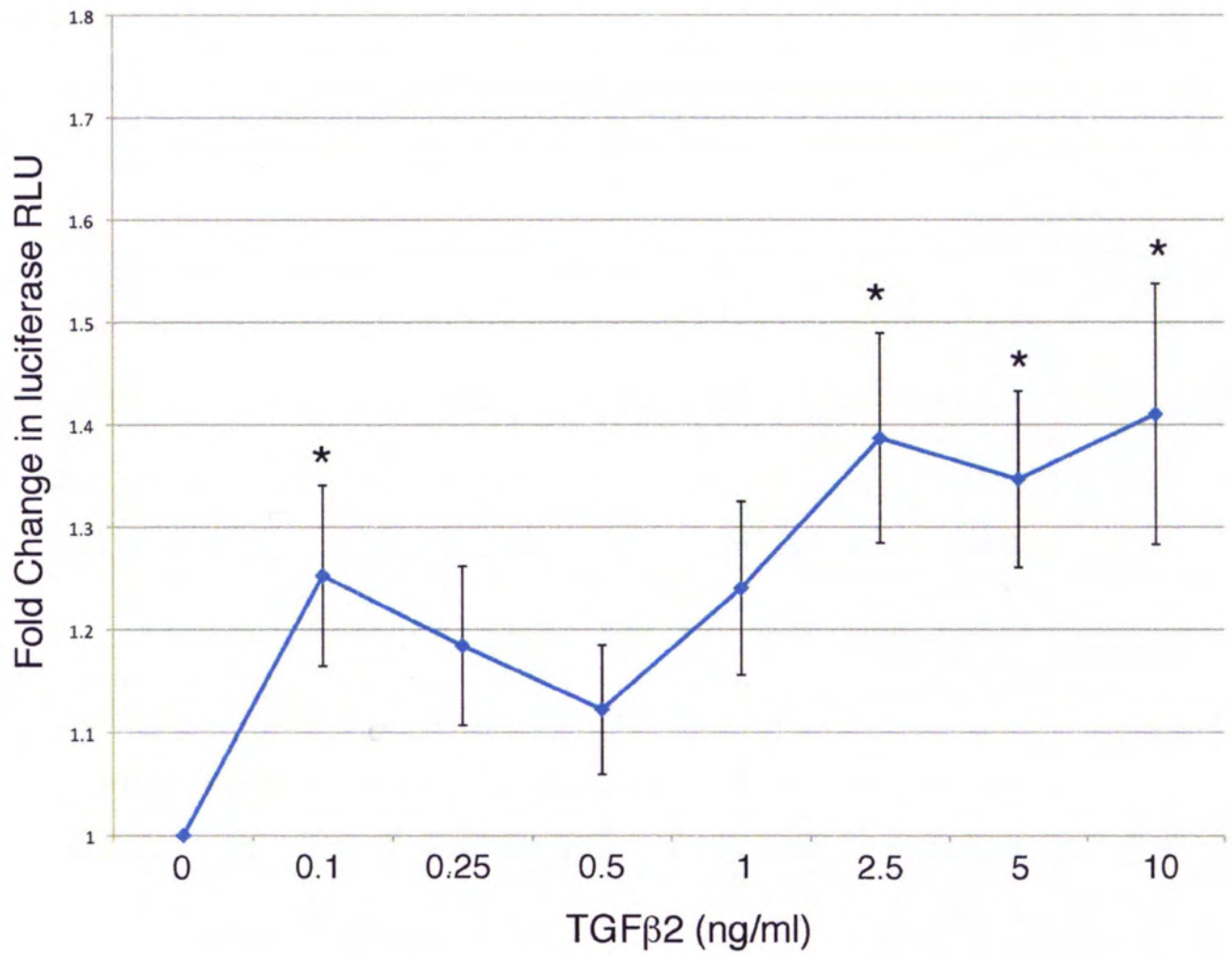


Figure 40: Concentration-response study of cells transfected with VC1889 luciferase expression plasmid and treated with varying TGF β 2 concentrations. Treatments with varying concentrations of TGF β 2 were done on REC cells transfected with VC1889 and CMV-Renilla. The firefly luciferase (VC1889) was normalized to the CMV-Renilla luciferase values. The normalized values were then expressed as a fold change from diluent. The asterisk (*) represents statistical significance between diluent and 0.1 ng/ml TGF β 2, 2.5 ng/ml TGF β 2, 5 ng/ml TGF β 2 and 10 ng/ml TGF β 2. These results represent 7 independent experiments performed in triplicate. The plotted values are the mean fold change from the diluent values. Error bars represent \pm SEM.



Alternatively, the retinoid consensus sites indentified on the promoter may not be functional retinoid binding sites.

Treatment with both TGF β 2 and 9-cisRA together shows a statistically significant increase in VCAM-luc activity compared to both diluent and 9-cisRA alone (Figure 39). However, there was no statistically significant difference in VCAM-1-luc activity between TGF β 2 alone and TGF β 2 plus 9-cisRA, indicating that TGF β 2 does not interact with 9-cisRA to have an influence on VCAM-1 expression at least not at the concentrations used in this experiment (Figure 39).

A dose response experiment was performed to evaluate the effect of TGF β 2 on induction of VCAM-1-luc activity. An apparent biphasic response curve was observed (Figure 40). At the lowest concentration of TGF β 2 (0.1 ng/ml), there was a statistically significant increase in VCAM-1-luc activity seen compared to diluent (Figure 40). At the next three concentrations tested (0.25 ng/ml, 0.5 ng/ml and 1 ng/ml), there was a decrease in the amount of VCAM-1-luc activity seen from 0.1 ng/ml treatment and there is no statistical significance in comparison to the diluent (Figure 40). When transfected cells are treated with the next three concentrations (2.5 ng/ml, 5 ng/ml and 10 ng/ml), the amount of VCAM-1-luc activity increased to levels that were significantly higher ($p < 0.05$) as compared to the diluent treatment (Figure 40). Previous studies using different concentrations of TGF β 2 in treatment suggested that at lower concentrations of TGF β 2 that p38 was being activated instead of Smads (Sauls, Hoover and Kubalak, unpublished). The biphasic response curve in this study could represent activation of the VCAM-1 promoter through both p38 (at lower concentrations) and Smad activation (at higher concentrations) by TGF β 2.

Chapter 4: Conclusions and Future Directions

From this study and those of others, it is concluded that VCAM-1, a cell adhesion molecule previously found to be necessary for epicardium formation (Kwee et al., 1995), is playing an integral role in the normal development of the heart following formation of the epicardium. Appropriate levels and cell-type specific expression of VCAM-1 is essential for normal cardiac morphogenesis including, but not limited to, the formation of EPDCs, which will contribute to the formation of coronary vasculature, ventricular chamber maturation and valve formation (Dettman et al., 1998; Gittenberger-de Groot et al., 1998; Manner, 1999, 2000; Mikawa and Fischman, 1992; Mikawa and Gourdie, 1996; Perez-Pomares et al., 1997; Vrancken Peeters et al., 1999). Using the $RXR\alpha^{-/-}$ mouse, a model of aberrant cardiac morphogenesis, alterations in VCAM-1 expression were found. This study showed an increase in VCAM-1 mRNA and protein in the myocardium of the $RXR\alpha^{-/-}$ heart from E11.5-E13.5 compared to the WT. In addition, VCAM-1 was misexpressed in the epicardium of the $RXR\alpha^{-/-}$ heart at E11.5-E13.5 compared to the WT, which normally has no VCAM-1 expression in the epicardium. Since VCAM-1 was increased and misexpressed in the $RXR\alpha^{-/-}$ heart, we wanted to look at regulation of this gene. Retinoid and Smad-binding elements were found on the VCAM-1 promoter (by *in silico* promoter analysis) and both $RXR\alpha$ and Smad4 were capable of binding to the VCAM-1 promoter (shown with CHIP analysis) suggesting regulation of VCAM-1 by retinoid and/or TGF β 2 signaling. TGF β 2 treatment induced expression of VCAM-1 in epicardial explants as well as in the epicardium in whole embryo culture while 9-cisRA treatment had no effect. Treating REC cells transfected with VC1889 luciferase expression plasmid with TGF β 2 demonstrated that TGF β 2 activates the VCAM-1 promoter to induce luciferase activity while treatment with 9-cisRA

does not activate the VCAM-1 promoter. The results from this study demonstrate that VCAM-1 is upregulated in the $RXR\alpha^{-/-}$ model of aberrant epicardium formation and that $TGF\beta 2$ is capable of upregulating VCAM-1 in the developing heart. Our current working model of the role of normal and aberrant VCAM-1 expression is present in Figure 41. Furthermore, these studies suggest that appropriate expression of VCAM-1 regulated by $TGF\beta 2$ is a significant contributing factor in normal heart development. The consequences of changes in VCAM-1 expression and cell type specific location to the developing heart are not fully known, however, several potential scenarios will be discussed.

Integrin Involvement

Integrin $\alpha 4$ and VCAM-1 have both been previously been shown to be essential to formation of the epicardium (Kwee et al., 1995; Yang et al., 1995), however, their role in cardiac morphogenesis following epicardium formation is not fully known. Currently it is thought that binding between integrin $\alpha 4$ (in the epicardium) and VCAM-1 (in the myocardium) helps to maintain close association of the myocardium and epicardium. Changing the levels of these two proteins could have detrimental consequences to cell-cell (epicardium to myocardium) and cell-ECM (epicardium to subepicardial space) binding. Increases in the amounts of VCAM-1 protein in the $RXR\alpha^{-/-}$ mouse could affect the normal stoichiometry of integrin $\alpha 4$ /VCAM-1 receptor interactions, thus affecting normal binding of the epicardium and myocardium possibly leading to epicardial detachment.

Epicardial explants from the $RXR\alpha^{-/-}$ mouse do attach to FN-coated slides, however, the amount of attachment has not been quantified. In one epicardial explant experiment using WT and $RXR\alpha^{-/-}$, most of the cells of the $RXR\alpha^{-/-}$ explant detached during the fixation process. However, in another experiment with WT and $RXR\alpha^{-/-}$

explants, epicardial cells remained attached during the fixation process. An attachment assay would need to be devised to further analyze epicardial cell attachment using $RXR\alpha^{-/-}$ epicardial explants.

Increased VCAM-1 could also bind to different receptors located in the epicardium and/or myocardium instead of binding to integrin $\alpha4$. There are no reports in the literature demonstrating VCAM-1/VCAM-1 binding so the formation of VCAM-1/VCAM-1 homodimers is unlikely. It is more likely that excess VCAM-1 could bind with another integrin in the developing heart. Typically, VCAM-1 binds to integrin $\alpha4/\beta1$ heterodimers. A study of the chick PE demonstrated that integrins $\alpha4$, $\alpha5$, $\alpha8$, αv , $\beta1$, $\beta3$ and $\beta5$ are all expressed in the PE (Pae et al., 2008). A recent study also found expression of integrin $\beta2$ in the mouse heart, particularly in the epicardium (Oliveira et al., 2010). Since integrin $\beta2$ is found in the epicardium, it is possible that it could interact with epicardially-expressed VCAM-1. VCAM-1 on endothelial cell walls was previously reported to bind to $\alpha D\beta2$ integrin on eosinophils (Grayson et al., 1998) but it is unknown if this interaction occurs within the heart. Under flow conditions, $\alpha D\beta2$ integrin expressed by lymphoid cells binds to VCAM-1 on endothelial cells at levels that were similar to binding of $\alpha4\beta1$ integrin-expressing inflammatory cells to VCAM-1 on endothelial cells (Van der Vieren et al., 1999). This would suggest that VCAM-1/ $\alpha D\beta2$ integrin binding could be as strong as VCAM-1/ $\alpha4\beta1$ integrin binding. Another study found that $\alpha9\beta1$ integrin in neutrophils binds to VCAM-1 on endothelial cells for migration across an endothelial monolayer during the inflammatory process (Taooka et al., 1999) suggesting that integrin $\alpha4$ is not always necessary for VCAM-1 binding. These alternative interactions of VCAM-1 with integrin subunits other than $\alpha4\beta1$ have only been reported in endothelial and lymphoid cells during inflammation. However, it is possible

that VCAM-1 interactions with other integrin subunits can occur in the heart since those subunits are expressed within the heart, particularly in the PE and epicardium.

PI3K/Akt

In the developing heart, PI3K/Akt can initiate proliferation of cardiomyocytes (Kang and Sucov, 2005) for ventricular chamber maturation. Binding of VCAM-1 and integrin $\alpha 4$ can activate PI3K/Akt signaling (Figure 7), which can induce myocardial proliferation in the normal developing heart (Kang and Sucov, 2005). Activation of PI3K/Akt signaling is downstream of integrin $\alpha 4$ /VCAM-1/FN binding is (Hynes, 2002). PI3K/Akt signaling has also been shown to be activated by an unknown factor secreted by epicardial cells in response to retinoic acid signaling (Kang and Sucov, 2005). Altering the normal ligand binding to integrin subunits could modify the downstream signaling in the developing heart such as PI3K/Akt and Erk signaling. The increased FN present in the RXR α -/- heart (Jenkins et al., 2005) could also alter the signaling that occurs from its binding with integrin $\alpha 4$. The RXR α -/- mouse has decreased PI3K/Akt and Erk signaling (Kang and Sucov, 2005), both of which are downstream of integrin binding. It is possible that the decreased signaling through those pathways is related to increased FN binding to integrin $\alpha 4$ or by VCAM-1 binding to another integrin heterodimer since each one of these interaction can initiate and modify integrin-mediated signaling.

A decrease in proliferation was found in the ventricular myocardium of the RXR α -/- heart as shown by a reduction in mitotic index of myocytes (Kastner et al., 1997) and a reduction of PI3K/Akt signaling (Kang and Sucov, 2005). Since the PI3K/Akt pathway is known to induce proliferation and is active in cardiomyocytes, the reduction in signaling from the PI3K/Akt pathway could decrease proliferation of cardiomyocytes in the RXR α -/- mouse (Kang and Sucov, 2005). This reduction in

PI3K/Akt signaling could be related to the disruption of VCAM-1/integrin α 4/FN stoichiometry because activation of PI3K/Akt signaling can occur downstream of integrin α 4 binding. Decreased proliferation due to a reduction of PI3K/Akt signaling could lead to a hypoplastic ventricular myocardium as seen in $\text{RXR}\alpha^{-/-}$ mice (Jenkins et al., 2005).

Using real time PCR, increased Rac mRNA was observed in $\text{RXR}\alpha^{-/-}$ mice (Brichler, Burton and Kubalak, unpublished). Rac is involved in initiation of migration downstream of integrin-mediated signaling (Figure 7) and has been found to increase invasiveness and transformation in cancer (Bosco et al., 2009). An increase in Rac would suggest an increase in EMT, but increased EMT is not what is observed in $\text{RXR}\alpha^{-/-}$ mice (Ruiz-Lozano and Kubalak, unpublished). VCAM-1/integrin α 4 signaling can activate Rac1 in mouse and human endothelial cells leading to the production of reactive oxygen species (ROS) (Cook-Mills, 2002; Deem and Cook-Mills, 2004; van Wetering et al., 2003). ROS have been shown to induce dissociation of cell-cell contacts in retinal pigment epithelial cells through the loss of cadherins on the cell surface without EMT occurring (Inumaru et al., 2009). It is possible in $\text{RXR}\alpha^{-/-}$ mice that increased VCAM-1 and increased Rac1 can induce dissociation of cell-cell contacts (possibly between epicardium and myocardium) without leading to the induction of EMT.

According to a recent study, Foxc proteins are activated by the PI3K/Akt pathway (Hayashi and Kume, 2008). The VCAM-1 promoter contains Fox-binding elements and the Foxc1 and Foxc2 transcription factors have been shown to activate the VCAM-1 promoter to increase VCAM-1 levels (Kang et al., 2006). Increased levels of VCAM-1 could, in turn, increase signaling downstream of integrin α 4 including the PI3K/Akt signaling (Figure 7). Similar to the $\text{RXR}\alpha^{-/-}$ mouse (Jenkins et al., 2005), the combination Foxc1 $^{+/-}$ /Foxc2 $^{-/-}$ mouse has been shown to have a detached epicardium (Seo and Kume, 2006). In $\text{RXR}\alpha^{-/-}$ mice, Foxc1 or Foxc2 expression has not been

examined. However, it is speculated that the reduction in PI3K/Akt signaling in $RXR\alpha^{-/-}$ mice (Kang and Sucov, 2005) could cause decreased Foxc1 and/or Foxc2. With decreased Foxc1 and/or Foxc2, there would be less activation of the VCAM-1 promoter, resulting in lower levels of VCAM-1. However, in $RXR\alpha^{-/-}$ mice, VCAM-1 is increased and is likely due to a mechanism independent of PI3K/Akt signaling and Foxc1/Foxc2. In this study, TGF β 2 signaling was shown to increase VCAM-1 expression so TGF β 2 is most likely the pathway affecting VCAM-1 expression in $RXR\alpha^{-/-}$ mice.

Effects on EMT

In normal cardiac morphogenesis, VCAM-1 could play a role in regulation of EMT through signaling by binding to integrin α 4 and through cell-cell adhesion. In order for EMT to occur, there must be some loss of cell adhesion. If VCAM-1 is increased or expressed in the wrong cells, there could be alterations in cell-cell adhesion and/or signaling that would impact EMT with increases in cell adhesiveness decreasing EMT. Recently, VCAM-1 has been shown to negatively impact EMT (Dokic and Dettman, 2006). Treatments with soluble VCAM-1 caused a reduction in EMT by strengthening β -catenin and E-cadherin association between epicardial cells, decreasing basal stress fibers and promoting formation of apical cortical actin fibers to maintain epicardial-epicardial cell attachment (Dokic and Dettman, 2006). The $RXR\alpha^{-/-}$ mouse has been previously shown to have decreased epicardial EMT (Ruiz-Lozano and Kubalak, unpublished). VCAM-1, in excess, could decrease epicardial EMT in $RXR\alpha^{-/-}$ mice. Similarly, other mouse models of aberrant epicardium formation have increased E-cadherin resulting in decreased epicardial EMT including the epicardial-specific Wt1 knockout (Martinez-Estrada et al., 2010) and the podoplanin knockout (Mahtab et al., 2008). Therefore, increased E-cadherin-mediated association between epicardial cells could decrease epicardial EMT. VCAM-1 was also found to antagonize EMT of

epicardial cells stimulated by TGF β by activating p190^{RhoGAP} thereby altering Rho activation by TGF β 3 (Dokic and Dettman, 2006). Since TGF β signaling is known to increase EMT, the TGF β 2 increase observed in RXR α ^{-/-} mice would be expected to increase EMT. However, since EMT is not increased in RXR α ^{-/-} mice (Ruiz-Lozano and Kubalak, unpublished), the increase in VCAM-1 might explain this discrepancy because VCAM-1 has been shown to reduce TGF β -induced EMT. A strategy to determine whether or not VCAM-1 elevation and misexpression in the epicardium alters EMT or causes epicardial detachment would be to create a mouse model overexpressing VCAM-1 in the epicardium. This could be done by creating a mouse line using the Wt1, Tbx18 or GATA5 promoter to drive expression of VCAM-1 in the epicardium. The phenotype of these transgenic embryos could then be analyzed for epicardial bubbling and alterations in epicardial EMT. Such experiments might provide insight into whether misexpression of VCAM-1 in the epicardium is responsible for any of the epicardial phenotype seen in RXR α ^{-/-} mice. Conversely, it could be determined if excess VCAM-1 is responsible for epicardial bubbling or decreased EMT by lowering VCAM-1 levels in the RXR α ^{-/-} mouse by creating a compound VCAM-1^{+/-}RXR α ^{-/-} mouse, in which VCAM-1 levels are genetically reduced.

N-cadherin

In the normal heart, N-cadherin is required for attachment of the epicardium to the myocardium (Luo et al., 2006). In this study, our findings indicate there may be a decrease in N-cadherin in the RXR α ^{-/-} mouse (Figure 33). N-cadherin is of interest because the N-cadherin KO mouse has a detached epicardium (Luo et al., 2006) and N-cadherin is involved in cell-cell attachment through desmosomes and adherens junctions. Desmosome dysfunction has been previously implicated in skin blistering diseases (Has and Bruckner-Tuderman, 2006). The phenotype of the skin in blistering

diseases is quite similar to the phenotype of the bubbled epicardium because the epithelial cell layer is detached from a loss of normal cell adhesion. Therefore, it is possible that improper formation of desmosomes is responsible for epicardium detachment in the $RXR\alpha^{-/-}$ mouse as well as other mouse models with epicardial bubbling/blistering. Cellular junctions between the epicardium and the myocardium were less apparent in the $RXR\alpha^{-/-}$ mouse than in the WT, as was seen in TEM analysis (Figure 21). Future studies examining epicardial/myocardial cellular junctions and analysis of N-cadherin in the developing heart are needed in order to determine N-cadherin's role in epicardium attachment.

Decreased N-cadherin has previously been observed in two models of detached epicardium. N-cadherin is decreased in the *Wt1* epicardial-specific knockout (Martinez-Estrada et al., 2010) and the *Alk5* epicardial-specific knockout (Sridurongrit et al., 2008), both of which have a decrease in epicardial EMT and a detached epicardium. The detachment of the epicardium in the $RXR\alpha^{-/-}$ mouse may be due to a decrease in N-cadherin and not necessarily to misregulation of VCAM-1, whereas an increase in VCAM-1 may contribute more to the decrease in EMT and EPDC formation. Therefore, the role of VCAM-1 in the normal heart following the formation of the epicardium could be in regulating epicardial EMT to form EPDCs that contribute cells and signals for normal cardiac morphogenesis.

TGF β 2 signaling

TGF β 2 signaling is known to be important for cardiac morphogenesis especially in activating EMT and in apoptosis in the endocardial cushions (Camenisch et al., 2002; Kubalak et al., 2002). TGF β 2 $^{-/-}$ mouse embryos have a multitude of cardiac defects including ventricular and outflow tract defects, hypoplastic ascending aorta, double outlet right ventricle and dual inlet left ventricle (Sanford et al., 1997), indicating the importance

of TGF β 2 signaling to the developing heart. An increase in TGF β 2 protein and mRNA was seen in the RXR α -/- heart in previous studies (Kubalak et al., 2002; Jenkins and Kubalak, unpublished) as well as this current study (Figures 26 and 33). TGF β 2 is known to regulate the transcription of several genes through its role as a growth factor and is expressed in the epicardium. Because of misexpression of VCAM-1 in the RXR α -/- epicardium and increased TGF β 2 in the heart of the RXR α -/- mouse occur during the same developmental timeframe, this study focused on whether TGF β 2 could regulate the expression of VCAM-1 in epicardial cells.

Both RXR α and Smad4 were shown to bind to the VCAM-1 promoter by using ChIP analysis (Figure 35). Binding of Smad4 to the promoter might indicate that any member of the TGF β and BMP family is capable of regulating the VCAM-1 promoter. TGF β 2 was shown to regulate VCAM-1 expression in epicardial explants (Figure 38), whole embryo culture (Figures 36 and 37) and VCAM-1 promoter luciferase assays (Figures 39 and 40). However, the effect of other TGF β family members on VCAM-1 expression is not known. Further analysis of the other TGF β family members would be necessary to determine if TGF β 2 is the only member regulating the VCAM-1 promoter. In the future, the effect of TGF β 1, TGF β 3, (because of its overlapped expression with TGF β 2 (Molin et al., 2003)) BMP2 and BMP4 (because of expression in the PE (Kruithof et al., 2006; Schlueter et al., 2006)) on VCAM-1 expression needs to be defined.

Using REC cells transfected with the VC1889 VCAM-1 promoter luciferase plasmid, TGF β 2 was shown to activate transcription from the VCAM-1 promoter. There are numerous putative SBEs present on the VCAM-1 promoter so promoter deletion constructs are needed to determine which possible SBEs are involved (due to their localization in the deleted region). Following promoter deletion studies, mutational

analysis of possible SBEs could be used to determine which SBEs are involved in the regulation of VCAM-1 transcription.

Retinoic Acid Signaling

A proper balance of retinoid signaling is required for cardiac morphogenesis to occur normally with too much or too little retinoid signaling resulting in heart defects as has been demonstrated previously with the VAD rat model and in gestational exposure to Accutane (isotretinoin) (de la Cruz et al., 1984; Wilson and Warkany, 1949). Retinoid consensus binding sites were found on the VCAM-1 promoter (Figure 14) suggesting that VCAM-1 could be regulated by retinoid signaling. However, treatment with 9-cisRA had no effect on the expression of VCAM-1 in epicardial explants or in embryos in WEC. Furthermore, 9-cisRA did not regulate the VCAM-1 promoter, in cells transfected with the VC1889 luciferase expression plasmid. Despite these findings, it is possible that another retinoid (such as all-transRA to activate RARs) or ligand that activates a retinoid receptor-binding partner (such as Vitamin D for the Vitamin D receptor) may play a role in regulating VCAM-1. It is also possible that the retinoid consensus elements found on the VCAM-1 promoter are not functional retinoid binding elements so, therefore, would have no effect on VCAM-1 activation. However, since RXR α bound to the VCAM-1 promoter, it is possible that RXR α acts as a heterodimer with another nuclear receptor. Therefore, in order for RXR α to have an effect on the VCAM-1 promoter, the heterodimer partner of RXR α would also need to be activated by ligand binding.

In the heart, RXR α may have more of a direct effect on TGF β 2 signaling than VCAM-1 since 9-cisRA treatment did not activate the VCAM-1 promoter. Previously it has been proposed that RXR α regulates activation of Smad2 since loss of RXR α (in the RXR α -/- mouse) or dual treatment with TGF β 2 and 9-cisRA (in NIH3T3 cells) will

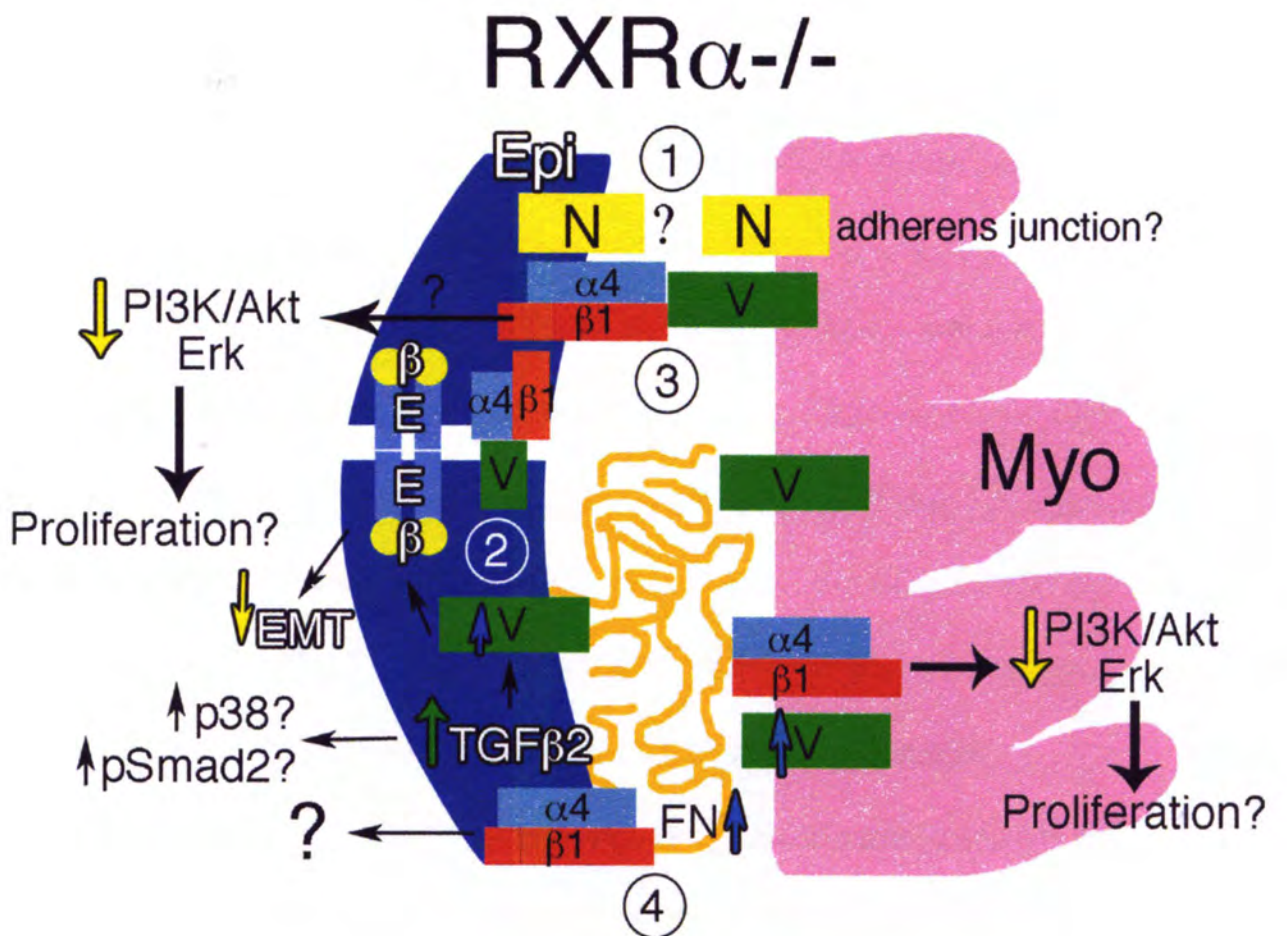
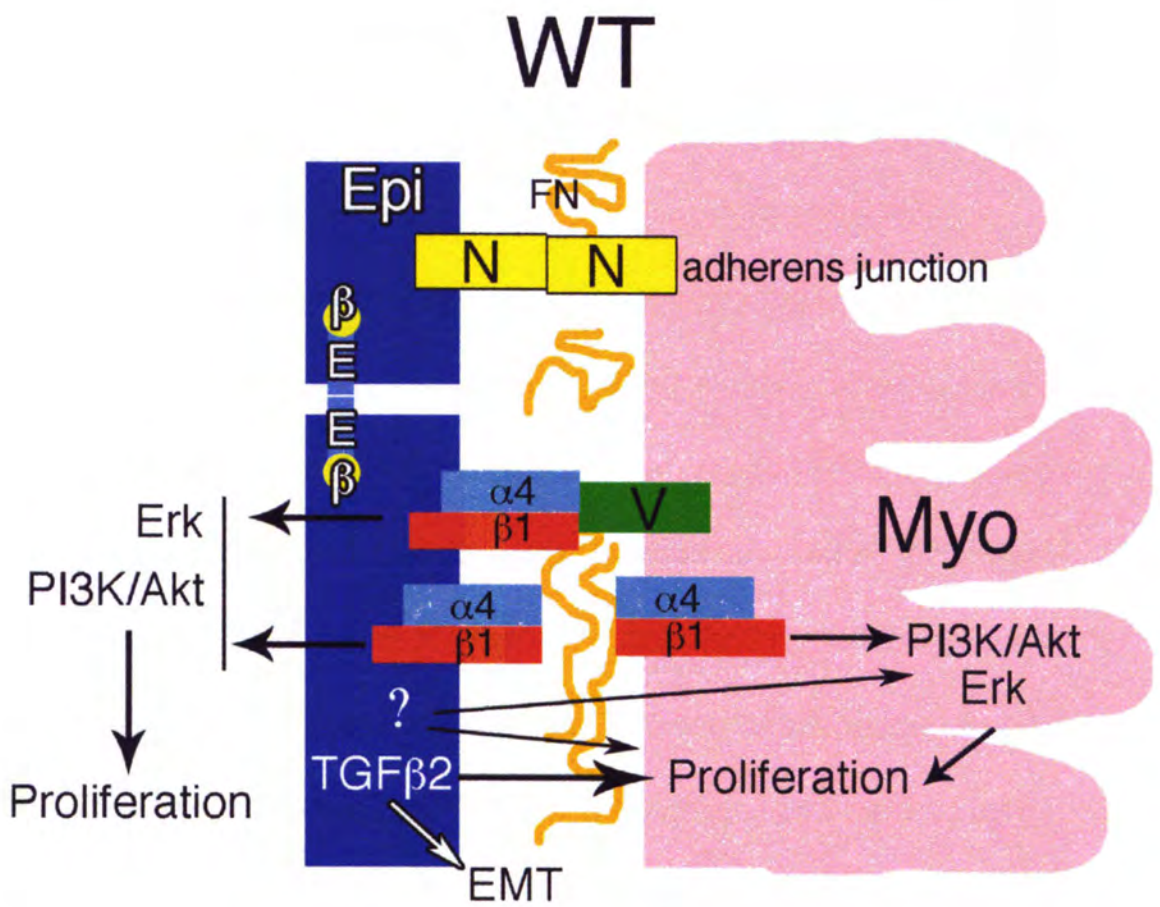
increase Smad2 phosphorylation (Hoover et al., 2008b). Although Smad phosphorylation was increased, nuclear localization of pSmad was decreased in both the RXR α -/- mouse and with TGF β 2/9-cisRA treatments (Hoover et al., 2008b). It was hypothesized that RXR α was acting as a nuclear shuttle for pSmad2 when it is located on the nuclear membrane (Hoover et al., 2008b). In the RXR α -/- mouse or with 9-cisRA treatment when RXR α is not present at the nuclear membrane, there is a decrease in pSmad2 in the nucleus, indicating an uncoupling of TGF β 2 signaling (Hoover et al., 2008b). The increase in TGF β 2 seen in the RXR α -/- mouse could be a compensatory mechanism since pSmad2 may be unable to get into the nucleus to signal (Hoover et al., 2008b). In response to the lack of TGF β 2 signaling, the cell could increase TGF β 2 levels (Hoover et al., 2008b). However, the uncoupling hypothesis would not explain the increase in VCAM-1 since in this current study it was found that TGF β 2 signaling can increase VCAM-1 expression. Importantly, the uncoupling of TGF β 2 signaling in the RXR α -/- mouse is not seen in the entire heart. For example, decreased nuclear localization of phosphorylated Smad2 was seen in the cushions of the heart but was not observed in the epicardium or myocardium (Hoover and Kubalak, unpublished). TGF β 2 could also activate p38 (part of MAPK signaling) to activate transcription of VCAM-1. TGF β 2 has been previously shown to cause phosphorylation of p38 by activation of TGF β associated kinase (TAK1) (Yamashita et al., 2008). Several studies have shown that induction of VCAM-1 expression is dependent on activation of p38. Inhibition of p38 has been shown to suppress VCAM-1 expression induced by tumor necrosis factor α (TNF α) (Ho et al., 2008), cadmium (Park et al., 2009), interleukin β (IL- β) (Wang et al., 2005) and C reactive protein (CRP) (Kawanami et al., 2006). Thus, the increased VCAM-1 may be independent of Smad-binding and instead a response to p38 activation by TGF β 2, which would still occur even if Smad2 is uncoupled.

Conclusion

From this study, it is proposed that VCAM-1 is playing roles in attachment, signaling and regulation of epicardial EMT in the developing heart, each of which will be discussed in this section. First, VCAM-1 is involved in epicardial cell attachment to the myocardium. VCAM-1 is necessary in the initial attachment of the PE cells to the myocardium to form the epicardium (Kwee et al., 1995; Yang et al., 1995) but may not play a role in the later attachment (starting at E11.5) to maintain epicardial adhesion to the myocardium. VCAM-1 and integrin $\alpha 4$ are essential for the initial attachment of PE buds to the myocardium as was demonstrated by both the integrin $\alpha 4$ and VCAM-1 KO mice, both of which fail to form an epicardium (Kwee et al., 1995; Yang et al., 1995). In both the VCAM-1 and integrin $\alpha 4$ knockout mice, PE buds form and migrate to the myocardium but fail to adhere to the myocardium. Therefore, VCAM-1 and integrin $\alpha 4$ are not required for PE bud formation (Kwee et al., 1995; Yang et al., 1995). In the RXR α ^{-/-} mouse, delay in epicardium formation is likely due to an increase in VCAM-1 expression, resulting in increased adhesiveness of PE cells within the PE. Increased PE cell adhesion could prevent or slow the formation of PE buds resulting in a delay of epicardium formation. Furthermore, findings from a previous study demonstrating decreased cell outgrowth in PE explants could be indicative of increased cell adhesion (Jenkins and Kubalak, unpublished).

As for the epicardial cell detachment in the RXR α ^{-/-} mouse, N-cadherin is likely responsible for maintenance of epicardial cell adhesion following epicardium formation (Figure 41, 1). The N-cadherin KO mouse has a detached epicardium and N-cadherin is expressed in both the epicardium and myocardium (Luo et al., 2006). Data from this study suggest that N-cadherin levels are decreased, which would decrease epicardial

Figure 41: Diagrammatic representation of the current working hypothesis. See text for further explanation. N-cadherin is necessary for binding of the epicardium to the myocardium (1). Increased VCAM-1 levels strengthen epicardial-epicardial cell adhesion through increasing interactions of β -catenin and E-cadherin between epicardial cells (2). Binding of VCAM-1 to integrin $\alpha 4\beta 1$ can activate signaling through the PI3K/Akt and Erk signaling cascades (3). Increased FN could increase signaling downstream of integrin $\alpha 4\beta 1$ (4). V, VCAM-1; N, N-cadherin; $\alpha 4$, integrin $\alpha 4$; $\beta 1$, integrin $\beta 1$; β , β -catenin; E, E-cadherin



cell adhesion to the myocardium. Further analysis of N-cadherin in the RXR α -/- mouse would need to be performed to support this conclusion.

It is proposed that VCAM-1 plays a role in regulating epicardial EMT either through cell adhesion of epicardial cells or through signaling with integrin α 4. Previously, it has been demonstrated that soluble VCAM-1 can decrease epicardial cell EMT by strengthening epicardial cell-cell association with β -catenin and E-cadherin on the cell surface (Dokic and Dettman, 2006). Decreased epicardial EMT is observed in the RXR α -/- mouse (Ruiz-Lozano and Kubalak, unpublished) as well as increased VCAM-1. If the increased VCAM-1 in the RXR α -/- mouse heart is increasing epicardial cell-cell association with β -catenin and E-cadherin, then there could be increased epicardial cell-cell adhesion and a decrease in EMT through cell-cell binding by E-cadherin (Figure 41, 2). Decreased epicardial EMT could contribute to some of the cardiac phenotype of the RXR α -/- mouse, including the hypoplastic ventricular myocardium which can occur as a result of fewer EPDCs (Jenkins et al., 2005).

Finally, it is suggested that VCAM-1 is playing a role in signaling in the developing heart (Figure 41, 3). By binding with integrin α 4, VCAM-1 can initiate several possible signaling cascades (Figure 7). PI3K/Akt and Erk signaling are activated downstream of VCAM-1/integrin α 4 binding (Figure 7). Both PI3K/Akt and Erk signaling are decreased in the RXR α -/- mouse (Kang and Sucov, 2005). Both PI3K/Akt and Erk signaling can initiate proliferation of myocytes and decreased PI3K/Akt or Erk signaling could decrease myocyte proliferation (Kang and Sucov, 2005). Increased PI3K/Akt or Erk signaling might be expected if there is increased VCAM-1/integrin α 4 binding. However, this is not seen in the RXR α -/- mouse (Ruiz-Lozano and Kubalak, unpublished), so the decrease in PI3K/Akt or Erk signaling may be unrelated to VCAM-1/integrin α 4 signaling or may reflect a decrease in interactions between α 4 integrin and

VCAM-1. Alternatively, the loss of RXR α in the RXR α -/- mouse could also affect signaling through the loss of gene transcription or through its role as a nuclear shuttle. The decrease in PI3K/Akt could be directly related to loss of RXR α . Since there is also increased FN in the RXR α -/- heart (Jenkins et al., 2005), an increase in FN binding to integrin α 4 could also alter downstream signaling, including PI3K/Akt and Erk signaling (Figure 41, 4). However, since the FN network is disorganized, signaling from FN/integrin α 4 binding could be adversely affected. Thus, increased FN may not increase integrin α 4-mediated signaling in the developing heart due the disorganization in the FN network in the subepicardial space.

From this study, increased VCAM-1 was found in the RXR α -/- mouse heart and can be regulated by TGF β 2 signaling. Several roles of VCAM-1 were proposed in the developing heart. Our study and those of others illustrate that cell adhesion molecules, particularly VCAM-1, play a significant role in cell adhesion as well as in signaling and EMT during heart development and demonstrates the importance of correct cell-type specific expression of cell adhesion molecules during the formation of the heart.

References

- Abbas, A.E., Appleton, C.P., Liu, P.T., and Sweeney, J.P. (2005). Congenital absence of the pericardium: case presentation and review of literature. *Int J Cardiol* 98, 21-25.
- Anagnostou, A., Lee, E.S., Kessimian, N., Levinson, R., and Steiner, M. (1990). Erythropoietin has a mitogenic and positive chemotactic effect on endothelial cells. *Proc Natl Acad Sci U S A* 87, 5978-5982.
- Bosco, E.E., Mulloy, J.C., and Zheng, Y. (2009). Rac1 GTPase: a "Rac" of all trades. *Cell Mol Life Sci* 66, 370-374.
- Bouchey, D., Drake, C.J., Wunsch, A.M., and Little, C.D. (1996). Distribution of connective tissue proteins during development and neovascularization of the epicardium. *Cardiovasc Res* 31 *Spec No*, E104-115.
- Bruneau, B.G. (2008). The developmental genetics of congenital heart disease. *Nature* 451, 943-948.
- Buckingham, M., Meilhac, S., and Zaffran, S. (2005). Building the mammalian heart from two sources of myocardial cells. *Nat Rev Genet* 6, 826-835.
- Cai, C.L., Martin, J.C., Sun, Y., Cui, L., Wang, L., Ouyang, K., Yang, L., Bu, L., Liang, X., Zhang, X., *et al.* (2008). A myocardial lineage derives from Tbx18 epicardial cells. *Nature* 454, 104-108.
- Camenisch, T.D., Molin, D.G., Person, A., Runyan, R.B., Gittenberger-de Groot, A.C., McDonald, J.A., and Klewer, S.E. (2002). Temporal and distinct TGFbeta ligand requirements during mouse and avian endocardial cushion morphogenesis. *Dev Biol* 248, 170-181.
- Chambon, P. (1996). A decade of molecular biology of retinoic acid receptors. *FASEB J* 10, 940-954.
- Chen, J., Kubalak, S.W., and Chien, K.R. (1998). Ventricular muscle-restricted targeting of the RXRalpha gene reveals a non-cell-autonomous requirement in cardiac chamber morphogenesis. *Development* 125, 1943-1949.
- Chen, T.H., Chang, T.C., Kang, J.O., Choudhary, B., Makita, T., Tran, C.M., Burch, J.B., Eid, H., and Sucov, H.M. (2002). Epicardial induction of fetal cardiomyocyte proliferation via a retinoic acid-inducible trophic factor. *Dev Biol* 250, 198-207.
- Chien, K.R., Domian, I.J., and Parker, K.K. (2008). Cardiogenesis and the complex biology of regenerative cardiovascular medicine. *Science* 322, 1494-1497.
- Christoffels, V.M., Grieskamp, T., Norden, J., Mommersteeg, M.T., Rudat, C., and Kispert, A. (2009). Tbx18 and the fate of epicardial progenitors. *Nature* 458, E8-9; discussion E9-10.

Cohen-Gould, L., and Mikawa, T. (1996). The fate diversity of mesodermal cells within the heart field during chicken early embryogenesis. *Dev Biol* 177, 265-273.

Cook-Mills, J.M. (2002). VCAM-1 signals during lymphocyte migration: role of reactive oxygen species. *Mol Immunol* 39, 499-508.

de la Cruz, E., Sun, S., Vangvanichyakorn, K., and Desposito, F. (1984). Multiple congenital malformations associated with maternal isotretinoin therapy. *Pediatrics* 74, 428-430.

Deem, T.L., and Cook-Mills, J.M. (2004). Vascular cell adhesion molecule 1 (VCAM-1) activation of endothelial cell matrix metalloproteinases: role of reactive oxygen species. *Blood* 104, 2385-2393.

Derynck, R., and Feng, X.H. (1997). TGF-beta receptor signaling. *Biochim Biophys Acta* 1333, F105-150.

Desvergne, B. (2007). RXR: from partnership to leadership in metabolic regulations. *Vitam Horm* 75, 1-32.

Dettman, R.W., Denetclaw, W., Jr., Ordahl, C.P., and Bristow, J. (1998). Common epicardial origin of coronary vascular smooth muscle, perivascular fibroblasts, and intermyocardial fibroblasts in the avian heart. *Dev Biol* 193, 169-181.

Dettman, R.W., Pae, S.H., Morabito, C., and Bristow, J. (2003). Inhibition of alpha4-integrin stimulates epicardial-mesenchymal transformation and alters migration and cell fate of epicardially derived mesenchyme. *Dev Biol* 257, 315-328.

Dokic, D., and Dettman, R.W. (2006). VCAM-1 inhibits TGFbeta stimulated epithelial-mesenchymal transformation by modulating Rho activity and stabilizing intercellular adhesion in epicardial mesothelial cells. *Dev Biol* 299, 489-504.

Duester, G. (2000). Families of retinoid dehydrogenases regulating vitamin A function: production of visual pigment and retinoic acid. *Eur J Biochem* 267, 4315-4324.

Dyer, L.A., and Kirby, M.L. (2009). The role of secondary heart field in cardiac development. *Dev Biol* 336, 137-144.

Dyson, E., Sucov, H.M., Kubalak, S.W., Schmid-Schonbein, G.W., DeLano, F.A., Evans, R.M., Ross, J., Jr., and Chien, K.R. (1995). Atrial-like phenotype is associated with embryonic ventricular failure in retinoid X receptor alpha $-/-$ mice. *Proc Natl Acad Sci U S A* 92, 7386-7390.

Eisenberg, L.M., and Markwald, R.R. (1995). Molecular regulation of atrioventricular valvuloseptal morphogenesis. *Circ Res* 77, 1-6.

Elangbam, C.S., Qualls, C.W., Jr., and Dahlgren, R.R. (1997). Cell adhesion molecules--update. *Vet Pathol* 34, 61-73.

- Feng, X.H., and Derynck, R. (2005). Specificity and versatility in tgf-beta signaling through Smads. *Annu Rev Cell Dev Biol* 21, 659-693.
- Fuxe, J., Vincent, T., and de Herreros, A.G. (2010). Transcriptional crosstalk between TGFbeta and stem cell pathways in tumor cell invasion: Role of EMT promoting Smad complexes. *Cell Cycle* 9.
- Garcia-Martinez, V., and Schoenwolf, G.C. (1993). Primitive-streak origin of the cardiovascular system in avian embryos. *Dev Biol* 159, 706-719.
- George, E.L., Georges-Labouesse, E.N., Patel-King, R.S., Rayburn, H., and Hynes, R.O. (1993). Defects in mesoderm, neural tube and vascular development in mouse embryos lacking fibronectin. *Development* 119, 1079-1091.
- Gittenberger-de Groot, A.C., Vrancken Peeters, M.P., Mentink, M.M., Gourdie, R.G., and Poelmann, R.E. (1998). Epicardium-derived cells contribute a novel population to the myocardial wall and the atrioventricular cushions. *Circ Res* 82, 1043-1052.
- Gourdie, R.G., Ghatnekar, G.S., O'Quinn, M., Rhatt, M.J., Barker, R.J., Zhu, C., Jourdan, J., and Hunter, A.W. (2006). The unstoppable connexin43 carboxyl-terminus: new roles in gap junction organization and wound healing. *Ann N Y Acad Sci* 1080, 49-62.
- Grayson, M.H., Van der Vieren, M., Sterbinsky, S.A., Michael Gallatin, W., Hoffman, P.A., Staunton, D.E., and Bochner, B.S. (1998). alphadbeta2 integrin is expressed on human eosinophils and functions as an alternative ligand for vascular cell adhesion molecule 1 (VCAM-1). *J Exp Med* 188, 2187-2191.
- Green, K.J., and Simpson, C.L. (2007). Desmosomes: new perspectives on a classic. *J Invest Dermatol* 127, 2499-2515.
- Gruber, P.J., Kubalak, S.W., Pexieder, T., Sucov, H.M., Evans, R.M., and Chien, K.R. (1996). RXR alpha deficiency confers genetic susceptibility for aortic sac, conotruncal, atrioventricular cushion, and ventricular muscle defects in mice. *J Clin Invest* 98, 1332-1343.
- Guadix, J.A., Carmona, R., Munoz-Chapuli, R., and Perez-Pomares, J.M. (2006). In vivo and in vitro analysis of the vasculogenic potential of avian proepicardial and epicardial cells. *Dev Dyn* 235, 1014-1026.
- Hagel, M., George, E.L., Kim, A., Tamimi, R., Opitz, S.L., Turner, C.E., Imamoto, A., and Thomas, S.M. (2002). The adaptor protein paxillin is essential for normal development in the mouse and is a critical transducer of fibronectin signaling. *Mol Cell Biol* 22, 901-915.
- Harvey, R.P. (1999). Seeking a regulatory roadmap for heart morphogenesis. *Semin Cell Dev Biol* 10, 99-107.
- Has, C., and Bruckner-Tuderman, L. (2006). Molecular and diagnostic aspects of genetic skin fragility. *J Dermatol Sci* 44, 129-144.

- Hayashi, H., and Kume, T. (2008). Foxc transcription factors directly regulate Dll4 and Hey2 expression by interacting with the VEGF-Notch signaling pathways in endothelial cells. *PLoS One* 3, e2401.
- Hertig, C.M., Kubalak, S.W., Wang, Y., and Chien, K.R. (1999). Synergistic roles of neuregulin-1 and insulin-like growth factor-I in activation of the phosphatidylinositol 3-kinase pathway and cardiac chamber morphogenesis. *J Biol Chem* 274, 37362-37369.
- Hildreth, V., Webb, S., Bradshaw, L., Brown, N.A., Anderson, R.H., and Henderson, D.J. (2008). Cells migrating from the neural crest contribute to the innervation of the venous pole of the heart. *J Anat* 212, 1-11.
- Hirose, T., Karasawa, M., Sugitani, Y., Fujisawa, M., Akimoto, K., Ohno, S., and Noda, T. (2006). PAR3 is essential for cyst-mediated epicardial development by establishing apical cortical domains. *Development* 133, 1389-1398.
- Ho, A.W., Wong, C.K., and Lam, C.W. (2008). Tumor necrosis factor-alpha up-regulates the expression of CCL2 and adhesion molecules of human proximal tubular epithelial cells through MAPK signaling pathways. *Immunobiology* 213, 533-544.
- Hoover, L.L., Burton, E.G., Brooks, B.A., and Kubalak, S.W. (2008a). The expanding role for retinoid signaling in heart development. *ScientificWorldJournal* 8, 194-211.
- Hoover, L.L., Burton, E.G., O'Neill, M.L., Brooks, B.A., Sreedharan, S., Dawson, N.A., and Kubalak, S.W. (2008b). Retinoids regulate TGFbeta signaling at the level of Smad2 phosphorylation and nuclear accumulation. *Biochim Biophys Acta* 1783, 2279-2286.
- Hosking, B.M., Wang, S.C., Downes, M., Koopman, P., and Muscat, G.E. (2004). The VCAM-1 gene that encodes the vascular cell adhesion molecule is a target of the Sry-related high mobility group box gene, Sox18. *J Biol Chem* 279, 5314-5322.
- Hurd, T.W., Fan, S., Liu, C.J., Kweon, H.K., Hakansson, K., and Margolis, B. (2003). Phosphorylation-dependent binding of 14-3-3 to the polarity protein Par3 regulates cell polarity in mammalian epithelia. *Curr Biol* 13, 2082-2090.
- Hurle, J.M., Kitten, G.T., Sakai, L.Y., Volpin, D., and Solursh, M. (1994). Elastic extracellular matrix of the embryonic chick heart: an immunohistological study using laser confocal microscopy. *Dev Dyn* 200, 321-332.
- Hutson, M.R., and Kirby, M.L. (2007). Model systems for the study of heart development and disease. Cardiac neural crest and conotruncal malformations. *Semin Cell Dev Biol* 18, 101-110.
- Hynes, R. (1985). Molecular biology of fibronectin. *Annu Rev Cell Biol* 1, 67-90.
- Hynes, R.O. (1992). Integrins: versatility, modulation, and signaling in cell adhesion. *Cell* 69, 11-25.
- Hynes, R.O. (2002). Integrins: bidirectional, allosteric signaling machines. *Cell* 110, 673-687.

- Ilic, D., Furuta, Y., Kanazawa, S., Takeda, N., Sobue, K., Nakatsuji, N., Nomura, S., Fujimoto, J., Okada, M., and Yamamoto, T. (1995). Reduced cell motility and enhanced focal adhesion contact formation in cells from FAK-deficient mice. *Nature* 377, 539-544.
- Inumaru, J., Nagano, O., Takahashi, E., Ishimoto, T., Nakamura, S., Suzuki, Y., Niwa, S., Umezawa, K., Tanihara, H., and Saya, H. (2009). Molecular mechanisms regulating dissociation of cell-cell junction of epithelial cells by oxidative stress. *Genes Cells* 14, 703-716.
- Ittner, L.M., Wurdak, H., Schwerdtfeger, K., Kunz, T., Ille, F., Leveen, P., Hjalt, T.A., Suter, U., Karlsson, S., Hafezi, F., *et al.* (2005). Compound developmental eye disorders following inactivation of TGFbeta signaling in neural-crest stem cells. *J Biol* 4, 11.
- Jenkins, K.J., Correa, A., Feinstein, J.A., Botto, L., Britt, A.E., Daniels, S.R., Elixson, M., Warnes, C.A., and Webb, C.L. (2007). Noninherited risk factors and congenital cardiovascular defects: current knowledge: a scientific statement from the American Heart Association Council on Cardiovascular Disease in the Young: endorsed by the American Academy of Pediatrics. *Circulation* 115, 2995-3014.
- Jenkins, S.J., Hutson, D.R., and Kubalak, S.W. (2005). Analysis of the proepicardium-epicardium transition during the malformation of the RXRalpha-/- epicardium. *Dev Dyn* 233, 1091-1101.
- Joberty, G., Petersen, C., Gao, L., and Macara, I.G. (2000). The cell-polarity protein Par6 links Par3 and atypical protein kinase C to Cdc42. *Nat Cell Biol* 2, 531-539.
- Kalman, F., Viragh, S., and Modis, L. (1995). Cell surface glycoconjugates and the extracellular matrix of the developing mouse embryo epicardium. *Anat Embryol (Berl)* 191, 451-464.
- Kang, J.O., and Sucov, H.M. (2005). Convergent proliferative response and divergent morphogenic pathways induced by epicardial and endocardial signaling in fetal heart development. *Mech Dev* 122, 57-65.
- Kang, M., Gregory, D., and Kume, T. (2006). Forkhead Transcription Factors, Foxc1 and Foxc2, Directly Regulate VCAM-1 Gene Expression in Endothelial Cells: P118. *Circ Res* 99, e39.
- Kastner, P., Grondona, J.M., Mark, M., Gansmuller, A., LeMeur, M., Decimo, D., Vonesch, J.L., Dolle, P., and Chambon, P. (1994). Genetic analysis of RXR alpha developmental function: convergence of RXR and RAR signaling pathways in heart and eye morphogenesis. *Cell* 78, 987-1003.
- Kastner, P., Messaddeq, N., Mark, M., Wendling, O., Grondona, J.M., Ward, S., Ghyselinck, N., and Chambon, P. (1997). Vitamin A deficiency and mutations of RXRalpha, RXRbeta and RARalpha lead to early differentiation of embryonic ventricular cardiomyocytes. *Development* 124, 4749-4758.
- Kawanami, D., Maemura, K., Takeda, N., Harada, T., Nojiri, T., Saito, T., Manabe, I., Imai, Y., and Nagai, R. (2006). C-reactive protein induces VCAM-1 gene expression through NF-kappaB activation in vascular endothelial cells. *Atherosclerosis* 185, 39-46.

- Kelly, R.G., Brown, N.A., and Buckingham, M.E. (2001). The arterial pole of the mouse heart forms from Fgf10-expressing cells in pharyngeal mesoderm. *Dev Cell* 1, 435-440.
- Kim, H., Yoon, C.S., and Rah, B. (1999). Expression of extracellular matrix components fibronectin and laminin in the human fetal heart. *Cell Struct Funct* 24, 19-26.
- Kirschner, K.M., Wagner, N., Wagner, K.D., Wellmann, S., and Scholz, H. (2006). The Wilms tumor suppressor Wt1 promotes cell adhesion through transcriptional activation of the alpha4 integrin gene. *J Biol Chem* 281, 31930-31939.
- Komiyama, M., Ito, K., and Shimada, Y. (1987). Origin and development of the epicardium in the mouse embryo. *Anat Embryol (Berl)* 176, 183-189.
- Krantz, S.B. (1991). Erythropoietin. *Blood* 77, 419-434.
- Kruithof, B.P., van Wijk, B., Somi, S., Kruithof-de Julio, M., Perez Pomares, J.M., Weesie, F., Wessels, A., Moorman, A.F., and van den Hoff, M.J. (2006). BMP and FGF regulate the differentiation of multipotential pericardial mesoderm into the myocardial or epicardial lineage. *Dev Biol* 295, 507-522.
- Kubalak, S.W., Hutson, D.R., Scott, K.K., and Shannon, R.A. (2002). Elevated transforming growth factor beta2 enhances apoptosis and contributes to abnormal outflow tract and aortic sac development in retinoic X receptor alpha knockout embryos. *Development* 129, 733-746.
- Kuhn, H.J., and Liebherr, G. (1988). The early development of the epicardium in *Tupaia belangeri*. *Anat Embryol (Berl)* 177, 225-234.
- Kwee, L., Baldwin, H.S., Shen, H.M., Stewart, C.L., Buck, C., Buck, C.A., and Labow, M.A. (1995). Defective development of the embryonic and extraembryonic circulatory systems in vascular cell adhesion molecule (VCAM-1) deficient mice. *Development* 121, 489-503.
- Laugwitz, K.L., Moretti, A., Caron, L., Nakano, A., and Chien, K.R. (2008). Islet1 cardiovascular progenitors: a single source for heart lineages? *Development* 135, 193-205.
- Lee, R.Y., Luo, J., Evans, R.M., Giguere, V., and Sucov, H.M. (1997). Compartment-selective sensitivity of cardiovascular morphogenesis to combinations of retinoic acid receptor gene mutations. *Circ Res* 80, 757-764.
- Li, W.E., Waldo, K., Linask, K.L., Chen, T., Wessels, A., Parmacek, M.S., Kirby, M.L., and Lo, C.W. (2002). An essential role for connexin43 gap junctions in mouse coronary artery development. *Development* 129, 2031-2042.
- Little, M., Holmes, G., and Walsh, P. (1999). WT1: what has the last decade told us? *Bioessays* 21, 191-202.
- Luo, J., Sucov, H.M., Bader, J.A., Evans, R.M., and Giguere, V. (1996). Compound mutants for retinoic acid receptor (RAR) beta and RAR alpha 1 reveal developmental functions for multiple RAR beta isoforms. *Mech Dev* 55, 33-44.

- Luo, Y., High, F.A., Epstein, J.A., and Radice, G.L. (2006). N-cadherin is required for neural crest remodeling of the cardiac outflow tract. *Dev Biol* 299, 517-528.
- Mahtab, E.A., Wijffels, M.C., Van Den Akker, N.M., Hahurij, N.D., Lie-Venema, H., Wisse, L.J., Deruiter, M.C., Uhrin, P., Zaujec, J., Binder, B.R., *et al.* (2008). Cardiac malformations and myocardial abnormalities in podoplanin knockout mouse embryos: Correlation with abnormal epicardial development. *Dev Dyn* 237, 847-857.
- Makita, T., Duncan, S.A., and Sucov, H.M. (2005). Retinoic acid, hypoxia, and GATA factors cooperatively control the onset of fetal liver erythropoietin expression and erythropoietic differentiation. *Dev Biol* 280, 59-72.
- Manasek, F.J. (1969). Embryonic development of the heart. II. Formation of the epicardium. *J Embryol Exp Morphol* 22, 333-348.
- Manner, J. (1992). The development of pericardial villi in the chick embryo. *Anat Embryol (Berl)* 186, 379-385.
- Manner, J. (1999). Does the subepicardial mesenchyme contribute myocardioblasts to the myocardium of the chick embryo heart? A quail-chick chimera study tracing the fate of the epicardial primordium. *Anat Rec* 255, 212-226.
- Manner, J. (2000). Cardiac looping in the chick embryo: a morphological review with special reference to terminological and biomechanical aspects of the looping process. *Anat Rec* 259, 248-262.
- Manner, J., Perez-Pomares, J.M., Macias, D., and Munoz-Chapuli, R. (2001). The origin, formation and developmental significance of the epicardium: a review. *Cells Tissues Organs* 169, 89-103.
- Mark, M., Ghyselinck, N.B., and Chambon, P. (2006). Function of retinoid nuclear receptors: lessons from genetic and pharmacological dissections of the retinoic acid signaling pathway during mouse embryogenesis. *Annu Rev Pharmacol Toxicol* 46, 451-480.
- Mark, M., Ghyselinck, N.B., Wendling, O., Dupe, V., Mascrez, B., Kastner, P., and Chambon, P. (1999). A genetic dissection of the retinoid signalling pathway in the mouse. *Proc Nutr Soc* 58, 609-613.
- Markwald, R.R., Fitzharris, T.P., and Manasek, F.J. (1977). Structural development of endocardial cushions. *Am J Anat* 148, 85-119.
- Martin-Puig, S., Wang, Z., and Chien, K.R. (2008). Lives of a heart cell: tracing the origins of cardiac progenitors. *Cell Stem Cell* 2, 320-331.
- Martin-Villar, E., Scholl, F.G., Gamallo, C., Yurrita, M.M., Munoz-Guerra, M., Cruces, J., and Quintanilla, M. (2005). Characterization of human PA2.26 antigen (T1alpha-2, podoplanin), a small membrane mucin induced in oral squamous cell carcinomas. *Int J Cancer* 113, 899-910.

- Martinez-Estrada, O.M., Lettice, L.A., Essafi, A., Guadix, J.A., Slight, J., Velecela, V., Hall, E., Reichmann, J., Devenney, P.S., Hohenstein, P., *et al.* (2010). Wt1 is required for cardiovascular progenitor cell formation through transcriptional control of Snail and E-cadherin. *Nat Genet* 42, 89-93.
- Martinsen, B.J. (2005). Reference guide to the stages of chick heart embryology. *Dev Dyn* 233, 1217-1237.
- Mendelsohn, C., Lohnes, D., Decimo, D., Lufkin, T., LeMeur, M., Chambon, P., and Mark, M. (1994). Function of the retinoic acid receptors (RARs) during development (II). Multiple abnormalities at various stages of organogenesis in RAR double mutants. *Development* 120, 2749-2771.
- Merki, E., Zamora, M., Raya, A., Kawakami, Y., Wang, J., Zhang, X., Burch, J., Kubalak, S.W., Kaliman, P., Belmonte, J.C., *et al.* (2005). Epicardial retinoid X receptor alpha is required for myocardial growth and coronary artery formation. *Proc Natl Acad Sci U S A* 102, 18455-18460.
- Mikawa, T., and Fischman, D.A. (1992). Retroviral analysis of cardiac morphogenesis: discontinuous formation of coronary vessels. *Proc Natl Acad Sci U S A* 89, 9504-9508.
- Mikawa, T., and Gourdie, R.G. (1996). Pericardial mesoderm generates a population of coronary smooth muscle cells migrating into the heart along with ingrowth of the epicardial organ. *Dev Biol* 174, 221-232.
- Mjaatvedt, C.H., Nakaoka, T., Moreno-Rodriguez, R., Norris, R.A., Kern, M.J., Eisenberg, C.A., Turner, D., and Markwald, R.R. (2001). The outflow tract of the heart is recruited from a novel heart-forming field. *Dev Biol* 238, 97-109.
- Molin, D.G., Bartram, U., Van der Heiden, K., Van Iperen, L., Speer, C.P., Hierck, B.P., Poelmann, R.E., and Gittenberger-de-Groot, A.C. (2003). Expression patterns of Tgfbeta1-3 associate with myocardialisation of the outflow tract and the development of the epicardium and the fibrous heart skeleton. *Dev Dyn* 227, 431-444.
- Moore, A.W., McInnes, L., Kreidberg, J., Hastie, N.D., and Schedl, A. (1999). YAC complementation shows a requirement for Wt1 in the development of epicardium, adrenal gland and throughout nephrogenesis. *Development* 126, 1845-1857.
- Moss, J.B., Xavier-Neto, J., Shapiro, M.D., Nayeem, S.M., McCaffery, P., Drager, U.C., and Rosenthal, N. (1998). Dynamic patterns of retinoic acid synthesis and response in the developing mammalian heart. *Dev Biol* 199, 55-71.
- Moustakas, A., Souchelnytskyi, S., and Heldin, C.H. (2001). Smad regulation in TGF-beta signal transduction. *J Cell Sci* 114, 4359-4369.
- Munoz-Chapuli, R., and Hamlett, W.C. (1996). Epilogue: comparative cardiovascular biology of lower vertebrates. *J Exp Zool* 275, 249-251.
- Munoz-Chapuli, R., Macias, D., Ramos, C., de Andres, V., Gallego, A., and Navarro, P. (1994). Cardiac development in the dogfish (*Scyliorhinus canicula*): a model for the study of vertebrate cardiogenesis. *Cardioscience* 5, 245-253.

- Nahirney, P.C., Mikawa, T., and Fischman, D.A. (2003). Evidence for an extracellular matrix bridge guiding proepicardial cell migration to the myocardium of chick embryos. *Dev Dyn* 227, 511-523.
- Nakamura, T., Colbert, M.C., and Robbins, J. (2006). Neural crest cells retain multipotential characteristics in the developing valves and label the cardiac conduction system. *Circ Res* 98, 1547-1554.
- Niederreither, K., McCaffery, P., Drager, U.C., Chambon, P., and Dolle, P. (1997). Restricted expression and retinoic acid-induced downregulation of the retinaldehyde dehydrogenase type 2 (RALDH-2) gene during mouse development. *Mech Dev* 62, 67-78.
- Niederreither, K., Vermot, J., Messaddeq, N., Schuhbauer, B., Chambon, P., and Dolle, P. (2001). Embryonic retinoic acid synthesis is essential for heart morphogenesis in the mouse. *Development* 128, 1019-1031.
- Niessen, C.M. (2007). Tight junctions/adherens junctions: basic structure and function. *J Invest Dermatol* 127, 2525-2532.
- Oliveira, L.A., Baker, R.K., Klewer, S.E., and Kitten, G.T. (2010). Expression of beta 2 integrin (CD18) in embryonic mouse and chicken heart. *Braz J Med Biol Res* 43, 25-35.
- Pae, S.H., Dokic, D., and Dettman, R.W. (2008). Communication between integrin receptors facilitates epicardial cell adhesion and matrix organization. *Dev Dyn* 237, 962-978.
- Park, S.L., Kim, Y.M., Ahn, J.H., Lee, S.H., Baik, E.J., Moon, C.H., and Jung, Y.S. (2009). Cadmium stimulates the expression of vascular cell adhesion molecule-1 (VCAM-1) via p38 mitogen-activated protein kinase (MAPK) and JNK activation in cerebrovascular endothelial cells. *J Pharmacol Sci* 110, 405-409.
- Pasutto, F., Sticht, H., Hammersen, G., Gillessen-Kaesbach, G., Fitzpatrick, D.R., Nurnberg, G., Brasch, F., Schirmer-Zimmermann, H., Tolmie, J.L., Chitayat, D., *et al.* (2007). Mutations in STRA6 cause a broad spectrum of malformations including anophthalmia, congenital heart defects, diaphragmatic hernia, alveolar capillary dysplasia, lung hypoplasia, and mental retardation. *Am J Hum Genet* 80, 550-560.
- Perez-Pomares, J.M., Carmona, R., Gonzalez-Iriarte, M., Atencia, G., Wessels, A., and Munoz-Chapuli, R. (2002). Origin of coronary endothelial cells from epicardial mesothelium in avian embryos. *Int J Dev Biol* 46, 1005-1013.
- Perez-Pomares, J.M., Macias, D., Garcia-Garrido, L., and Munoz-Chapuli, R. (1997). Contribution of the primitive epicardium to the subepicardial mesenchyme in hamster and chick embryos. *Dev Dyn* 210, 96-105.
- Perez-Pomares, J.M., Macias, D., Garcia-Garrido, L., and Munoz-Chapuli, R. (1998). The origin of the subepicardial mesenchyme in the avian embryo: an immunohistochemical and quail-chick chimera study. *Dev Biol* 200, 57-68.

- Peters, J.H., and Hynes, R.O. (1996). Fibronectin isoform distribution in the mouse. I. The alternatively spliced EIIIB, EIIIA, and V segments show widespread codistribution in the developing mouse embryo. *Cell Adhes Commun* 4, 103-125.
- Pinco, K.A., Liu, S., and Yang, J.T. (2001). alpha4 integrin is expressed in a subset of cranial neural crest cells and in epicardial progenitor cells during early mouse development. *Mech Dev* 100, 99-103.
- Potts, J.D., Dagle, J.M., Walder, J.A., Weeks, D.L., and Runyan, R.B. (1991). Epithelial-mesenchymal transformation of embryonic cardiac endothelial cells is inhibited by a modified antisense oligodeoxynucleotide to transforming growth factor beta 3. *Proc Natl Acad Sci U S A* 88, 1516-1520.
- Ream, M., Ray, A.M., Chandra, R., and Chikaraishi, D.M. (2008). Early fetal hypoxia leads to growth restriction and myocardial thinning. *Am J Physiol Regul Integr Comp Physiol* 295, R583-595.
- Rhee, D.Y., Zhao, X.Q., Francis, R.J., Huang, G.Y., Mably, J.D., and Lo, C.W. (2009). Connexin 43 regulates epicardial cell polarity and migration in coronary vascular development. *Development* 136, 3185-3193.
- Rodgers, L.S., Lalani, S., Runyan, R.B., and Camenisch, T.D. (2008). Differential growth and multicellular villi direct proepicardial translocation to the developing mouse heart. *Dev Dyn* 237, 145-152.
- Rosen, G.D., Sanes, J.R., LaChance, R., Cunningham, J.M., Roman, J., and Dean, D.C. (1992). Roles for the integrin VLA-4 and its counter receptor VCAM-1 in myogenesis. *Cell* 69, 1107-1119.
- Ruiz-Lozano, P., and Chien, K.R. (2003). Cre-constructing the heart. *Nat Genet* 33, 8-9.
- Ruiz-Lozano, P., Smith, S.M., Perkins, G., Kubalak, S.W., Boss, G.R., Sucov, H.M., Evans, R.M., and Chien, K.R. (1998). Energy deprivation and a deficiency in downstream metabolic target genes during the onset of embryonic heart failure in RXRalpha^{-/-} embryos. *Development* 125, 533-544.
- Sakai, Y., Meno, C., Fujii, H., Nishino, J., Shiratori, H., Saijoh, Y., Rossant, J., and Hamada, H. (2001). The retinoic acid-inactivating enzyme CYP26 is essential for establishing an uneven distribution of retinoic acid along the antero-posterior axis within the mouse embryo. *Genes Dev* 15, 213-225.
- Sanford, L.P., Ormsby, I., Gittenberger-de Groot, A.C., Sariola, H., Friedman, R., Boivin, G.P., Cardell, E.L., and Doetschman, T. (1997). TGFbeta2 knockout mice have multiple developmental defects that are non-overlapping with other TGFbeta knockout phenotypes. *Development* 124, 2659-2670.
- Scheffe, J.H., Lehmann, K.E., Buschmann, I.R., Unger, T., and Funke-Kaiser, H. (2006). Quantitative real-time RT-PCR data analysis: current concepts and the novel "gene expression's CT difference" formula. *J Mol Med* 84, 901-910.

- Schlueter, J., Manner, J., and Brand, T. (2006). BMP is an important regulator of proepicardial identity in the chick embryo. *Dev Biol* 295, 546-558.
- Schroeder, J.A., Jackson, L.F., Lee, D.C., and Camenisch, T.D. (2003). Form and function of developing heart valves: coordination by extracellular matrix and growth factor signaling. *J Mol Med* 81, 392-403.
- Schulte, I., Schlueter, J., Abu-Issa, R., Brand, T., and Manner, J. (2007). Morphological and molecular left-right asymmetries in the development of the proepicardium: a comparative analysis on mouse and chick embryos. *Dev Dyn* 236, 684-695.
- Sengbusch, J.K., He, W., Pinco, K.A., and Yang, J.T. (2002). Dual functions of [alpha]4[beta]1 integrin in epicardial development: initial migration and long-term attachment. *J Cell Biol* 157, 873-882.
- Seo, S., and Kume, T. (2006). Forkhead transcription factors, Foxc1 and Foxc2, are required for the morphogenesis of the cardiac outflow tract. *Dev Biol* 296, 421-436.
- Sheppard, A.M., Onken, M.D., Rosen, G.D., Noakes, P.G., and Dean, D.C. (1994). Expanding roles for alpha 4 integrin and its ligands in development. *Cell Adhes Commun* 2, 27-43.
- Smith, T.K., and Bader, D.M. (2007). Signals from both sides: Control of cardiac development by the endocardium and epicardium. *Semin Cell Dev Biol* 18, 84-89.
- Snarr, B.S., Kern, C.B., and Wessels, A. (2008). Origin and fate of cardiac mesenchyme. *Dev Dyn* 237, 2804-2819.
- Sridurongrit, S., Larsson, J., Schwartz, R., Ruiz-Lozano, P., and Kaartinen, V. (2008). Signaling via the Tgf-beta type I receptor Alk5 in heart development. *Dev Biol* 322, 208-218.
- Srivastava, D. (2006). Making or breaking the heart: from lineage determination to morphogenesis. *Cell* 126, 1037-1048.
- Stuckmann, I., Evans, S., and Lassar, A.B. (2003). Erythropoietin and retinoic acid, secreted from the epicardium, are required for cardiac myocyte proliferation. *Dev Biol* 255, 334-349.
- Subbarayan, V., Mark, M., Messadeq, N., Rustin, P., Chambon, P., and Kastner, P. (2000). RXRalpha overexpression in cardiomyocytes causes dilated cardiomyopathy but fails to rescue myocardial hypoplasia in RXRalpha-null fetuses. *J Clin Invest* 105, 387-394.
- Sucov, H.M., Dyson, E., Gumeringer, C.L., Price, J., Chien, K.R., and Evans, R.M. (1994). RXR alpha mutant mice establish a genetic basis for vitamin A signaling in heart morphogenesis. *Genes Dev* 8, 1007-1018.

- Taooka, Y., Chen, J., Yednock, T., and Sheppard, D. (1999). The integrin alpha9beta1 mediates adhesion to activated endothelial cells and transendothelial neutrophil migration through interaction with vascular cell adhesion molecule-1. *J Cell Biol* 145, 413-420.
- Tevosian, S.G., Deconinck, A.E., Tanaka, M., Schinke, M., Litovsky, S.H., Izumo, S., Fujiwara, Y., and Orkin, S.H. (2000). FOG-2, a cofactor for GATA transcription factors, is essential for heart morphogenesis and development of coronary vessels from epicardium. *Cell* 101, 729-739.
- Tidball, J.G. (1992). Distribution of collagens and fibronectin in the subepicardium during avian cardiac development. *Anat Embryol (Berl)* 185, 155-162.
- Tomanek, R.J. (2005). Formation of the coronary vasculature during development. *Angiogenesis* 8, 273-284.
- Van den Eijnde, S.M., Wenink, A.C., and Vermeij-Keers, C. (1995). Origin of subepicardial cells in rat embryos. *Anat Rec* 242, 96-102.
- Van der Vieren, M., Crowe, D.T., Hoekstra, D., Vazeux, R., Hoffman, P.A., Grayson, M.H., Bochner, B.S., Gallatin, W.M., and Staunton, D.E. (1999). The leukocyte integrin alpha D beta 2 binds VCAM-1: evidence for a binding interface between I domain and VCAM-1. *J Immunol* 163, 1984-1990.
- van Wetering, S., van den Berk, N., van Buul, J.D., Mul, F.P., Lommerse, I., Mous, R., ten Klooster, J.P., Zwaginga, J.J., and Hordijk, P.L. (2003). VCAM-1-mediated Rac signaling controls endothelial cell-cell contacts and leukocyte transmigration. *Am J Physiol Cell Physiol* 285, C343-352.
- van Wijk, B., van den Berg, G., Abu-Issa, R., Barnett, P., van der Velden, S., Schmidt, M., Ruijter, J.M., Kirby, M.L., Moorman, A.F., and van den Hoff, M.J. (2009). Epicardium and myocardium separate from a common precursor pool by crosstalk between bone morphogenetic protein- and fibroblast growth factor-signaling pathways. *Circ Res* 105, 431-441.
- Verberne, M.E., Gittenberger-de Groot, A.C., and Poelmann, R.E. (1998). Lineage and development of the parasympathetic nervous system of the embryonic chick heart. *Anat Embryol (Berl)* 198, 171-184.
- Verzi, M.P., McCulley, D.J., De Val, S., Dodou, E., and Black, B.L. (2005). The right ventricle, outflow tract, and ventricular septum comprise a restricted expression domain within the secondary/anterior heart field. *Dev Biol* 287, 134-145.
- Viragh, S., and Challice, C.E. (1981). The origin of the epicardium and the embryonic myocardial circulation in the mouse. *Anat Rec* 201, 157-168.
- Viragh, S., Gittenberger-de Groot, A.C., Poelmann, R.E., and Kalman, F. (1993). Early development of quail heart epicardium and associated vascular and glandular structures. *Anat Embryol (Berl)* 188, 381-393.

- Vrancken Peeters, M.P., Gittenberger-de Groot, A.C., Mentink, M.M., and Poelmann, R.E. (1999). Smooth muscle cells and fibroblasts of the coronary arteries derive from epithelial-mesenchymal transformation of the epicardium. *Anat Embryol (Berl)* **199**, 367-378.
- Waldo, K.L., Kumiski, D.H., Wallis, K.T., Stadt, H.A., Hutson, M.R., Platt, D.H., and Kirby, M.L. (2001). Conotruncal myocardium arises from a secondary heart field. *Development* **128**, 3179-3188.
- Wang, C.C., Lin, W.N., Lee, C.W., Lin, C.C., Luo, S.F., Wang, J.S., and Yang, C.M. (2005). Involvement of p42/p44 MAPK, p38 MAPK, JNK, and NF-kappaB in IL-1beta-induced VCAM-1 expression in human tracheal smooth muscle cells. *Am J Physiol Lung Cell Mol Physiol* **288**, L227-237.
- Watt, A.J., Battle, M.A., Li, J., and Duncan, S.A. (2004). GATA4 is essential for formation of the proepicardium and regulates cardiogenesis. *Proc Natl Acad Sci U S A* **101**, 12573-12578.
- Wheelock, M.J., and Johnson, K.R. (2003). Cadherin-mediated cellular signaling. *Curr Opin Cell Biol* **15**, 509-514.
- Wilson, J.G., and Warkany, J. (1949). Aortic-arch and cardiac anomalies in the offspring of vitamin A deficient rats. *Am J Anat* **85**, 113-155.
- Wozniak, M.A., Modzelewska, K., Kwong, L., and Keely, P.J. (2004). Focal adhesion regulation of cell behavior. *Biochim Biophys Acta* **1692**, 103-119.
- Wu, H., Lee, S.H., Gao, J., Liu, X., and Iruela-Arispe, M.L. (1999). Inactivation of erythropoietin leads to defects in cardiac morphogenesis. *Development* **126**, 3597-3605.
- Xavier-Neto, J., Shapiro, M.D., Houghton, L., and Rosenthal, N. (2000). Sequential programs of retinoic acid synthesis in the myocardial and epicardial layers of the developing avian heart. *Dev Biol* **219**, 129-141.
- Yamashita, M., Fatyol, K., Jin, C., Wang, X., Liu, Z., and Zhang, Y.E. (2008). TRAF6 mediates Smad-independent activation of JNK and p38 by TGF-beta. *Mol Cell* **31**, 918-924.
- Yang, J.T., Rayburn, H., and Hynes, R.O. (1993). Embryonic mesodermal defects in alpha 5 integrin-deficient mice. *Development* **119**, 1093-1105.
- Yang, J.T., Rayburn, H., and Hynes, R.O. (1995). Cell adhesion events mediated by alpha 4 integrins are essential in placental and cardiac development. *Development* **121**, 549-560.
- Zaffran, S., Kelly, R.G., Meilhac, S.M., Buckingham, M.E., and Brown, N.A. (2004). Right ventricular myocardium derives from the anterior heart field. *Circ Res* **95**, 261-268.
- Zhou, B., Ma, Q., Rajagopal, S., Wu, S.M., Domian, I., Rivera-Feliciano, J., Jiang, D., von Gise, A., Ikeda, S., Chien, K.R., and Pu, W.T. (2008a). Epicardial progenitors contribute to the cardiomyocyte lineage in the developing heart. *Nature* **454**, 109-113.

Zhou, B., von Gise, A., Ma, Q., Rivera-Feliciano, J., and Pu, W.T. (2008b). Nkx2-5- and Isl1-expressing cardiac progenitors contribute to proepicardium. *Biochem Biophys Res Commun* 375, 450-453.

Zhou, Y., Kato, H., Asanoma, K., Kondo, H., Arima, T., Kato, K., Matsuda, T., and Wake, N. (2002). Identification of FOXC1 as a TGF-beta1 responsive gene and its involvement in negative regulation of cell growth. *Genomics* 80, 465-472.